SEDIMENTATION PROCESSES IN ANCHIALINE CAVES OF THE YUCATAN PENINSULA – THE ROLE OF KARST TOPOGRAPHY AND VEGETATION

SEDIMENTATION PROCESSES IN ANCHIALINE CAVES OF THE YUCATAN PENINSULA – THE ROLE OF KARST TOPOGRAPHY AND VEGETATION

By

SHAWN COLLINS, B.Sc. (HONS.), M.Sc.

A Thesis

Submitted to the School of Graduate Studies

in Partial Fulfillment of the Requirements

for the Degree

Doctor of Philosophy

McMaster University

McMaster University
Doctor of Philosophy (2015)
Hamilton, Ontario, Canada
(Geography and Earth Sciences)

TITLE: SEDIMENTATION PROCESSES IN ANCHIALINE CAVES OF THE YUCATAN PENINSULA – THE ROLE OF KARST TOPOGRAPHY AND VEGETATION

Author: Shawn V. Collins B.Sc.(Hons) McMaster University M.Sc. McMaster University

SUPERVISOR: Professor Eduard G. Reinhardt

NUMBER OF PAGES: xxii, 160

Abstract

Understanding the mechanisms that control sedimentation in the anchialine caves of the Yucatan Peninsula, Mexico is vital for interpreting the sedimentary deposits therein. External forcing mechanisms of varying scales, such as eustatic sea-level rise and large storm events, can have a significant influence on the rate and composition of sediment transported and deposited in the cave. Using sediment cores, high resolution radiocarbon dating, cave mapping and continuous aquifer attribute data, it was shown that sedimentation patterns in the cave were not controlled by sea-level rise/fall alone. Overlying vegetation and cave physiography were controlling factors which resulted in sedimentation in the cave being transient in time and space.

The coastal aquifer responded to seasonal variations in precipitation but also showed a broad regional response to intense rainfall associated with Hurricane Ingrid in 2013. Due to the extensive hydraulic conductivity of the aquifer, the hydrologic response to Hurricane Ingrid was shorted lived (weeks) while its effect on sedimentation in the cave lasted for months. Sedimentation rates in the cave did not respond to elevated precipitation alone but showed a link with overlying vegetation. In regions of the cave with overlying mangrove forest, sedimentation was significantly higher than areas with tropical forest coverage. Mangrove forests baffled sediment creating an aquitard which resulted in the ponding of meteoric waters and subsequent enrichment in nutrients. Nutrient rich meteoric waters were funneled into cenotes increasing primary productivity for organic matter sediment production.

Sedimentary deposits in anchialine caves are subject to punctuated sedimentation as a result of external forcing mechanisms or triggers. In the case of Yax Chen the trigger for sedimentation was not contemporaneous with Holocene sea-level rise. This has important implications for the use of cave sediments as proxies for sea-level research and paleo hurricane studies.

Acknowledgements

Truth be told, I have a lot of people to thank for the opportunity to complete my doctorate. At the top of the list were all of the GUE, MCEP volunteers that helped me collect data and break the first rule of cave diving by interacting with the sediments in the cave. There are far too many to list but rest assured I appreciate all of your contributions to my work. I would like to especially thank a few volunteers who decided to spend their time and money cave diving with me year after year. Jan, Arno and Allie were always happy to contribute in any way, and did it with a smile and a laugh, with the exception of surface manager days (Allie)! I owe a large debt to my dive partner Onno. He not only came diving with me year after year and put up with my terrible SAC rate (when compared to his) but asked me to complete the cave 2 class with him. Onno you provided technical diving instruction and are one of the most solid dive partners I have ever had. I certainly attribute your rock solid diving skills as one of the main reasons I passed our cave 2 course and completed the removal of the longest underwater sediment core in Ox Bel Ha. I appreciate your help over the years and I am so happy you now have your better half to dive with! Yvonne is much better looking than me anyway.

I could not have done this work in Mexico without the help, instruction and support of Zero Gravity Dive Center and the consummate professionals in the GUE organization. Fred Devos and Chris Le Maillot are both responsible for teaching me not only how to dive in a cave safely but how to conduct science in a cave safely. They allowed the project to overrun the dive shop and were always around to discuss anything

I needed. I thank both of you very much for all of your help and hope to visit next time as a vacationing cave diver! I would love to be able to dive wherever I please and to leave the science gear at home!

A quick shout out goes to the purple diving dinosaur! Brady, you always made me laugh and I enjoyed our stress relieving runs around the indoor track.

I would like to thank Ed Reinhardt for helping me achieve my dream of completing my Ph.D. Ed, you have been a positive influence on my scholastic career for some time. The first contribution was to convince me that I should continue on to graduate school after my Bachelor's degree. The second contribution was convincing me to return to McMaster to complete my doctorate. I apologize for making you edit my long winded manuscripts and I promise to continue to look for ways to shorten my writing. I would also like to thank my committee members Chris Werner, Dominique Rissolo and Joe Boyce for all of their time and insight into my work. A special thanks to Chris who travelled all the way from Huston to participate in my comprehensive exams.

I need to thank my mother, family and close friends (you know who you are) for always being there when I needed you. Special thanks goes out to my son Kieran who never questioned why I was away in the field or got upset when I had to work late or spend the evening writing on the computer. He was especially proficient at helping me build sediment traps and loved the fact that he was "doing science"! I can't wait to help you with your science projects!

As with most things in life the final stages to get something done is the most difficult time. It can be a tough to see the "silver lining" or "the light at the end of the tunnel" when you are working on a project like this. It can be overwhelming but I was blessed to find a girlfriend who was so patient and supportive. Crystal Ripa volunteered her time to proof read and put up with my rants about this and that (there were a few). She was especially supportive when my father passed away in 2014. I can never repay her for the help and support she has given me over the last two years. Although, I hope I have a long time trying.

My Dad never got the chance to see me complete my doctorate. I hope that before he passed he was content in the knowledge that I was way too stubborn to give up on this dream.

Declaration of Academic Achievement

Chapter 2 - Reconstructing water level in Hoyo Negro with implications for early Paleoamerican and faunal access.

For this paper, all of the data was collected in the field (sediment cores and organic matter samples) by S.V. Collins, E.G. Reinhardt and A. Nava Blank. Processing of laboratory samples was completed by S.V. Collins. The manuscript and figures were prepared by S.V. Collins and E.G. Reinhardt with comments and assistance from D. Rissolo and J. Chatters. Mexican government cooperation was provided by P. Luna Erreguerena.

Chapter 3 - Regional response of the coastal aquifer to Hurricane Ingrid and sedimentation flux in the Yax Chen cave system (Ox Bel Ha) Yucatan, Mexico.

For this paper, design of sediment traps was completed by S.V. Collins. Placement and retrieval of sediment traps was completed by S.V. Collins, E.G. Reinhardt, C.L. Werner, F. Devos and C. Le Maillot. Processing of laboratory samples was completed by S.V. Collins. Data processing of weather and water level data was completed by S.V. Collins. All GIS and Google Earth imagery interpolation and processing was completed by S.V. Collins with the exception of the mangrove vector overly which was provided by S. Meacham. Figures were prepared by S.V. Collins and E.G. Reinhardt. Manuscript preparation was completed by S.V. Collins and E.G. Reinhardt with comments from C.L. Werner.

Chapter 4 - Late Holocene Mangrove development and onset of sedimentation in the Yax Chen cave system (Ox Bel Ha) Yucatan, Mexico implications for using cave sediments as a sea-level indicator

For this paper, design of sediment depth survey was by S.V. Collins. Collection of sediment depths and cores were completed by S.V. Collins and E.G. Reinhardt. F. Devos and C. Le Maillot were responsible for cave diving logistics and consulted on all cave diving matters. All data processing was completed by S.V. Collins. All GIS and Google Earth imagery interpolation and processing was completed by S.V. Collins. Figures were prepared by S.V. Collins and E.G. Reinhardt. Manuscript preparation was completed by S.V. Collins and E.G. Reinhardt with comments from C.L. Werner.

Table of Contents

Table of Figures

Chapter 2

Chapter 3

Chapter 4

List of Tables

Chapter 1 - Introduction

The extensive underground cave systems in the Yucatan Peninsula, Mexico have played a pivotal role in both the natural and anthropogenic history of the area. As early as thirteen thousand years before present, the cave systems have provided shelter and access to potable water during colonization of North America by Paleoamericans (Chatters et al., 2014; Gill et al., 2007; González et al., 2013). In later times, the caves also played a central role in Mayan society in both a spiritual and domestic capacity (Back, 1995; Colas et al., 2000; Rissolo, 2001). Presently, the freshwater that occupies the phreatic cave system continues to be the only source of drinking water for most of the Yucatan Peninsula (Gondwe et al., 2010; Steinich and L.E. Marin, 1997). Contamination of this fresh groundwater mass is an ongoing concern due to porosity of the carbonate host rocks and increasing anthropogenic stresses (Mahler et al., 2007). Until now, minimal work has been done to monitor changes in the aquifer to external factors such as sea-level fluctuations, hurricanes and anthropogenic stresses (Neuman and Rahbek, 2007). In the absence of continuous monitoring data, scientists have relied on speleothems and sedimentary records found in the caves to provide information on the past variations to water chemistry and paleoenvironment as a result of these external forcing mechanisms. Previous work has demonstrated that sedimentary deposits in the phreatic caves are capable of recording and preserving local environmental changes due to their unique geology and generally low energy regimes (van Hengstum et al., 2010). Proxies such as foraminifera, thecamoebians, stable isotopes, pollen and ostracods have been established as reliable indicators of past hydrologic conditions in surficial and cave environments

(DeDeckker and R.M. Forester, 1988; Gabriel et al., 2009; Patterson et al., 1995; Pohlman et al., 1997; Reinhardt et al., 2005; van Hengstum et al., 2009b). In addition, factors such as low concentrations of dissolved oxygen, high concentrations of hydrogen sulphide, fluctuating salinities and a lack of photosynthetic organisms, keep bioturbation and oxidation low, thus increasing the preservation potential of paleo records (Bauer-Gottwein et al., 2011; Coke, 1991; Gabriel et al., 2009; van Hengstum et al., 2009b). The sedimentary information recorded in the caves in Mexico have implications for understanding a vast array of problems, such as the ancestry of the Americas (Chatters, 2000; Chatters et al., 2014; Dixon, 1999), local sea-level history (Milne and Peros, 2013; Toscano and Macintyre, 2003) and paleolimnological conditions (Gabriel et al., 2009; van Hengstum et al., 2009a; van Hengstum et al., 2008). However, a more extensive knowledge of phreatic cave sedimentation processes and the effects of external forcing mechanisms are required to gain a complete understanding of this complex sedimentary record.

This research will utilize two different cave systems within the province of Quintana Roo, Mexico, Sac Actun and Ox Bel Ha. These two cave systems are the two longest underwater cave systems in the world (Quintana Roo Speleological Survey, 2014). Both caves are part of the Yucatan Peninsula aquifer which is classified as an open system with hydrologic connections to the Caribbean Sea (Bauer-Gottwein et al., 2011; Beddows et al., 2007). Sediment cover in the caves varies from greater-than three meters to non-existent, depending on the location. Large variations are observed over short distances in the cave. Even cave passages in the same system can display significantly different sediment coverages. The aquifer is a density stratified system with a freshwater lens sitting on top of warm dense saline groundwater. The boundary layer between these two groundwater masses is the mixing zone and displays significant variability in thickness, depth, and chemistry. Largely, the variations seen in the mixing layer can be attributed to distance from the Caribbean coast, with it becoming shallower and thicker as the coastline is approached (Smart et al., 2006). The fluctuating elevations of the mixing zone through time are a result of eustatic sea-level cycles. These sea-level cycles along with the $CaCo_3$ dissolution capabilities of the mixing zone have been documented as the main mechanism of cave formation in the Yucatan aquifer. Repeated cycles have resulted in enhanced dissolution of these cave passages (Back et al., 1986; Smart et al., 2006). Access to the subterranean caves was via sinkholes known locally as cenotes.

This dissertation will be divided into three papers. The first will apply proven sedimentological and micropalentological methods to sediment cores collected in the Outland Cave (part of the Actun Ha Cave System), Cenotes Ich Balam, Oasis and Hoyo Negro to determine the paleohydrological history of the Hoyo Negro archaeological site. In addition to these proven methods, the cave conduit morphology will be examined to determine the effect it has on the timing and spatial variability of the sedimentological processes active over the history of this cave passage, during the Holocene sea-level transgression. The second paper will characterize the current sedimentation rates and examine the effects that large storms have on the sediment flux in Yax Chen Cave (part of the Ox Bel Ha Cave System). The determination of modern sedimentation rates were accomplished by deploying a series of specially designed sediment traps which were developed for use in the hydrologic conditions of Yax Chen Cave. Sediment traps were positioned in the cave to determine the effect the overlying vegetation and cenotes had on sedimentation rates in the cave. As sedimentation patterns appear to be linked directly with climatic variables, weather station data from the Sian Ka'an Biosphere Reserve were collected contemporaneously with "in cave" temperature and water level data. Finally, the third paper will review all the available geologic data in the context of the facies model developed in the first paper to determine the sedimentation history of Yax Chen. In addition to the cave physiography, data utilized in this study consisted of sediment core data, geochronology, current sedimentation rates and sediment depth measurements from the cave. Determination of the sediment initiation, providence and preferred pathways into the cave environment will help to determine variations in sedimentation patterns though time as a result of external forcing mechanisms. This study will examine the utility of cave sediments in a karstic terrain as a proxy for local sea-level and paleo-hurricane research in the circum-Caribbean region.

Chapter 2 - Reconstructing water level in Hoyo Negro with implications for early Paleoamerican and faunal access.

Quaternary Science Reviews.

Collins S.V.*, Reinhardt E.G., Rissolo D., Chatters J., Nava Blank A., Luna Erreguerena, P.

*Corresponding author – shawnvcollins@icloud.com

Keywords: Cave sediments; Paleoamericans; Anchialine; Hoyo Negro; Paleoenvironmental reconstruction; Yucatan

2.1 Abstract

The skeletal remains of a Paleoamerican (Naia; HN5/48) and extinct megafauna (e.g. gomphotheres, Shasta ground sloths) were found at the base (62 m diam., -40 to -43 mbsl) of a submerged dissolution chamber named Hoyo Negro (HN) in the Sac Actun Cave system, Yucatan Peninsula, Mexico. The remains were dated to between 12-13 Ka making this one of the oldest in the Yucatan. A series of 12 sediment cores were used to reconstruct the flooding history of the now phreatic cave passages and cenotes (Ich Balam, Oasis) that connect to HN. Four facies were found: 1. bat guano and Seed (SF), 2. lime Mud (MF), 3. Calcite Rafts (CRF) and 4. Organic Matter/Calcite Rafts

(OM/CRF) which were defined by their lithologic characteristics but also ostracod, foraminifera and testate amoebae content. Basal radiocarbon ages (AMS) of aquatic sediments (SF) combined with cave bottom and ceiling height profiles determined the flooding history of HN and when access was blocked for human and animal entry. Our results show that the bottom of HN was flooded at least by 9850 cal yr BP but likely earlier, and the pit was blocked for human and animal entry at ≈8100 cal yr BP when water reached the cave ceiling effectively blocking entry. Water level continued to rise between ≈ 6000 - 8100 cal yr BP filling the cave passages and entry points to HN (Cenotes Ich Balam and Oasis). Analysis of cave facies revealed that both Holocene sea-level rise and cave ceiling height determined the configuration of airways and the deposition of floating and bat derived OM (guano and seeds). Calcite rafts which form on the water surface are dependent on airways but also isolated air domes which affect their loci of deposition on the cave bottom. These results indicated that aquatic cave sedimentation is transient in time and space requiring multiple cores to determine a limit after which flooding occurred.

2.2 Introduction

In 2007, cave divers Alberto Nava Blank, Alex Alvarez and Franco Attolini were exploring a previously unmapped section of the Sac Actun Cave System in Quintana Roo, Mexico. During exploration, they discovered a 55 m (maximum) deep underwater pit they named Hoyo Negro (HN; Chatters et al., 2014). At the bottom of the pit were the remains of at least 26 large mammals including extinct Pleistocene megafauna (e.g. extinct: sabertooth [*Smilodon fatalis*], gomphothere [*Cuvieronius cf. tropicus*, a proboscidean], Shasta ground sloth [*Nothrotheriops shastensis*]; a bear of the genus *Tremarctos* and sloth of the family Megalonychidae; extant: puma, bobcat, coyote, Baird's tapir, collared peccary and white-nosed coati, (Chatters et al., 2014). Amongst this Lagerstätten of terrestrial animals, were the remains of a 15-16 year old woman who the dive team named Naia (HN5/48; Chatters et al., 2014). U/Th dating of calcite florets which precipitated on the bones post-mortem provided a minimum age of 12 ± 2 Ka, while AMS radiocarbon ages of tooth enamel bioapatite provided a maximum age of 13 Ka. Naia's craniofacial similarity with other Paleoamericans and her Beringian-derived mtDNA contributes to the debate on the arrival and dispersal of early humans in North and South America (see Chatters et al., 2014 for a full discussion; Anderson and Gillam, 2000; Chatters, 2000; Dixon, 1999; González et al., 2008). As summarized in Chatters et al. (2014), the Yucatan caves provide a unique environment for preservation that is unparalleled. Few early Paleoamerican remains have been found in terrestrial sites and none have been associated with extinct megafauna (Chatters et al., 2014; González et al., 2013; Chatters, 2000). However, radiocarbon dating bone material found in the flooded Yucatan caves is not without complications (see Chatters et al., 2014). Hard-water effects and collagen leaching result in contamination which can make dating difficult (e.g. Dixon, 1999; González et al., 2008; Taylor, 2009). Dating of associated artifacts can be used, but is problematic, and more so with HN as there was little sediment coverage to provide any stratigraphic association or context (Chatters, 2000; Chatters et al., 2014). In Naia's case, there was insufficient bone collagen for radiocarbon dating necessitating the use of small quantities of tooth enamel. Her age was constrained using U-Th dating of calcite florets that formed on the bones post-mortem but also with water level reconstructions from cave deposits (as presented in Chatters et al., 2014).

The goal of this study was to provide constraining data on Naia's age through reconstructing water levels in the cave as her taphonomic condition indicated she fell and died in water at the bottom of HN (Chatters et al., 2014), but also contribute to understanding site formation for further studies on the HN Lagerstätten.

2.2.1 Geologic Setting

The Yucatan Peninsula, Mexico is a large Paleogene to Quaternary limestone platform with an area of over 350,000 Km^2, of which, half is submerged under the Gulf of Mexico (Weidie, 1985). Metamorphic basement rocks underlie the Cenozoic units (Ward et al., 1995). The limestone platform has been largely unaffected by tectonic uplift or orogenic events. As a result, the stratigraphy is largely sub-horizontal with minimal differential tilting (Beddows, 2004; Coke, 1991).

In the Yucatan, as with other anchialine settings, the aquifer is density stratified and composed of a freshwater meteoric lens sitting on top of saline water. Marine water intrudes from the coast via the porous limestone with the fresh (or slightly brackish) meteoric water mass thickening landward and separated by a halocline (underground estuary; Moore, 1999). Density contrasts between the warmer, denser saline water (PSU 35) and the cooler freshwater (PSU <1) lens are responsible for the stratification (Esterson, 2003). The main interface (halocline) between the two water bodies is termed the mixing zone and has PSU values ranging from 1-35 (Werner, 2007). The mixing zone can have changes in temperature, pH, dissolved oxygen and salinity depending on the location in the cave and the time of year (Esterson, 2003). The meteoric and marine water masses have uniform characteristics. Mixing occurs at the halocline through a variety of mechanisms including tidal pumping, precipitation patterns, cave conduit roughness etc., which produces spatial variation in meteoric salinity but with a gradient inland (e.g. Yax Chen @ 6 PSU vs Hoyo Negro @ 1 PSU; Collins et al., 2015 a, b; Chatters et al., 2014). Hoyo Negro is ≈ 7 km from the coast and has a halocline at 15-22 m depth while Yax Chen is ≈1.5 km and its halocline is at 10 m (Collins et al., 2015 a, b). Groundwater level rises gradually away from the coast (10-15 cm/km; ≈1-2 m above msl at HN). Due to the high hydraulic conductivity of the limestone the flow velocities in the meteoric lens are typically low (generally <6 cm/sec; Beddows, 2004; Moore, 1999). No rivers drain the Yucatan since rainfall quickly penetrates through the porous vadose zone to the water table (Bauer-Gottwein et al., 2011). Presumably, based on modern studies of groundwater response, Holocene sea-level rise controlled the water levels in the caves and aquifer, although there is no verifying data.

Cave and cenote formation has been attributed to processes driven by glacio-eustatic sea-level cycles (Beddows, 2004; Smart et al., 2006). Meteoric water was found to be saturated with respect to calcite ($CaCO_3$-) until mixed with saline groundwater. In the mixing zone, the water was undersaturated with respect to $CaCO_3$- resulting in dissolution of limestone and cave passage enlargement (Beddows, 2004; Esterson, 2003; Smart et al., 2006). Smart et al, 2006 studied cave speleothems and determined that numerous phases of subaqueous/subaerial conditions had occurred over the life of the cave passages, as evidenced by repeated dissolution/recrystallization sequences.

2.2.2 Late Pleistocene – Early Holocene Climate and Vegetation

Vegetation in the Yucatan Peninsula has varied since the Late Pleistocene as a result of climatic variability, sea-level rise and anthropogenic influences in the late Holocene (Carrillo-Bastos et al., 2010; Leyden et al., 1998). Pollen records from lowland Guatemala have demonstrated that temperate oak forests were firmly established between 14,000 – 10,000 cal yr BP. The climate was inferred to be drier and cooler resulting in an increased prevalence of natural forest fires (Islebe et al., 1996). As a result of increased temperature and precipitation in the early Holocene, the vegetation shifted to a lowland tropical forest as evidenced by significant increases in Moraceae – Urticaceae taxa. Islebe et al., 1996, report that the high forest was established by ~ 8600 cal yr BP and persisted until ~5600 cal yr BP. Pollen analysis from Lake Tzib, Mexico showed that by 7900 cal yr BP the vegetation in Quintana Roo was consistent with a diverse, low to medium statured forest with traces of *C. erecta* pollen indicating the existence of limited mangrove nearby (Carrillo-Bastos et al., 2010). The onset of drier conditions between 6500 – 4700 cal yr BP resulted in a decrease in forest taxa (*Ficus* and Moraceae) resulting in an assemblage of medium statured forests and grasses (Carrillo-Bastos et al., 2010; Islebe et al., 1996). Increased climate variability in the pan-Caribbean has been ascribed to the changing positon of the intertropical convergence zone (ITCZ) resulting in fluctuations between mesic and drought conditions as evidenced by sediment cores from the Cariaco Basin (Haug et al., 2001). This is reflected in the Yucatan pollen record as increases/decreases in *Ficus* and Moraceae pollen between 4600 – 4100 cal yr BP, followed by drought conditions circa 3500 cal yr BP (Carrillo-Bastos et al., 2010;). As a result of Holocene sea-level rise, by 3800 cal yr BP the costal vegetation on the Quintana Roo coast was consistent with the assemblage of mangroves currently present on the eastern coast of the Yucatan (Torrescano and Islebe, 2006).

2.2.3 Hoyo Negro - Sac Actun Cave System

HN is a dissolution feature found in the Outland Cave which is part of Sac Actun the world's second longest subaqueous cave system, (Quintana Roo Speleological Survey, 2014) located in the Mexican state of Quintana Roo, near the town of Tulum (Fig. 1). The Outland Cave is part of a network of over 540 kilometers of anastomosing phreatic caves that trend sub-perpendicular to the Caribbean Coast from Puerto Morelos to Tulum (Beddows, 2004). As the anastomosing conduits drain the upland areas, flow is generally to the east towards the coast (Neuman and Rahbek, 2007). HN is a bell shaped dissolution chamber with a diameter of 32 m at the top and 62 m near the bottom. The rim of the pit is located at a water depth of approximately -12 m while the bottom ranges from -33 m on the north wall and -48 m on the south wall but also has crevices that extend to -55 m (Chatters et al., 2014). Three phreatic cave passages merge into HN. Such cross-linked passages are common in the anastomosing network of the Yucatan (Fig. 2a). The passages have an approximate mean depth of -12 m, with sidewall widths that are > 10 m in some instances. This elliptical tabular morphology is one of the more common passage types in the Yucatan (Smart et al., 2006) and generally does not follow bedding planes. The wide horizontal shape is a result of dissolution in the mixing zone and shows little evidence of past flow direction or velocities (Smart et al., 2006). The northeast passage from the pit leads to Cenote La Concha which is over ≈ 600 meters upstream from HN but has a very narrow passage (Fig. 2a). The downstream southeast passage, which is wider than La Concha, leads to Cenotes Ich Balam (60 m) and Oasis (≈600m; Chatters et al., 2014).

2.2.4 Paleoamerican remains in Hoyo Negro

HN was not the first significant Paleoamerican site found in the submerged caves of the Yucatan Peninsula. González et al. (2013) reports, that to-date, eight prehistoric sites with human remains have been discovered in the caves in the Tulum region, Mexico. Currently, (with the exception of HN) none of these human remains have been reported to be associated with any fauna of Pleistocene age. Indirect evidence of Paleoamerican occupation such as; charcoal, fossil animal bones and lithic tools is reported but not in association with the skeletons (González et al., 2008). HN is the first prehistoric site where both human and extinct Pleistocene megafauna skeletal material have been found co-mingled (Chatters et al., 2014).

Previous to the discovery of Naia, the most significant find in the Yucatan was the human remains of a female found in Naharon Cave by Jim Coke and Tom Young. She was 80% intact and was considered to be in fair taphonomic condition (González et al., 2008). Radiocarbon dating of amino acids indicated that the remains were from 13.4-13.8 Ka (González et al., 2013) although the age has been questioned due to the leaching and degradation of amino acids necessary to calculate an accurate date (Chatters et al., 2014; Taylor, 2009). No primary environmental data was collected to assess its taphonomic history or the skeletal age.

In the case of HN, there were questions on how Naia and the animals entered the cave system and ultimately fell into the pit, with the possibilities including accidental (trap; cenote Ich Balam) and/or a "willing" entry scenarios (Cenotes Oasis and La Concha). The three cave passages leading to Hoyo Negro are relatively shallow at ≈ -12 mbsl. The bottom has irregular topography due to the ceiling breakdown with the scattered but intact skeletal material laying on and in crevices between the limestone blocks. The closest entry point was Ich Balam located 60 meters downstream of the pit followed by Cenotes Oasis (≈ 600 m) and La Concha (≈ 600 m; Fig. 2a). Both La Concha and Oasis have enlarged central pits that are open to the surface due to the collapse of the cavern ceiling. They have low, sloping walls and cave passages that are open at ground level, providing easy access for animals or humans (Chatters et al., 2014; Finch, 1965). The entrance of Ich Balam measures only 1.2 x 5 m and is located at the apex of the ceiling in an otherwise roofed cavern. Branches and leaves could have concealed the opening, allowing unsuspecting animals to fall 8 m to the cavern floor. The domed shape of the cavern roof, with its speleothem coated walls, would have prevented escape, forcing movement through either of the two existing cave passages present in Ich Balam. If they chose poorly, unsuspecting animals would fall into HN. This would be applicable for smaller fauna such as cats but not for the larger gomphotheres or sloths. The "willing" entry scenario is more difficult to assess since animals would need to enter a dark cave passage. However, animals may have smelled groundwater, or in the case of the carnivores may have heard the cries of animals in distress or smelled carrion and in desperation may have entered the cave passage and unsuspectingly fallen into HN. Oasis and La Concha entry points are the farthest away (i.e. ≈ 600m) necessitating navigating long and restricted passages in the dark.

The skeletons found at HN are well-preserved, but most are not articulated, suggesting they fell into water and progressively decayed with body parts falling in different parts of the pit as the corpses floated on the surface. The lower half of Naia showed greater articulation suggesting that this portion of the skeleton settled and decomposed insitu. There is no speleothem covering the skeletons other than calcite florets, suggesting the skeletons were deposited in water or quickly became covered by rising water levels. However, during our investigations there were many questions about when the pit flooded, and how water levels may have fluctuated or whether they reflected Holocene sea-level changes.

Our research throughout the investigation of HN was to provide the environmental context of site evolution while assessing entry points and determining when access to HN was ultimately blocked with rising water levels. We accomplished this through dating aquatic sediments in HN, cave passages and the cenotes (Ich Balam and Oasis) and reconstructing water levels and sedimentation patterns in the context of the cave configuration. This provided important water level information to assess the age of Naia, but also provides a minimum age for faunal accumulation in HN. This research will be important for future studies addressing site formation and taphonomy of the skeletal material in similar sites in the Yucatan but also worldwide (e.g. Gabriel et al., 2009; Gregory et al., in press; Hodell et al., 2005; Peros et al., 2007).

2.2.5 Cave Sedimentation and Microfossil Proxies

Aqueous cave sedimentation is an area of research that is underdeveloped in terms of the process and contributing factors. Yucatan cave sediment contains minimal amounts of siliciclastics, being composed largely of either organic matter (OM) or secondarily precipitated calcite rafts. OM enters the cave via transport from terrestrial sources or through primary productivity in sunlit cenote water bodies (Collins et al., 2015a, b; van Hengstum et al., 2010). Calcite rafts form on surface waters in cenotes or in air domes in the cave as a result of CO_2 degassing from the $CaCO_{3}$- saturated meteoric water mass. When degassing occurs, calcite is precipitated at the air-water interface (Taylor and Chafetz, 2004; van Hengstum et al., 2015). Gabriel et al. (2009) was the first to examine how water level affected cenote development in the Yucatan while van Hengstum used microfossils (foraminifera and testate amoebae) and cave sediment records to reconstruct groundwater salinity over the past 4.5 Ka (van Hengstum et al., 2009b; van Hengstum et al., 2008; van Hengstum et al., 2010). Subsequent work in Bermuda and Bahamas used similar techniques (van Hengstum et al., 2011; van Hengstum et al., 2009a; van Hengstum et al., 2013). However, much of the previous research relating cave sedimentation to sea-level was inferred from limited background data (eg. Bermuda; van Hengstum et al., 2011; also van Hengstum et al., 2009a; Bahamas; van Hengstum et al, 2013). Subsequent research by Collins et al. (2015a, b) was conducted to enhance this body of research documenting sources and controls of sedimentation in Yax Chen (part of the Ox Bel Ha Cave System) and its relationship with an extensive mangrove system but also with a recent hurricane (Ingrid Sept 2013; Collins et al, 2015a, b). The results from HN provide an extension of that research, but in a cave system where terrestrial vegetation dominates (forest vs mangrove) and where sedimentation is more focused and less extensive. The HN results are unique; as they take into account both the bottom and ceiling heights of the cave showing its role in focusing OM and calcite raft deposition a factor that has not been considered previously.

2.3 Methods

2.3.1 Field

Twelve push cores (5 cm diam, 11-136 cm long) were obtained from Ich Balam, Oasis, HN and the passage leading from Ich Balam to HN using SCUBA (Self-Contained Underwater Breathing Apparatus). All cores reached refusal on the underlying cave bottom (Fig. 2b-d). In order to develop a flooding history of the cave, core locations were selected according to three criteria: spatial coverage, the availability of sediment, and depth. Core sites tended to be focused close to the cenotes where accumulations are thicker as opposed to the cave passages that contained no or very thin (< 1cm) sediment coverage. Sediment coverage in HN consisted of isolated calcite raft piles and concentrations of OM including seeds, branches and charcoal which were concentrated in small piles and scattered on the cavern floor as well as on limestone and speleothem ledges on the side of the cavern. The HN core (C9) was taken through one of the calcite raft piles. Core compaction was measured before removal and averaged ≈ 50% which is typical of cave sediments in the Yucatan (Gabriel et al., 2009; van Hengstum et al., 2010). Core sites were positioned using previously collected cave maps of the sites with depths measured using a digital depth gauge (± 10cm).

Cave passage profiles were measured at tie-off points along the cave line which were installed during initial exploration of the cave. At each tie-off, ceiling and bottom elevations were measured with a digital depth gauge (± 10cm). Sidewall dimensions were also measured with a tape measure from tie-off points. Line azimuth (compass) and also distance between tie-off points were measured providing an overall direction and distance of the cave passage and spatially corrected with hand-held GPS (Garmin etrex) at cenotes (Fig. 2a).

2.3.2 Laboratory Analyses

Cores were split, logged and analyzed for particle size at 1 cm resolution for each core (with the exception of OC3). Particle sizes were measured using a Beckman Coulter LS230 using the Fraunhofer optical model. Mean, median, mode and standard deviations were computed.

Petrographic analysis was also performed to document microfossil and calcite raft components with a sampling resolution of 5 cm. Approximately, 0.5 cm^3 of sediment was wet sieved using a 45 µm sieve to remove silts and clays and examined with a binocular dissecting microscope at 60-80X magnification. Foraminifera, testate amoebae and ostracods were counted and recorded as numbers of specimens per cm^3 (Scott and Hermelin, 1993). Since the determination of waterborne sedimentation was the focus of this study, the species were noted but not analyzed further. Calcite raft crystal habit (equant – prismatic vs acicular) was also documented as well as their relative abundance (no./cm^3). Cenote Borge a site with a partially collapsed cavern ceiling, located approximately 30 Km SW of HN was used as a modern analogue for the facies analysis (Fig 3 c-f).

Twenty-nine AMS-radiocarbon dates were obtained on a variety of materials throughout the cores but targeting basal ages with aquatic sediments (Table 1). Seeds and fruit endocarps were preferentially selected where possible but also twigs, charcoal and bulk organic matter (OM) were used. Samples HN4 – HN12 were collected from ledges on the wall of HN at various water depths (Table 1).

Radiocarbon dates were calibrated using the northern hemisphere terrestrial calibration curve IntCal13.14C (Reimer et al., 2013) using the R-statistical software package Clam (Blaauw, 2010 v2.2; RStudio, 2014) and reported as ranges in calibrated years before present (Cal BP) to the 2σ confidence interval.

2.4 Results

2.4.1 Cave Facies

Four facies were recognized based primarily on sediment composition (OM and calcite rafts, mud) however; mean particle size, calcite raft abundance, crystal habits, and microfossils (ostracods, foraminifera and testate amoebae) also were utilized. Most cores showed a typical facies progression up-core (Figs. 4-7). These include: Mud, Seed, Calcite Raft, and an OM/Calcite Raft Facies and are described in their stratigraphic order from bottom to top.

2.4.1.1 Mud *Facies* (MF)

The carbonate Mud Facies (MF), clay/silt sized limestone with a mean size of 4.7 μm, was found in four cores (C2, C4, C6 - Ich Balam, C7 - cave passage at edge of HN) (Fig. 4a, b). The MF generally lacked microfossils and had only small fragments of OM although a few specimens of foraminifera were found in C2 and C4. Mud facies thickness was generally thin but variable in the cores, ranging from ≈ 5cm in C6 to 23 cm in C7 which was entirely mud. The MF at the base of C4 may represent deposition in a pool of water on the cave bottom before full flooding of the cave, while the MF in C2 may represent mud deposition between limestone blocks of the breakdown pile in Ich Balam. C6 is more difficult to interpret as it is within the Calcite Raft (CR) facies, but again may be deposition between limestone boulders on the top of the breakdown pile. C7, taken near the edge of HN, was entirely limestone mud but contained small fragments of charcoal. This area was slightly depressed in the cave passage on the edge of HN and likely represents deposition when water level had risen to the base of the cave passage but not fully flooded it. The charcoal that was radiocarbon dated in C7 was likely reworked and out of context. However, in all these cases, the mud represents deposition in small isolated pools with limited inputs of sediment that likely was originating from the overlying limestone during rainfall events.

2.4.1.2 Seed Facies (SF)

The Seed Facies (SF) is characterized by seeds and fruit endocarps with undifferentiated OM and was found at the base of six cores (C1-5, 9; Fig. 4 a, b). Two fruiting taxa dominate in this facies: *Byrsonima crassifolia* a member of the

Malpighiaceae family, and *Thevetia peruviana* or yellow oleander, a species of Apocynaceae both of which are still common in the Yucatan (Morell-Hart, 2012). Ostracods were abundant in this assemblage, consisting of *Darwinula spp.* and *Cypridopsis spp.* Small numbers of foraminifera, including *Physalidia simplex* and *Conicosprillina* sp. were also present (n < 16; C1, C2 and C5; Fig. 5 d-g). Acicular calcite rafts were present in most cores in addition to the equant - prismatic variety (Fig 4 a, b; 5 a-c). The acicular rafts formed in the pore and interstitial space in the sediment or at the sediment/water interface and maybe similar to the larger calcite florets from HN (Chatters et al., 2014). However, the presence of equant calcite rafts, which likely formed at the air/water interface, and the abundant ostracods indicate water was present, although shallow enough (likely < 1m) to allow piles of seeds and bat guano to form. These would become dispersed in deeper water (Fig. 3e). A modern analogue was observed in Cenote Borge which shows a bat guano/seed pile (≈10-15cm water depth) below an overhead rookery (Fig. 3 c-e; Laprida, 2006; Taylor and Chafetz, 2004).

2.4.1.3 Calcite Raft Facies (CRF)

The CRF consists of abundant calcite rafts that have well-developed equant – prismatic crystal habit (Fig. 5 a,b). Mean particle size was 563 µm due to this abundance of calcite rafts. This facies also contained variable abundances of ostracods, thecamoebians and foraminifera (Fig. 4a, b). The CRF had low OM content, consisting of ≈ 1-4 cm thick laminations/beds or occasional seed or wood fragments (e.g. C2, C5; Fig 4a). CRF represents an increased water level from the SF but depth is difficult to estimate since calcite rafts formed at the surface can accumulate on the bottom over a range of water depths. Spatial and temporal calcite raft accumulation also requires suitable conditions to produce rafts. Changes in water chemistry such as rates of CO_2 degassing, ionic concentration, temperature, pressure, fluid flow and magnesium concentration have all been shown to have an influence on raft development but the process is still not well understood (González et al., 1992; Hanor, 1978; Jones et al., 1989; Palmer, 1996). However, on a physical basis, calcite raft formation requires the presence of air-water interface (e.g. air domes) so CO_2 degassing can occur in addition to water disturbances that cause rafts to sink and accumulate on the bottom (e.g. water drips, water ripples etc.; Taylor and Chafetz (2004). In Cenote Borge, rafts were only forming in one part of the water body when observed in May 2014 (Fig. 3f). The radiocarbon ages show variable accumulation rates from core to core suggesting that the focus of raft accumulation varied (e.g. C2 and C3). Particle sizes exhibit a general fining upwards in many of the Ich Balam cores (C1, C3, and C4) likely reflecting a change in water depth around the breakdown pile. As the water body increased in area from a ring surrounding the breakdown pile to a larger body of water when the central breakdown pile became flooded, it may have caused increased surface disturbance (i.e. ripples) preventing the rafts from attaining a larger size.

2.4.1.4 Organic Matter/Calcite Rafts Facies (OM/CRF)

This mixed facies had high OM content relative to the CRF with a diverse assemblage of microfauna; ostracods (*Darwinula spp.* and *Cypridopsis spp.*), foraminifera (*Physalidia simplex* and *Conicosprillina spp.*) and thecamoebians

(*Centropyxis aculeata*). The mean particle-size (≈ 325 μm) was less than the CRF but greater than the SF (Figs. 4a, b).

The transition to the OM/CRF is due to the continued water level rise from CRF and is not present in all the cores. The OM/CRF is different from the SF as it contains more calcite rafts and a variety of OM (e.g. seeds, leaves, twigs, etc.). The higher OM content in this facies is likely from rising water levels creating a larger, deeper water body that redistributed the OM on the water surface and bottom. In Cenote Borge, coarse OM deposition (leaves and twigs) was focused in areas open to the surface with a transition to fine OM and calcite rafts coincident with the overlying drip line of the cavern (Fig. 3c). In Ich Balam, the small opening and cavern would focus OM sedimentation directly on the apex of the breakdown pile with some downslope movement but only fine particulates would move deeper into the cave with the low flow regime. In Oasis, the presence of a cave airway with lower water level would allow the OM to be distributed deeper into the cave but would move towards the cenote as water level rose. The OM/CRF gets thicker towards the cenote opening and thinner with increasing distance from openings. The presence of airways would also allow bat transported OM which would also be redistributed in a similar fashion (Fig. 4 a, b).

2.4.2 Radiocarbon Ages

Twenty-nine radiocarbon dates obtained from sediment range from 1007 to 11,328 cal yr BP with no age reversals (Figs. 4a, 4b; Table 1). The ages from Ich Balam are older (3782 to 8090 cal yr BP) and deeper (mostly -9.6 to -12.3 m) compared to Oasis (1007 to 5370 cal yr BP; -1.8 to -4.1 m). The basal charcoal date of 11,328 cal yr BP from the lip of HN (C7) is the oldest radiocarbon date in the cores but is likely affected by reworking and/or an old wood effect. We have three ages for the HN core (C9), two on seeds (9,526 - 9,954 cal yr BP) and one older age on charcoal (11,162 -11,240 cal yr BP). Again, the charcoal may reflect an old wood effect or be reworked or transported from an older deposit.

The surface samples collected from the ledges (n=9) on the side of HN show age reversals with water depth. The radiocarbon samples were collected on lower ledges (≈ -40 to -49 m) of the bell-shaped pit (i.e. under an overhang), so seeds, twigs and charcoal could only lodge there if floating on the water surface. The OM could only get to HN through large storm events or hurricanes, washing material originating from the cenotes into the pit. The age reversals indicate water level fluctuations in HN caused by these extreme rainfalls could have also refloated OM from the base or ledges (Collins et al., 2015a). The seeds and fruit endocarps ranged from 9600 to 9850 cal yr BP while the twigs and charcoal yielded older ages ranging from 10,000 to 12,500 cal yr BP. The seeds and endocarps likely were transported into HN via bats while the twigs and charcoal maybe allochthonous, having eroded from older deposits in the cenote and cave passages during hurricane or storm events.

2.4.3 Facies and Water Level Reconstructions

Flooding history can be inferred from the elevations of basal radiocarbon dates for aquatic sediments with the underlying limestone providing the elevation. This data has one important caveat; aquatic sedimentation is not necessarily coincident with flooding since sediment deposition is controlled by the availability and transport of OM (bats or water) into the cave or the existence of suitable conditions for the formation and deposition of calcite rafts (e.g. water chemistry, air domes and water disturbance). Many caves in the Yucatan have been water filled for thousands of years but lack a sedimentary record of that inundation (Collins et al., 2015b). Therefore, basal radiocarbon ages on aquatic sediment may only provide a limit before which flooding occurred. This was addressed to some degree by taking numerous cores and using the oldest date for a given elevation to provide an age that approached the actual timing of flooding. The water level data is concentrated between -1.8 to -12.3 m in Cenotes Ich Balam and Oasis since they have the most sediment as a result of being open to the air and in proximity to OM inputs (Fig. 7b, c). The HN data is from a calcite raft core (C9; - 42.5 m) and the ledge on the pit wall (≈ -40 to -49 m). Many of the points coincide with documented Holocene sea-level rise, showing the influence of sea-level on water levels in the epikarst and cave (Fig. 7a, d). The Toscano and Macintyre (2003) and the GIA (Glacial Isostatic Adjustment) model of Milne and Peros (2013) are similar over the past 9 Ka and were used to assess the relationship between cave flooding and sea-level (Fig. 7a-c). The ages (n=8) of basal aquatic sediments in Ich Balam and Oasis generally follow sea-level rise although four dates are either too young (n=2) or too old (n=2) for their given elevation. As described, either sediment accumulation began after flooding (too young) or could have included reworked OM (too old) but four of the ages are coincident with the sea-level curves.

For HN we use Medina-Elizalde (2013) modeled relative sea-level curve (9-13 Ka) which has been GIA adjusted by 3.5m (Chatters et al. 2014; Bard et al., 1990). The seed ages (SF; n=2) from the base of aquatic sediment in C9 range between 9526 and 9954 cal yr BP matching the sea-level estimates. However, radiocarbon ages from the ledges vary which as discussed is likely due to variation in water levels in the pit due to extreme precipitation events. For example, Hurricane Ingrid (Sept 2013; Collins et al., 2015a) caused higher than normal water levels in the Tulum area cave systems. In Yax Chen, instrumentally recorded water levels reached +1m from background levels, and a nearby cave system Temple of Doom had water levels that reached +3 m and lasted for several days. This recent example demonstrates considerable regional variability so it is uncertain how groundwater level in HN would have responded to storms when sea-levels were much lower. However, the upper cave passages entering HN may have acted as conduits funneling water into the pit, raising water levels during rainfall events which may have lasted hours or days. The vadose porosity of the limestone would likely limit the flows; however, the flowstones developed on the floor of the cave passages would have occluded infiltration, enhancing flows in the cave passages leading to HN. The twigs, trunks and other OM found in HN could have only arrived though wash-in events, reinforcing this interpretation. High water levels in HN would not last long, but would allow OM to be deposited on higher than normal ledges on the pit wall.

Based on the water level reconstructions and the ceiling and bottom profiles of the cave, the pit was accessible until ≈ 8.1 Ka at which point water level blocked the passage at the ceiling at HN proper. Continued water level rise eventually filled the cave passages as documented in the Oasis cores (OC1-3).

2.5 Discussion

The spatial and temporal distribution of sediment facies, along with the changing elevation of the base of aquatic sedimentation allow us to reconstruct the water level history of HN and its connecting passages. Three intervals were recognizedin this process.

2.5.1 Initial inundation of HN 9850 – 13,000 cal yr BP

In this early phase the upper cave passages leading to HN were open to animals and humans which could have entered from the three cenotes (Ich Balam, Oasis, La Concha; Fig. 8, 9a). Ich Balam and Oasis are viewed as the likely entry points since they have wide and easily navigated passages especially for the large gomphotheres. There were questions on the antiquity of the Ich Balam trap as it is a small opening in the ceiling. The basal core ages for Ich Balam indicate that the cenote opening was in existence at least by ≈ 8.1Ka, as entry of OM and bat guano could only occur if there was a karst window opening to the surface. However, it was likely open earlier (i.e. >13 Ka), as OM preservation is unlikely when the cenote was dry - i.e. decay would be rapid and OM accumulation would be thin and patchy. Better OM preservation occurred with flooding of the upper passage which will be discussed. One stick on the HN ledge dated to 12,372 - 12,573 cal yr BP which if transported into pit via the cave passage; Ich Balam represents the closest and likely source of that material thus extending the date to at least ≈ 13 Ka and the time Naia was in the pit.

Determining the water level history in HN is more difficult (Fig. 8, 9a-d). Based on the correspondence of water level points from the shallower locations in Ich Balam and Oasis from which there is more data, it appears that flooding largely reflects rising Holocene sea-level (Fig. 7a). In HN however, the record appears more complicated due to the configuration of the cave passages and their relationship with the pit. Less data are available due to the lack of sedimentary deposits in HN, but also because earlier Holocene sea-level reconstructions have greater uncertainty due to the rarity of data and the high rate of sea-level rise during this period. Our basal age from the SF in C9 indicates that water was at -42 mbsl (and possibly higher) in HN at least by 9.5-10 Ka, but possibly earlier. Other bat guano deposits in HN date from 9.7- 10.2 Ka Chatters et al., (2014), while the age range of the majority of OM on the ledges spans 9.5 - 11.2 Ka which shows water, but albeit fluctuating water levels in HN as well.

The age of Naia (11.8 - 12.9 Ka; -42 mbsl) was determined through radiocarbon dating of her tooth, which was constrained with U-Th dates from calcite florets on her bones (≈ 9.5 - 12 Ka). Naia's skeletal condition indicated that she had fallen into water. Her disarticulated skeleton lacked evidence of serious trauma that would occur with a fall on a hard substrate (e.g. bone breaks or skull fractures). She and most other animal bones in the pit also lack speleothem covering supporting the theory that they fell into water or were quickly covered by rising water.

Our water level data fits well with the GIA corrected sea-level curve of Medina-Elizalde (2013) as presented in Chatters et al., (2014) but the skeletal taphonomy and age of Naia doesn't correspond as well. Sea-level and by correspondence water level in HN would have been -80 mbsl at 12-13 Ka, necessitating a short-term rise of 40m in water level during rainfall events which seems unlikely due to the high permeability of Yucatan limestone. The Milne and Peros (2013), Caribbean derived GIA sea-level curve if extrapolated to 13 Ka fits the Naia data better as sea-level was close to 42 mbsl at 13 Ka. However, the ledge data does not fit this curve well, since it means that the sampled OM is too young for a given depth and does not match the proposed model of deposition of floating OM on rising water levels during precipitation events (i.e. water levels will rise but not fall below base level). Medina-Elizalde, (2013) fits the HN data better since there is OM on the ledges that is generally too old for a given depth. This argument assumes that OM deposition does not occur from above because of the overhang, although it is possible that turbulent currents in the pit could suspend and deposit OM on the ledges, however, floating OM is a more likely cause.

2.5.2 Rising water levels in HN 9850-8100 cal yr BP

Water levels continued to rise in HN, following Holocene sea-level change,with the CRF in C9 representing deepening water above -41 m after 9850 cal yr BP (Medina-Elizalde, 2013; Milne and Peros, 2013; Toscano and Macintyre, 2003). The majority of our radiocarbon ages from OM are older than 9.5 Ka but this is likely biased as we preferentially sampled guano piles that would have accumulated in shallow water and the OM from the ledges spanned only a short depth range over a short time period (40-49m). As water levels in the pit increased, sediment would become more dispersed on the water surface and with sinking would be more dispersed on the bottom of the pit (Gregory et al., submitted; Fig. 9b). The calcite raft piles could have accumulated over greater water depths as their formation would be based on suitable chemical conditions for their formation but the loci of deposition would be based on water disturbance (i.e. overhead drip water in HN) which would be static over periods of time. Further coring in the pit may provide more information on the spatial and temporal patterning of sedimentation in HN, but based on our data we assume that water levels steadily increased in the pit with episodic OM inputs from the cenotes but also from overhead bat rookeries. Since HN would be isolated during rising water levels, all OM would be contained in the pit. The pit was the depo-center at this time but this changed when the floors of the cave passages leading to HN were flooded at ≈ 8.1 Ka (Fig. 9b, c).

2.5.3 Cave Passages flooded <8100 cal yr BP

The upper cave passages leading to HN were flooded and continued to fill after 8.1 Ka as documented in the Ich Balam stratigraphy (Fig. 8, 9c). Soon after, access to HN would have been blocked by rising water levels reaching the cave ceiling at the pit. Evidence for the initial flooding comes from core 7 on the rim of HN. This core was entirely muddy and represents ponding of water at the edge of HN as water levels rose prior to 8.1 Ka. Basal radiocarbon ages on bulk charcoal fragments provided an old age (11,162 - 11,240 cal yr BP) and there is extensive scatter of charcoal in this area. This charcoal could be from torches and fires used in the cave passage to access HN but charcoal is easily floated and could be allochthonous (i.e. sourced from forest fires). The evidence of flooding is provided by the basal SF ages from Ich Balam. At this point the focus of deposition changed. HN was no longer accessible to humans or animal thus provides a minimum age for the age of the skeletal material in HN (Fig. 8, 9c). HN was also cut off from OM inputs brought in by bats or floated from cenotes during extreme events; however, the presence of an air dome in HN would still allow calcite raft deposition. Suspension transport of OM could still occur perhaps with extreme events but normal meteoric water flows are low with transport eastward from HN. Thus meteoric flow would transport sediment from Ich Balam and Oasis away from HN. This is seen in our core data, which shows thicker sediment accumulation in cores downstream of Ich Balam. Input from upstream La Concha, which is > 600m away is not a likely contributor of OM sediment. Our radiocarbon ages of OM in the cave reflect that as well, with earlier ages in HN (≈ 9.5 - 11.5 Ka) relative to Ich Balam (≈ 3.8 - 8.1 Ka). As water levels in the cave passages reached ceiling heights, the depo-center would move closer to the open water areas in cenotes. Cave passages leading from Ich Balam and Oasis became further restricted by rising water levels and eventually became fully blocked by ≈ 6 Ka (Fig. 8, 9d).

2.5.4 Comparisons with Green Bay and Walsingham Cave, Bermuda.

Similar core studies conducted in Green Bay Cave in Bermuda show similar depositional patterns as Hoyo Negro (van Hengstum et al., 2011). Twelve cores were collected in a transect through the cave passage from Cliff Pool sinkhole to an opening in Harrington Sound. Most of the cores are at a similar depth of ~19-20 m below SL. Basal ages of calcite rafts show an age that is too young by ~ 500-1000 yrs. for its elevation indicating that there may have been water in the cave before calcite rafts began to form. Ceiling elevation fits better with the radiocarbon dated termination of calcite rafts deposition (Fig. 8; C5 in van Hengstum et al., 2011). Green Bay also exhibits a shifting depo-center for OM sediment which is moving closer to the Cliff pool sinkhole as water level rises. Core one closest to the sinkhole has a radiocarbon age of ~ 3.1 Ka at 10 cm from the core top indicating that OM is being deposited further upslope and in the sinkhole itself with rising water level.

Walsingham cave also shows departure between flooding ages from basal aquatic sediments and sea-level. One core has a basal vadose facies which is overlain by an aquatic sediment facies (carbonate mud with foraminifera; Fig 3 and 4 in van Hengstum et al, in press). The base of the carbonate mud has a radiocarbon age (~ 3 ka cal yrs BP) that is ~ 5 Ka too young for its elevation at ~ 20 mbsl (van Hengstum et al., in press).

2.6 Conclusion

This study inferred the water level history in HN and its connecting tunnels from the age and facies content of cave sediments. Water was continuously present in the bottom of HN at least by 9850 BP (C9) and maybe earlier based on the ledge data, which suggest that water was in the pit by 11 Ka. However, this age may be contaminated by the transport of old wood into the pit. The data matches Holocene sea-level rise of (Medina-Elizalde, 2013; GIA adjusted; Milne and Peros, 2013) indicating sea-level had a strong control on water level in the cave system, but the ledge data suggests short-term water level fluctuations from storms or hurricanes at least during the early Holocene. Blockage of the easiest access points (Ich Balam and Oasis) to HN occurred at ≈ 8.1 Ka due to rising water levels reaching the cave ceiling providing a minimum age for the bone accumulation in the pit.

This study also emphasizes that sedimentation patterns in the cave environment are not controlled by water level alone (i.e. sea-level; van Hengstum et al., 2011). Cave passage morphology including floor and ceiling height with water level, controls sedimentation. As demonstrated here, the availability of airways strongly controlled OM sediment vectors; both surface floatation and bat transport. Likewise, the presence of airways and air domes affected calcite raft deposition. Cave sedimentation is therefore transient in space and time and multiple cores are required to determine a minimum age for chamber and passage flooding.

2.7 Acknowledgements

The authors would like to thank Dr. Todd Kincaid for his insightful review and comments on the original manuscript. We gratefully acknowledge the support of; Global Underwater Explorers, The Mexican Cave Exploration Project (Fred Devos, Chris Le Maillot, S. Meecham, D. Riordan), Cindaq, and the awesome staff at Zero Gravity for dive support and logistics. Ceiling and cave mapping; Alex Alvarez, Roberto Chavez, Onno van Eijk, Ali Perkins, Cameron Russo and all of the volunteers on the Hoyo Negro Project. Underwater photography courtesy of, Roberto Chavez. Laboratory support was greatly appreciated from Mallory Coles and Kate Slamon. Funding was provided by National Sciences and Engineering Research Council of Canada (EGR – Discovery); National Geographic Research and Exploration Grant (DR, JC, ANB, EGR); PADI Grant (SVC).

2.8 References

Anderson, D. G., and J.C. Gillam, 2000. Paleoindian colonization of the Americas: Implications from an examination of physiography, demography, and artifact distribution: American Antiquity, v. 65, no. 1, p. 43-66.

Bard, E., B. Hamelin, R.G. Fairbanks, and A. Zindler, 1990. Calibration of the 14C timescale over the past 30,000 years using mass spectrometric U-Th ages from Barbados Corals: Nature, v. 345, p. 405-410.

Bauer-Gottwein, P., B.R.N. Gondwe, G. Charvet, L.E. Marin, M. Rebolledo-Vieyra, and G. Merediz-Alonso, 2011. Review: The Yucatan Peninsula karst aquifer, Mexico: Hydrogeology Journal, v. 19, p. 507-524.

Beddows, P. A. 2004. Groundwater Hydrology of a Coastal Conduit Carbonate Aquifer: Caribbean Coast of the Yucatan Peninsula, Mexico Unpublished doctoral disertation, University of Bristol.

Blaauw, M., 2010. Methods and code for "classical" age-modelling of radiocarbon sequences: Quaternary Geochronology, v. 5, p. 512-518.

Carrillo-Bastos, A., G.A. Islebe, N. Torrescano-Valle, and N.E. González, 2010, Holocene vegetation and climate history of central Quintana Roo, Yucatan Peninsula, Mexico: Review of Palaeobotany and Palynology, v. 160, p. 189-196.

Chatters, J. C., D.J. Kennett, Y. Asmerom, B.M. Kemp, V. Polyak, A.N. Blank, P.A. Beddows, E. Reinhardt, J. Arroyo-Cabrales, D.A. Bolnick, TR.S. Malhi, B.J. Culleton, P.Luna Erreguerena, D. Rissolo, S. Morell-Hart, and T.W. Stafford Jr., 2014. Late Pleistocene Human Skeleton and mtDNA Link Paleoamericans and Modern Native Americans: Science, v. 344, p. 750-754.

Chatters, J. C., 2000. The recovery and first analysis of an early Holocene human skeleton from Kennewick, Washington: American Antiquity, v. 65, no. 2, p. 291-316.

Coke, J., 1991. Sea-level Curve: Nature, v. 353, no. 5, p. 25.

Collins, S. V., E.G. Reinhardt, Werner, C. L., S. Meacham, F. Devos, and C. LeMaillot, 2015a, Hurricane Ingrid sedimentation in Yax Chen cave system (Ox Bel Ha) Yucatan, Mexico.:Manuscript submitted for publication.

Collins, S. V., Reinhardt, E. G., Devos, F., and LeMaillot, C., 2015b, Late Holocene Mangrove development and onset of sedimentation in Yax Chen cave system (Ox Bel Ha) Yucatan, Mexico.: Manuscript submitted for publication.

Dixon, E. J., 1999. Bones Boats and Bison, New Mexico, Univesity of New Mexico Press.

Esterson, K., 2003. Mixing Corrosion in a Coastal Aquifer, Unpublished Masters of Science: Florida State University, 66 p.

Finch, W. A., 1965. The Karst Landscape of Yucatan, University of Illinois at Urbana-Champaign.

Gabriel, J. J., E.G. Reinhardt, M.C. Peros, D.E. Davidson, P.J. van Hengstum, and P.A. Beddows, 2009. Palaeoenvironmental evolution of Cenote Actun Ha (Carwash) on the Yucatan Peninsula, Mexico and its response to Holocene sea-level rise: Journal of Paleolimnology, v. 42, p. 199-213.

González, A. H., A. Terrazas, W. Stinnesbeck, M.E. Benavente, J. Aviles, C. Rojas, J.M. Padilla, A. Velasquez, E. Acevez, and E. Frey, 2013. The First Humans in the Yucatan Penninsula Found in Drowned Caves: The Days of the Late Pleistocene-Early Holocene in a Changing Tropic, *in* K.E. Graf, C.V. Ketron, and M.R. Waters, eds., Paleoamreican Odyssey: New Mexico, Center fo rthe Study of the First Americans, p. 223-238.

González, A. H., C. Rojas Sandoval, A.Terrazas Mata, M.Benavente Sanvicente, W. Stinnesbeck, J.Aviles O., Magdalena de los Rios, and E. Acevez, 2008. The arrival of humans on the Yucatan Peninsula: evidence from submerged caves in the state of Quintana Roo, Mexico: Current Research in the Pleistocene, v. 25, p. 1-25.

González, L. A., Carpenter, S. J., and Lohmann, K. C., 1992. Inorganic calcite morphology: roles of fluid chemistry and fluid flow: Journal of Sedimentary Petrology, v. 62, p. 382-399.

Gregory, B. R. B., Eduard G. Reinhardt, and J.A. Gifford, submitted. The Influence of Morphology and Sea-Rise on Sinkhole Sedimentation: Evidence From Little Salt Springs, Florida Masters: McMaster University, 26 p.

Hanor, J. S., 1978. Precipitation of beachrock cements: mixing of marine and meteoric waters vs. CO_2 -degassing: Journal of Sedimentary Petrology, v. 48, p. 489-501.

Haug, G. H., K.A. Hughen, D.M. Sigman, L.C. Peterson, and U. Rohl, 2001, Southward Migration of the Intertropical Convergence Zone through the Holocene: Science, v. 293, p. 1304-1308.

Hodell, D. A., M. Brenner, and J.H. Curtis, 2005. Terminal Classic drought in the northern Maya lowlands inferred from multiple sediment cores in Lake Chichancanab (Mexico): Quaternary Science Reviews, v. 24, p. 1413-1427.

Islebe, G. A., H. Hooghiemstra, M. Brenner, J.H. Curtis, and D.A. Hodell, 1996, A Holocene vegetation history from lowland Guatemala: The Holocene, v. 6, p. 265-271.

Jones, B., R.W. Renaut, and M.R. Rosen, 1989. Trigonal dendritic calcite crystals forming from hot spring waters at Waikite, North Island, New Zealand: Journal of Sedimentary Research, v. 70, p. 586-603.

Laprida, C., 2006. Recent ostracods of the Pampas, Buenos Aires, Argentina: ecology and implications paleolimnological: Ameghiniana, v. 43, no. 1, p. 1-27.

Leyden, B. W., M. Brenner, D.A. Hodell, and J.H. Curtis, 1993. Late Pleistocene climate in the Central American lowlands., *in* Swart, P.K. et al., editors, Climate change in continental isotopic records. American Geophysical Union, Washington, DC, 1993, Geophysical Monograph 78: 135-152.

Leyden, B. W., M. Brenner, and B.H. Dahlin, 1998, Cultural and Climatic History of Coba a Lowland Maya City in Quintana Roo, Mexico: Quaternary Research, v. 49, p. 111-122.

Medina-Elizalde, M., 2013. A global compilation of coral sea-level benchmarks: Implications and new challenges: Earth and Planetary Science Letters, no. 362, p. 310-318.

Milne, G. A., and Peros, M., 2013. Data-model comparison of Holocene sea-level change in the circum-Caribbean Region: Global and Planetary Change, v. 107, p. 119-131.

Moore, W. S., 1999. The subterranean estuary: a reaction zone of ground water and sea water: Marine Chemistry, no. 65, p. 111-125.

Morell-Hart, S., 2012. Preliminary Analysis of Macrobotanical samples from Hoyo Negro (TP-M 001.1), Quintana Roo, College of William and Mary.

Neuman, B. R., and Rahbek, M. L., 2007. Modeling The Groundwater Catchment of the Sian Ka'an Reserve, Quintana Roo: National Speleological Society.

Palmer, M. V., Influence of carbon dioxide outgassing rates ans accessory ions on calcium carbonate crystal shapes, *in* Proceedings Geological Society of America, 28th Annual Meeting 1996. Volume 28, p. 48.

Peros, M. C., E.G. Reinhardt, and A.M. Davis, 2007a, A 6000-year record of ecological and hydrological changes from Laguna de la Leche, north coastal Cuba: Quaternary Research, v. 67, p. 69-82.

Quintana Roo Speleological Survey, 2014. List of Long Underwater Caves in Quintana Roo, Mexico: Tulum, Quintana Roo Speleological Survey.

Reimer, P. J., M.G.L. Bard, A. Bayliss, J.W. Beck, P.G. Blackwell, C.B. Ramsey, C.E. Buck, R.L. Edwards, M. Freidrich, P.M. Groots, T.P. Guilderson, H. Haflidason, I. Hajdas, C. Hatté, T.J. Heaton, D.L. Hoffmann, A.G. Hogg, K.A. Hughen, K.F. Kaiser, B. Kromer, S.W. Manning, M. Nui, R.W. Reimer, D.A. Richards, E.M. Scott, J.R. Southon, C.S.M. Turney, and J. van der Plicht, 2013, IntCal13 and Marine13 radiocarbon age calibration curves, 0-50,000 years Cal BP.: Radiocarbon, v. 55, p. 1896-1887.

RStudio (2014). RStudio: Integrated development environment for R (Version 0.98.1062) [Computer software]. Boston, MA. Retrieved Jan 5, 2014. Available from http://www.rstudio.org/

Scott, D. B., and Hermelin, J.O.R., 1993. A device for precision splitting of micropaleontological samples in liquid suspension.: Journal of Paleontology, v. 67, p. 151-154.

Smart, P. L., P.A. Beddows, J. Coke, S. Doerr, S. Smith, and Whitaker, F. F., 2006. Cave Development on the Caribbean coast of the Yucatan Peninsula, Quintana Roo, Mexico, *in* Harmon, R. S. a. C. W., ed., Perspectives on Karst geomorphology, hydrology and geochemistry - A tribute volume to Derek C. Ford and William B. White, Volume 404, Geological Society of America Special Paper, p. 105-128.

Taylor, P. M., and Chafetz, H. S., 2004. Floating Rafts of Calcite Crystals in Cave Pools, Central Texas, USA: Crystal Habit vs. Saturation State: Journal of Sedimentary Research, v. 74, no. 3, p. 328-341.

Taylor, R. E., 2009. Six Decades of Radiocarbon Dating in New World Archaeology: Radiocarbon, v. 51, no. 1, p. 173-212.

Torrescano, N., and Islebe, G. A., 2006, Tropical forest and Mangrove history from southeastern Mexico: a 5000 yr pollen record and implications for sea level rise: Veget Hist Archaeobot, v. 15, p. 191-195.

Toscano, M. A., and Macintyre, I. G., 2003. Corrected western Atlantic sea-level curve for the last 11,000 years based on calibrated ^{14}C dates from Acropora framework and intertidal mangrove peat: Coral Reefs v. 22, p. 257-270.
van Hengstum P.J., J.P. Donnelly, A.W. Kingston, B.E. Williams, D.B. Scott, E.G. Reinhardt, S.N. Little, and W.P. Patterson, in press, Low frequency storminess at Bermuda linked to cooling events in the North Atlantic region.
van Hengstum, P. J., J.P. Donnelly, M.R. Toomey, N.A. Albury, P. Lane, and B. Kakuk, 2013, Heightened hurricane activity on the Little Bahama Bank from 1350 to 1650 AD:Continental Shelf Research, v. 86, p. 103-115.
van Hengstum, P. J., D.A. Richards, B.P. Onac, and J.A. Dorale, 2015, Coastal caves and sinkholes, in Ian Shennan, A.J. Long, and B.J. Horton, eds., Handbook of Sea-Level Research, John Wiley and Sons Ltd.
van Hengstum, P. J., D.B. Scott, D.R. Grocke, and M.A. Charette, 2011. Sea level controls sedimentation and environments in coastal caves and sinkholes: Marine Geology, v. 286, p. 35-50.
van Hengstum, P. J., D.B. Scott, and E.J. Javaux, 2009a. Foraminifera in elevated Bermudian caves provide further evidence for +21 m eustatic sea-level during Marine Isotope Stage 11: Quaternary Science Reviews, v. 28, p. 1850-1860.
van Hengstum, P. J., E.G. Reinhardt, P.A. Beddows, H.P. Schwarcz, and J.J., G., 2009b. Foraminifera and testate amoebae (thecamoebians) in an anchialine cave: Surface distributions from Actun Ha (Carwash) cave system, Mexico: Limnology and Oceanography, v. 54, no. 1, p. 391-396.
van Hengstum, P. J., E.G. Reinhardt, P.A. Beddows, H.P. Schwarcz, R.J. Huang, and J.J. Gabriel, 2008. Thecamoebians (testate amoebae) and foraminifera from three anchialine cenotes in Mexico: low salinity (1.5-4.5 psu) faunal transitions Journal of Foraminiferal Research, v. 38, no. 4, p. 305-317.
van Hengstum, P. J., E.G. Reinhardt, P.A. Beddows, and J.J. Gabriel, 2010. Linkages between Holocene paleoclimate and paleohydrogeology preserved in a Yucatan underwater cave: Quaternary Science Reviews, v. 29, no. 19-20, p. 2788-2798.
Ward, W. C., G. Keller, W. Stinnesbeck, and T. Adatte, 1995. Yucatan subsurfacce stratigraphy: Implications and constraints for the Chicxulub impact: Geology, v. 23, no. 10, p. 873-876.
Weidie, A. E., 1985. Geology of Yucatan Platform: Part 1, 19 p.:
Werner, C., 2007. Double-Diffusive Fingering in Porous Media, Unpublished doctoral dissertation, Florida State University, United States, 114 p.

2.9 Tables

Table 1: Conventional and calibrated radiocarbon ages measured by atomic mass spectrometry from Cenote Ich Balam, Sac Actun Cave, Hoyo Negro and Cenote Oasis, Mexico.

Core / Sample	Location	Sample Depth (meters bmsl)	Depth in Core (cm)	Material dated	Conventional Radiocarbon age (14C yr BP)	δ13C (VPDB)	Laboratory Code	Calibrated yrs BP (2σ confidence interval)
Core 1	Cenote Ich Balam	-11.5	64	Seed	7088 ±31	-21.2	D-AMS 002363	7914-7970
Core 2	Cenote Ich Balam	-8.6	50	Seed	3565 ±30	-34.2	D-AMS 002361	3822-3929
Core 2	Cenote Ich Balam	-8.9	79	Seed	5315 ±30	-32.5	D-AMS 002365	5996-6186
Core 2	Cenote Ich Balam	-9.4	131	Seed	7270 ±40	-26	Beta 333187	8009-8172
Core 3	Cenote Ich Balam	-10.9	8	Seed	5990 ±32	-28.9	D-AMS 002371	6741-6911
Core 3	Cenote Ich Balam	-11.0	22	Seed	6400 ±39	-33.5	D-AMS 002369	7268-7418
Core 3	Cenote Ich Balam	-11.2	38	Seed	6994 ±31	-22.6	D-AMS 002368	7742-7817
Core 4	Cenote Ich Balam	-12.3	77	Seed	7269 ±38	-21.9	D-AMS 002374	8010-8170
Core 5	Cenote Ich Balam	11.7	107	Seed	5909 ±35	-26.9	D-AMS 002373	6658-6797
Core 5	Cenote Ich Balam	11.8	120	Seed	6300 ±40	-24.4	Beta 333188	7163-7310
Core 6	Cenote Ich Balam	-4.9	26	Seed	3510 ±31	-26.4	D-AMS 002372	3698-3865
Core 7	Cave Passage	-11.8	21	Charcoal	9941 ±42	-21.8	D-AMS 003402	11242-11413
Core 9	Pit Core	-42.5	47	Seed1	8630±50	-21.8	Beta 333189	9526-9700
Core 9	Pit Core	-42.5	47	Charcoal	9761±33	-26.5	D-AMS 003403	11162-11240
Core 9	Pit Core	-42.5	47	Seed2	8826±31	-33.8	D-AMS 003404	9731-9954
HN4	Pit Wall	-40.0	n/a	Wood	10467±38	-32.1	D-AMS 003409	12372-12573
HN5	Pit Wall	-41.5	n/a	Wood	9761±38	-29.7	D-AMS 003410	11145-11244
HN6	Pit Wall	-43.0	n/a	Wood	8935±46	-29.4	D-AMS 003412	9912-10103
HN7	Pit Wall	-44.8	n/a	Wood	9793±39	-29.4	D-AMS 003411	11176-11254
HN8	Pit Wall	-46.0	n/a	Wood	9626±36	-31.7	D-AMS 003408	10786-10976
HN9	Pit Wall	-47.6	n/a	Wood	9557±45	-26.9	D-AMS 003407	10918-11087
HN10	Pit Wall	-48.5	n/a	Wood	9416±39	-31.7	D-AMS 003406	10562-10745
HN11	Pit Wall	-49.1	n/a	Seed	8667±31	-32.3	D-AMS 003413	9546-9684
HN12	Pit Wall	-49.4	n/a	Seed	8815±34	-26.6	D-AMS 003405	9696-9949
OAC2	Cenote Oasis	-4.1	66	Wood	4704±29	-24.5	D-AMS 003397	5322-5418
OAC3	Cenote Oasis	-1.2	19	Seed	1090±23	-31.5	D-AMS 003398	956-1058
OAC3	Cenote Oasis	-1.4	40	Seed	2049±23	-27.4	D-AMS 003399	1946-2066
OAC3	Cenote Oasis	-1.6	62	Bulk OM	3129±33	-27.2	D-AMS 003401	3317-3409
OAC3	Cenote Oasis	-1.8	76	Bulk OM	3887±38	-15.7	D-AMS 003400	4230-4420

2.10 Figures

Fig. 1. The location of Cenote Ich Balam, which was used to access Hoyo Negro, on the Yucatan Peninsula, Mexico.

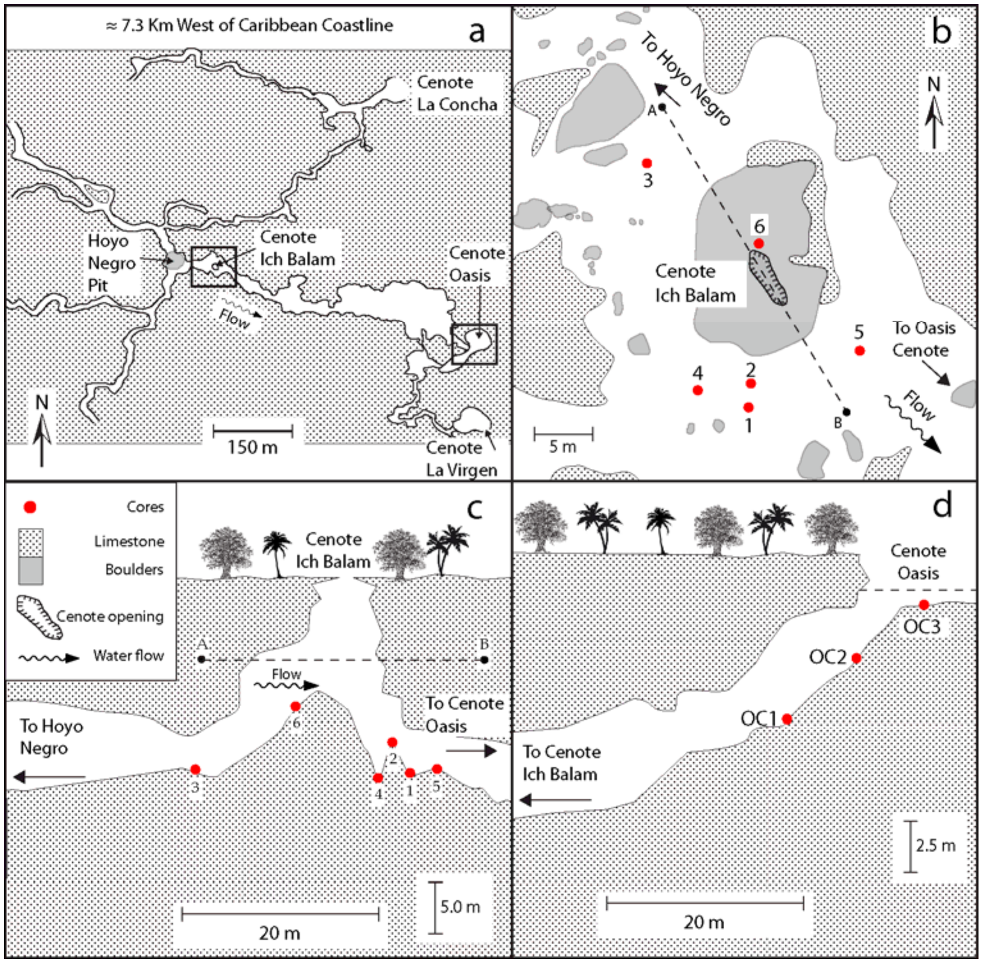

Fig. 2. a) The Outland Cave in the Sac Actun Cave System showing the cave passage geometry and proximity of Cenotes Ich Balam, Oasis, La Concha and La Virgen to Hoyo Negro (HN). b) Plan view of Ich Balam showing the core locations and general cave features. Sediment coverage is focused on the breakdown pile in the central area of the cenote. c, d) Cross-section of core locations in Cenote Oasis and Ich Balam (vertical exaggeration = 4 and 8, respectively).

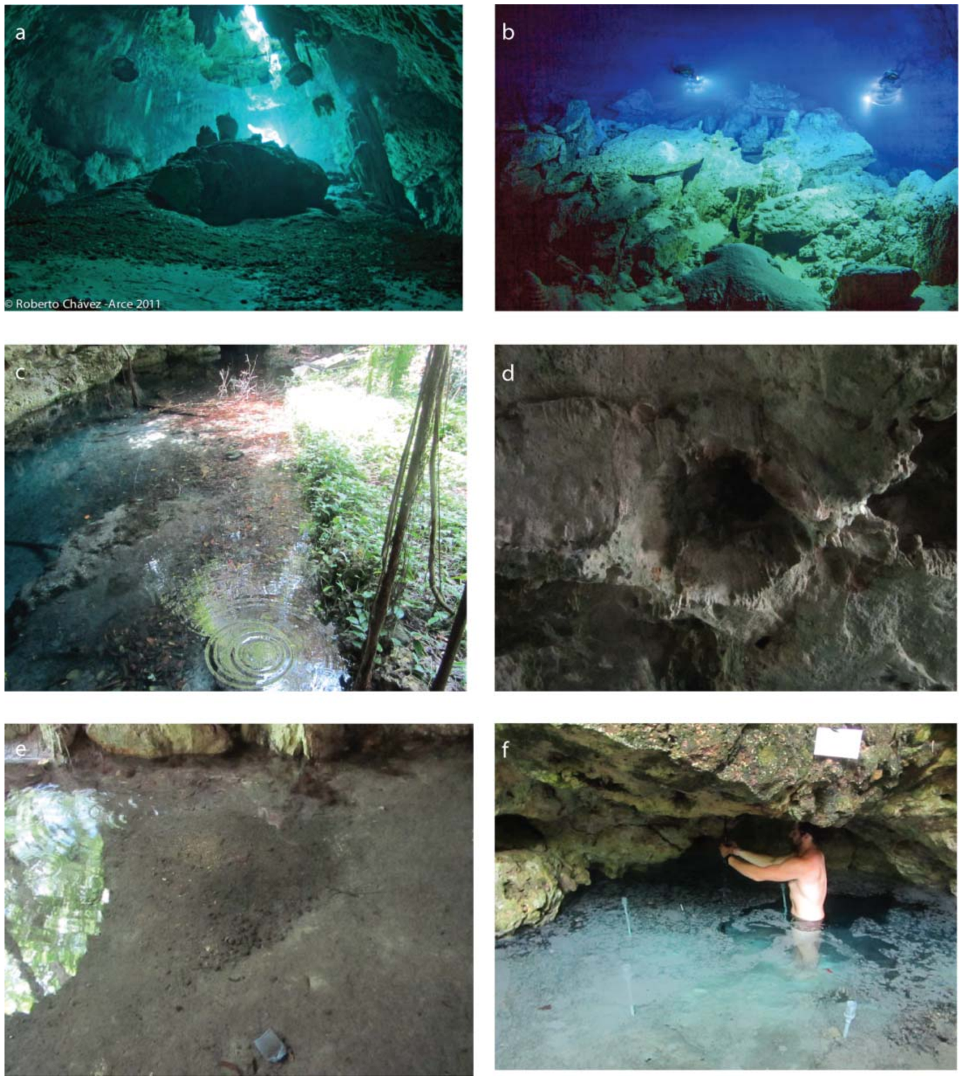

Fig. 3. a) View of Ich Balam looking up from the cave passage leading to HN. Note the size of the opening as well as the concentration of sediment on the central breakdown pile, as well as the calcite rafts forming on the surface waters (white film). b) The bottom of HN showing the limestone boulders from ceiling collapse, the lack of sediment coverage as well as isolated speleothem. Divers are approx. 1.5m in length. c) Cenote Borge showing the relationship between the cavern drip line and OM accumulations. Note the float leaves. d, e) Bat rookery (overhead) and guano pile including seeds and endocarps in Cenote Borge. Guano pile is approx. 40 cm wide and 15 cm high. f) Calcite raft formation in one section of Cenote Borge - note white film on the surface.

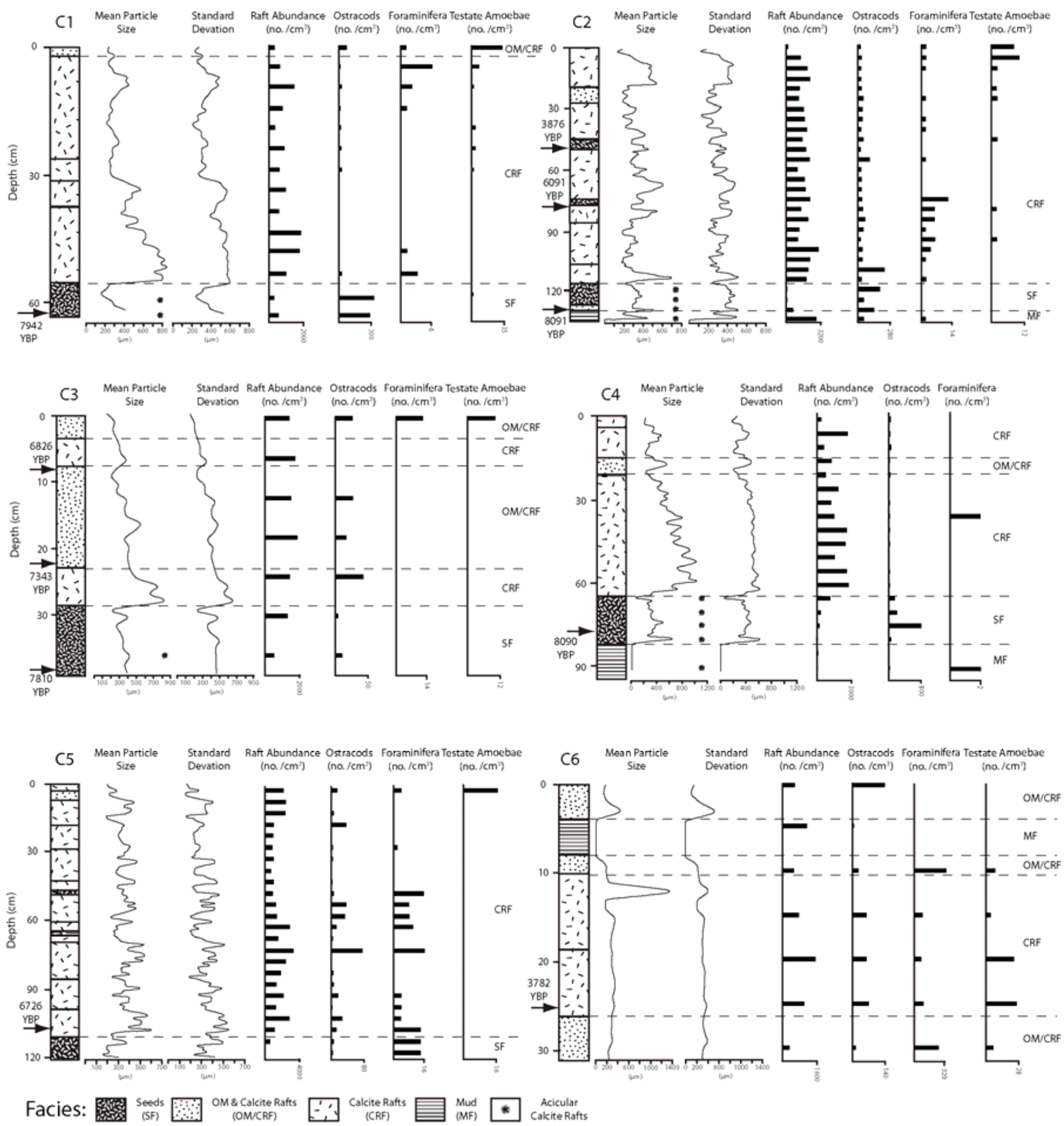

Fig. 4a The core results including mean particle size (μm), standard deviation (μm), calcite raft abundance (no./cm^3), microfossils (no./cm^3), and radiocarbon ages for Cenote Ich Balam (C1-8), HN (C9) and Oasis (OC1-3).

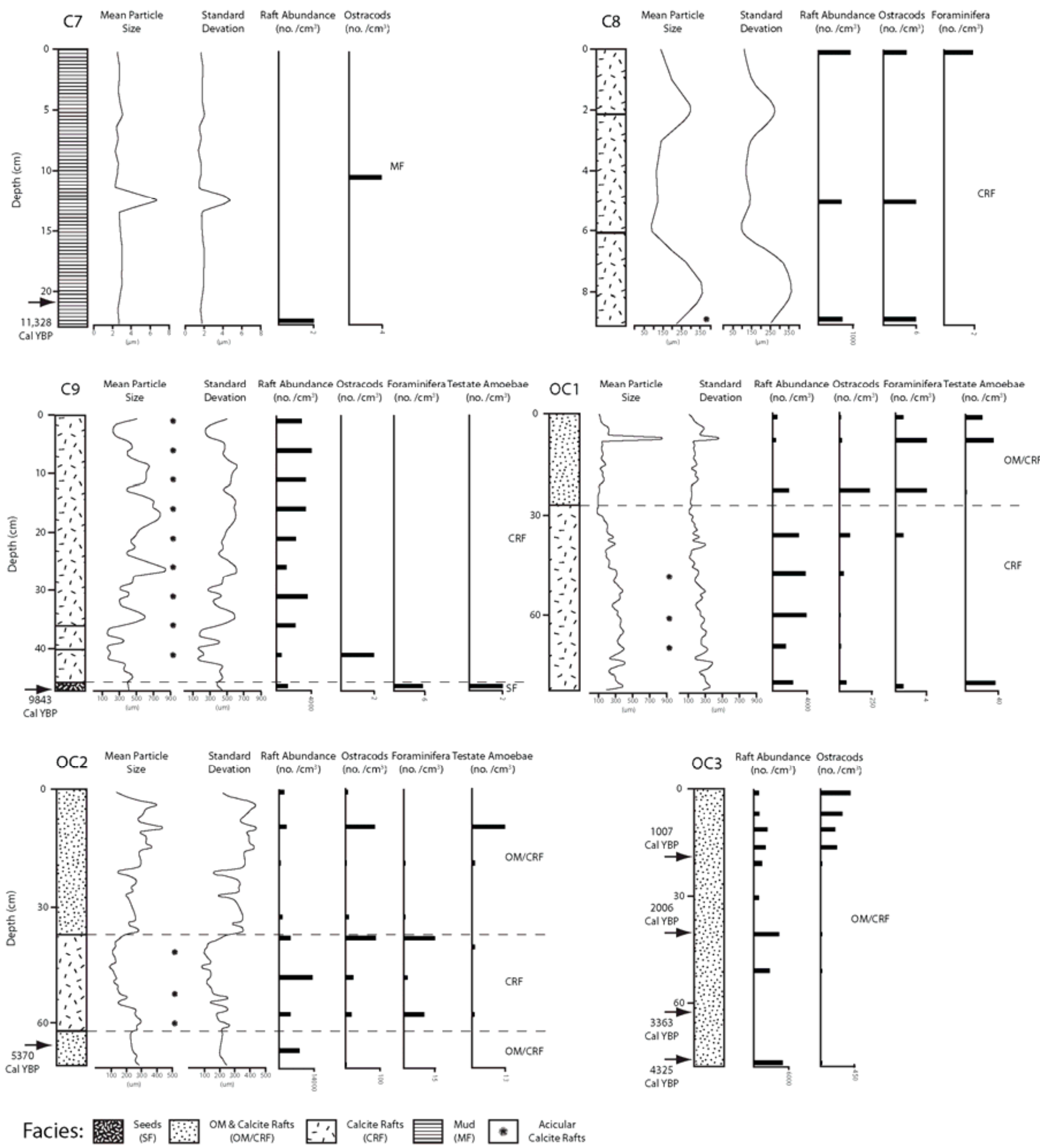

Fig. 4b The core results including mean particle size (μm), standard deviation (μm), calcite raft abundance (no./cm^3), microfossils (no./cm^3), and radiocarbon ages for Cenote Ich Balam (C1-8), HN (C9) and Oasis (OC1-3).

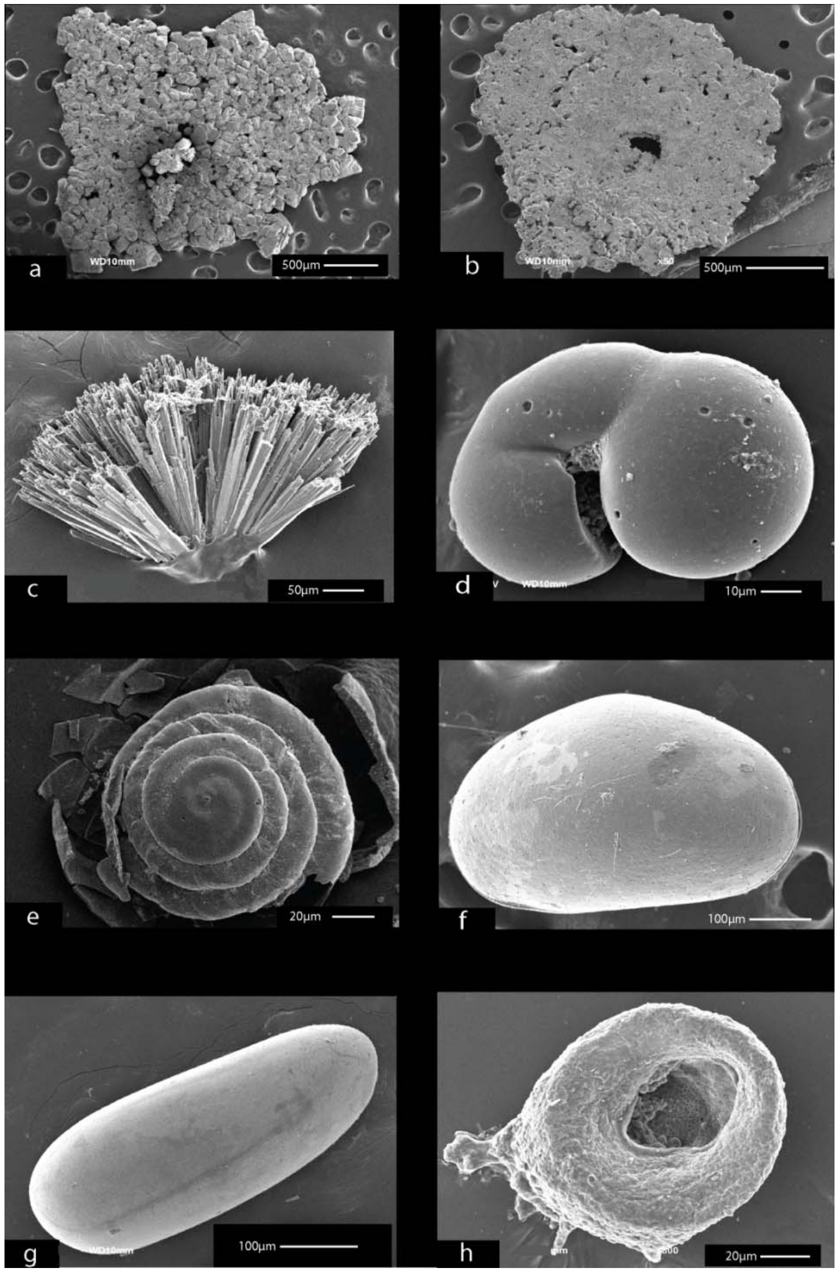

Fig. 5. a) Bottom surface of calcite raft showing irregular crystal terminations and equant calcite grains. b) Top surface of calcite raft showing fused fabric and smooth termination at air-water interface. c) Acicular calcite. d) *Physalidia simplex*. e) *Conicosprillina sp.* f) *Cypridopsis sp.* g) *Darwinula sp.* h) *Centropyxis aculeata*.

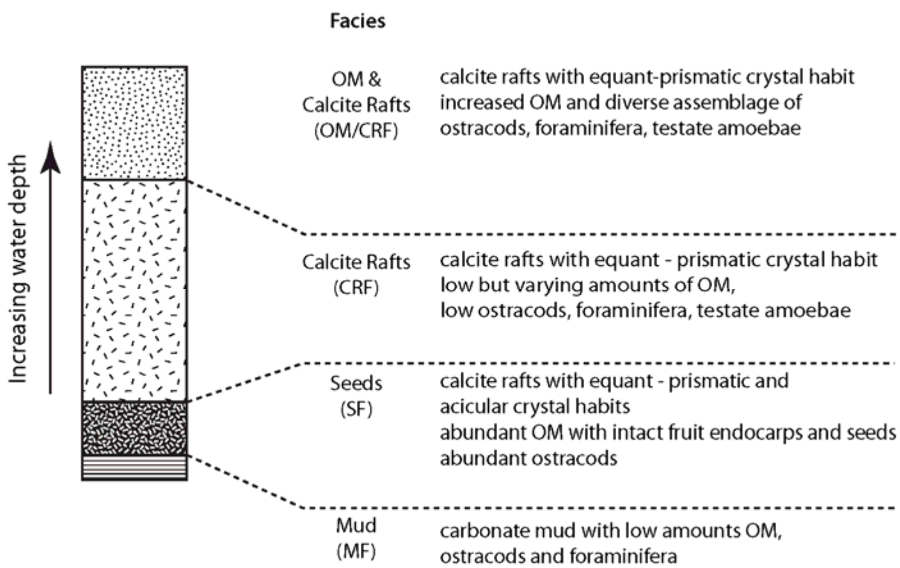

Fig. 6. Typical facies progression found in this study with their characteristics.

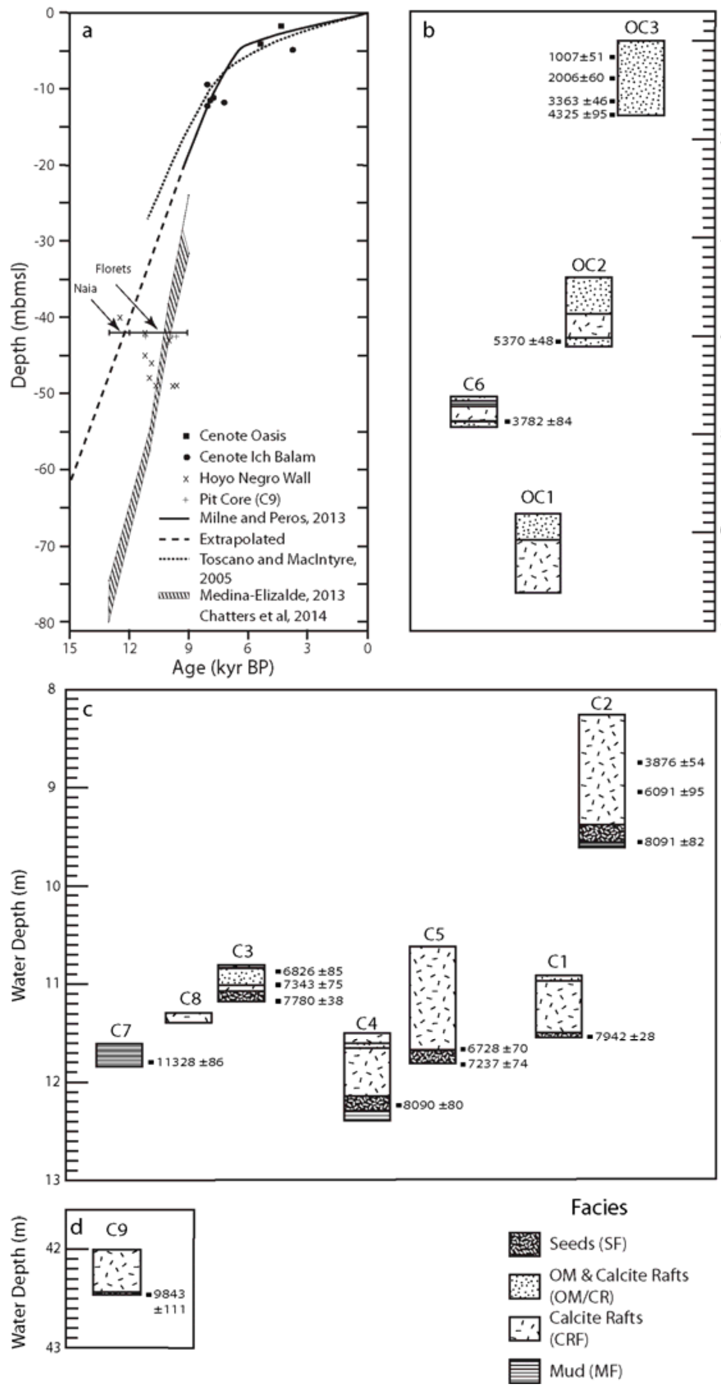

Fig. 7. Facies correlation from Cenotes Oasis (b) Ich Balam (c), and HN (d) showing rising water levels in the cave system and its relationship with Holocene sea-level rise (a). Basal radiocarbon ages on aquatic facies were used to reconstruct water levels.

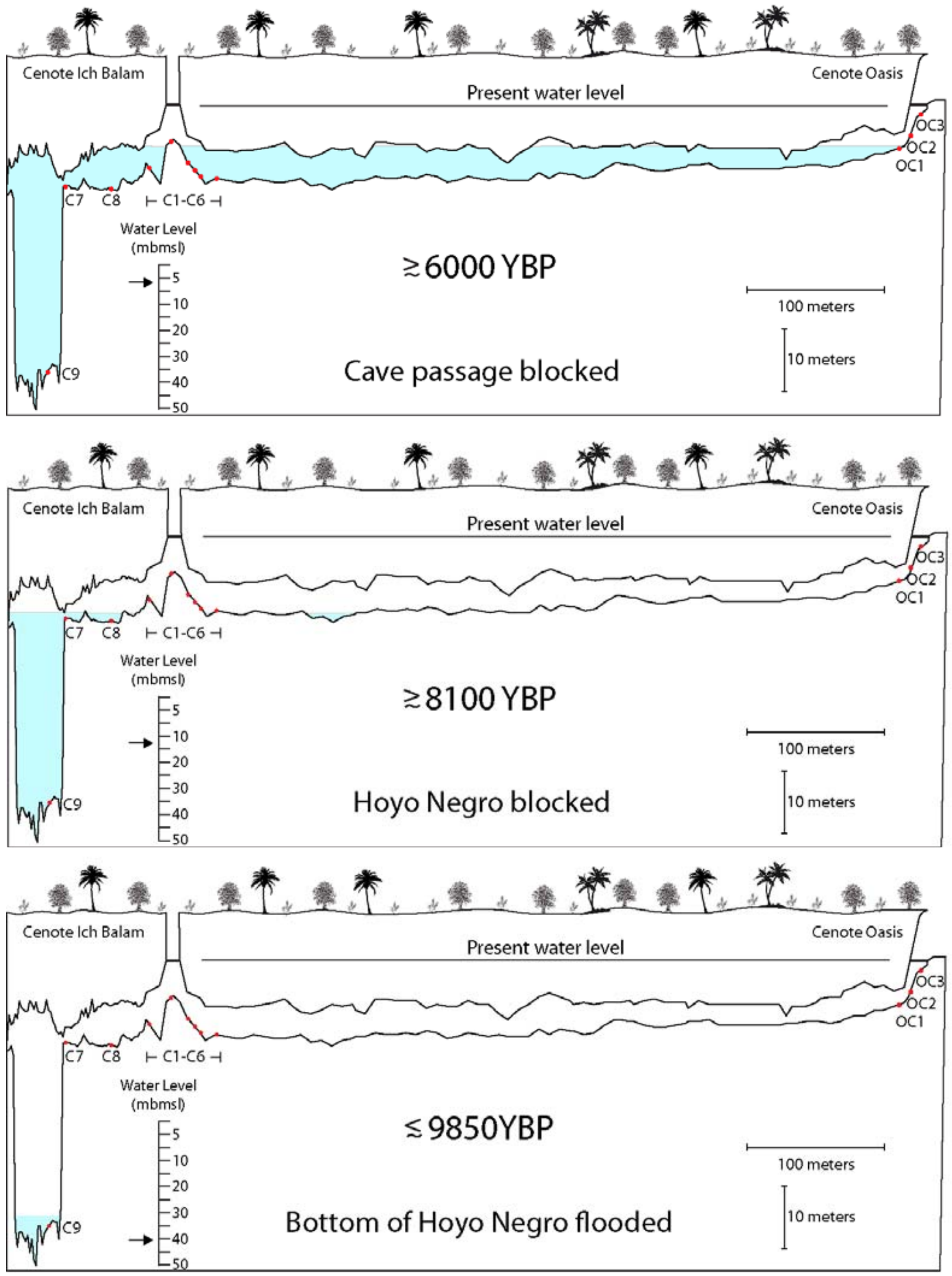

Fig. 8. Flooding history based on facies analysis and its relationship with measured cave ceiling and bottom elevations (vertical exaggeration = 10x).

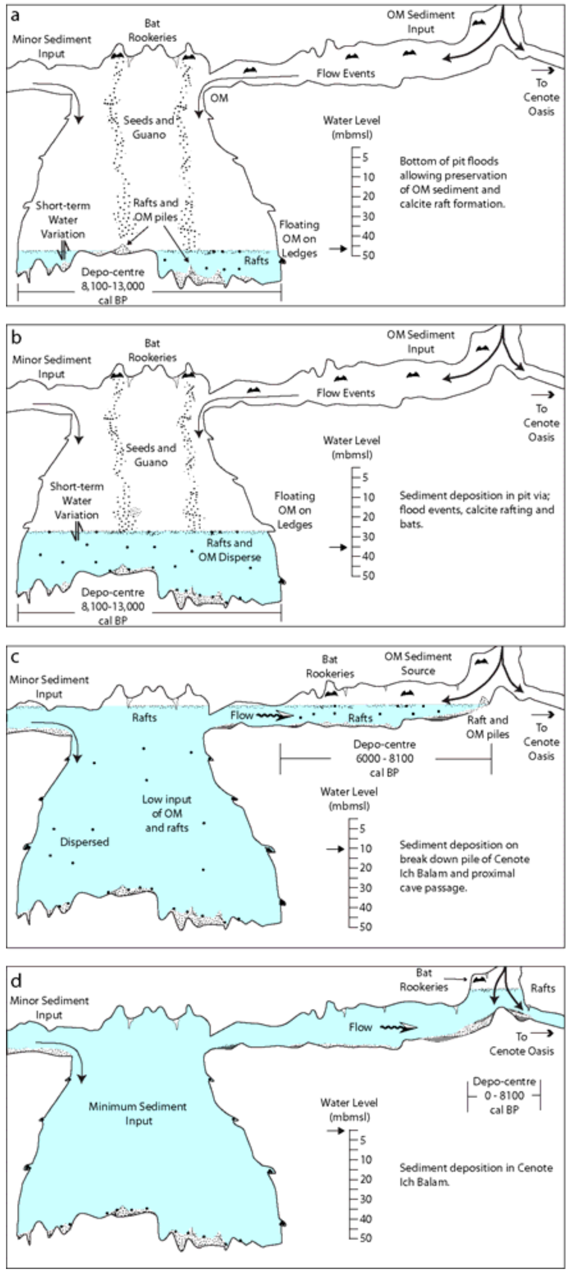

Fig. 9. Factors affecting sedimentation patterns through the flooding history of the cave as recorded in the cores and using cave passage morphology. a) Sediment deposition focused in the pit, subsequent deposits are concentrated under bat rookeries. b) Sedimentary deposits become dispersed with rising water level. c) Pit is isolated from surface. Organic matter sedimentation transitions proximal to cenote Ich Balam. d) Deposition in the pit decreases to minimal levels.

Chapter 3 – Regional response of the coastal aquifer to Hurricane Ingrid and sedimentation flux in the Yax Chen cave system (Ox Bel Ha) Yucatan, Mexico

Palaeogeography, Paleoclimatology, Palaeoecology

Collins S.V.*, Reinhardt E.G., Werner C.L., Devos F., Le Maillot C., Meacham S.

*Corresponding Author – shawnvcollins@icloud.com

Keywords: Cave Sediments; Anchialine; Yucatan; Hurricanes; Sea-level; Mangrove.

3.1 Abstract

Coastal karst aquifers are an important source of potable water which can be affected by external forcing on various temporal and spatial scales (e.g. sea-level) but there is minimal long-term data available to understand their response. Sediment cores and their proxy records have been used in lakes and oceans to assess long-term environmental change, but haven't been extensively applied to anchialine caves where there is less known about the physical, biological and chemical processes affecting sedimentation. Over fifty sediment traps were placed in Yax Chen which is part of the Ox Bel Ha cave system near Tulum, Mexico and four water level sensors were placed in two additional cave systems (Ponderosa, Sac Actun) for comparative water table fluctuations. Data collected over the past three years (2011 - 2013) captured seasonal and spatial sediment flux including the effect of an intense rainfall associated with Hurricane Ingrid (September 18, 2013). The data indicates that sediment deposition was controlled by

cenote size and the presence of mangrove. Areas upstream of Cenote Gemini had negligible sediment accumulation as there were few cenotes and the terrain is dominated by lowland tropical forest, while areas downstream from Cenote Gemini were dominated by mangrove forests and larger cenotes which resulted in higher sediment accumulation rates (0.014 vs. 0.22 mg/cm^2/day). Bi-annual sedimentation rates in 2013 - 2014 were higher in the months after the rainy season (0.2 vs. 0.5 mg/cm^2/day) indicating that cenote productivity was likely controlling sedimentation. Mangrove areas with their peat accumulations occlude the porous karst causing funneling of nutrient rich rainwater into the sunlit cenotes enhancing primary productivity and sedimentation in downstream areas. Hurricane Ingrid had little effect on the yearly sediment rate even though water table fluctuations were high (0.7m) compared to the yearly values (0.3m). This likely is due to water bypassing the cenotes with little residence time to enhance productivity and sedimentation in downstream areas.

3.2 Introduction

The Yucatan Peninsula has a coastal anchialine aquifer and has been used as a potable water source since the first Paleoamericans migrated to the area in the Late Pleistocene/Early Holocene (Back, 1995; González et al., 2008; Rissolo, 2001; Veni, 1984). As in other anchialine settings, freshwater sits on top of a denser saline water mass. Coastal communities around the world rely on this freshwater resource but there is little long-term information on how groundwater masses respond to sea-level or climate change. Most of our understanding comes from short-term instrumental monitoring as there are no developed proxies to examine long-term changes.

Sediment cores from lakes and oceans have been used extensively in the past to understand spatial and temporal trends in climate and oceanography and could be applied to cave sediments to examine long-term paleohydrology (e.g. van Hengstum et al., 2015). However, to take advantage of the information recorded by these proxies, a clear understanding of the sedimentation processes must be established, which currently does not exist.

Cave passages in the Yucatan often have karst windows or cenotes (collapsed caverns) which funnel allochthonous organic matter (OM) sediment into the cave, OM is either generated through primary productivity in the sunlit cenotes or transported from surrounding land areas via meteoric waters, but no primary OM productivity occurs in the dark cave (Benavente et al., 2001; Pohlman et al., 1997; van Hengstum et al., 2010). The input of OM sediment and associated nutrients defines much of the benthic life in the cave and there is little clastic sediment (e.g. aeolian dust, oxides; Gabriel et al., 2009; Steinich and Marin 1997; van Hengstum et al., 2010). Initial paleohydrological research in Actun Ha (Gabriel et al, 2009; van Hengstum et al, 2010) had uncertainties regarding the process of sedimentation (e.g. sources, sedimentation rates, microfossil transport). In this study from Yax Chen cave system (part of Ox Bel Ha cave system), we have mapped the cave passage (bottom, ceiling and sidewall), instrumented the cave (water depth sensors) and deployed sediment traps (n=51) along the length of the cave (2.5 km). For comparative purposes we also instrumented three other locations in two additional cave systems (Xtabay - Ponderosa cave system, Temple of Doom - Sac Actun cave system, Mayan Blue – Ox Bel Ha). The experiment was monitored for three years documenting sources and rates of sediment accumulation, but also the effects of Hurricane Ingrid (Sept 2013; Beven, 2014). This study documented the role of overlying vegetation (i.e. forest vs. mangrove type) and cenote size on sediment accumulation in the cave but also the regional water level response to Hurricane Ingrid. The results provide important background information for further paleoenvironmental studies in Yax Chen but also for cave studies worldwide, as it establishes comparative data for assessing sediment accumulations and their information on sea-level and paleohydrology of the aquifer.

3.2.1 Geologic/Hydrologic Setting

The Yucatan Peninsula (Fig. 1) platform is over 350,000 km^2 of Cenozoic limestone and hosts a largely unconfined coastal aquifer (Weidie, 1985) with low hydraulic gradients of 1-10 cm/km (Beddows, 2004; Gondwe et al., 2010; Marin, 1990; Moore et al., 1992). The area is tectonically stable with stratigraphy that is largely sub-horizontal (Beddows, 2004; Coke, 1991). The limestone has high porosity combined with large cave passages that vary in dimension but often are tens of meters in size (Smart et al., 2006). This high net porosity (14 - 51%) allows immediate penetration of rainwater through the vadose zone to the water table resulting in few lakes or rivers in the Yucatan (Beddows et al., 2007; Stoessell, 1995). Permeability in the subsurface is increased due to mixing zone dissolution and enlargement of fractures, bedding planes and joints (Smart et al., 2006). Repeated glacio-eustatic sea-level cycles have been the primary mechanism for dissolution enlargement of the caves in the Yucatan aquifer

(Back, 1995; Smart et al., 2006). There are over 540 km of subaqueous caves currently documented in the Yucatan Region, but this value increases every year with continued exploration (Beddows, 2004; Quintana Roo Speleological Survey, 2014). During sea-level low-stands, cavern ceiling collapse forms cenotes providing surficial access and allows the inputs of sediment to the cave passages through these karst windows (Chatters et al., 2014; Finch, 1965).

The Yucatan groundwater is density stratified with an upper meteoric lens (ML) which is positioned on top of a Marine Water Mass (MWM; Bauer-Gottwein et al., 2011; Steinich and Marin, 1997). The ML has low salinity (1-7 PSU vs 35 PSU, MWM) and a stable temperature (25.0 ±0.2 °C vs 25.50 - 28.0 °C, MWM) with a thickness ranging from 56 m at the center of the peninsula to 10 m closer to the coast (6 km; Stoessell, 1995; Stoessell and Coke, 2006). The halocline or Mixing Zone (MZ) between the ML and MWM also varies with distance from the coast, becoming deeper and thinner (Smart et al., 2006; Werner, 2007). ML flow increases towards the coast and is ~ 1 cm/s at ~10 km inland but rises to ~12 cm/s at the coastline and is due to coalescing cave passages and decreasing thickness of the ML (Moore et al., 1992).

Numerous environmental factors influence the flow dynamics in the unconfined aquifer. Regional variables such as sea-level fluctuations and differences in hydraulic head driven by climate can alter the circulation patterns in the MWM which can also affect the MZ and ML (Beddows et al., 2007; Whitaker and Smart, 1990). The response of smaller scale changes such as tides and seasonal variability are poorly understood as the effects may be subtle due to the high porosity of the aquifer. The tidal range for the

Caribbean Coast of the Yucatan is 0.3 m and seasonal water table variability has been reported as 0.1 - 0.2 m, although there is no long-term data on yearly or seasonal groundwater level change (Neuman and Rahbek, 2007; Stoessell, 1995). Fluctuations in the water table of the Yucatan aquifer to short term events such as, hurricanes has not been studied in detail, and there is no baseline hydrologic data available to study the effect on the aquifer in the past or with predicted future increases in magnitude or frequency (Bauer-Gottwein et al., 2011; Budd and Vacher, 1991; Maas, 2007; Neuman and Rahbek, 2007).

3.2.2 Climate

Yucatan climate is classified as tropical and precipitation depends strongly on the positioning and seasonal fluctuations of the Intertropical Convergence Zone (ITCZ; Hanstenrath and Greischar, 1993; Hughen et al., 1996; Peterson et al., 1991). The ITCZ moves northward and southward during summer/winter months bringing heavy rains to the Yucatan Peninsula from May to October (780-1426mm; 2012-2013; this study) with lesser amounts in the intervening period (171-651mm; 2012-2013; this study). Meteorological data for the coastal area of Quintana Roo (1998-2008) shows precipitation ranging from 550 – 1500 mm/yr with the majority of it occurring in the summer (Bauer-Gottwein et al., 2011). Rainfall can be temporally and spatially variable, so local and regional precipitation datasets often show inconsistencies (Gondwe et al., 2010; Leyden et al., 1998). Air temperatures can reach 34 °C between May and August (mean ~ 28 °C) and are lower in the winter months (Dec – April; mean ~ 25 °C). Tropical cyclonic activity usually occurs between June and November with the most intense storms during August – September (Boose et al., 2003). Since 1851 over 100 hurricanes with sustained winds of greater than 33 m/s, have affected the Maya lowlands (Boose et al., 2003). The return period for damaging storms over that time interval was ~ 2.4 years (defined as F1+; Boose et al., 2003).

3.2.3 Hurricane Ingrid - 2013

During 2013, two hurricanes developed near the Yucatan Peninsula and made landfall within 24 hours of each other (Beven, 2014; Pasch and Zelinsky, 2014). Hurricane Manuel developed off the Pacific Coast of Mexico and attained hurricane status on September 13, 2013, while Hurricane Ingrid developed in the Gulf of Mexico on September 12, 2013 near Campeche (Fig. 2a; Beven, 2014; Pasch and Zelinsky, 2014). Hurricane Manuel and Ingrid attained Category 1 status but were downgraded to tropical storms when they made landfall (Beven, 2014; Pasch and Zelinsky, 2014). Hurricane Ingrid's track moved W and then NE and attained hurricane status on Sept 14th with peak winds of 140 km/h making landfall south of La Pesca as a tropical storm on Sept 16th (Beven, 2014). Not since 1958 have two tropical cyclones simultaneously hit opposing coasts in one day (Appendini, 2014). The storm combination resulted in 162 billion m^3 of rainfall with a peak of 511 mm in Tuxpan, Veracruz with widespread flooding damaging homes and infrastructure (estimated $5.7 billion USD). Although hurricane Ingrid did not directly impact the eastern coast of the Yucatan, rainfall in this area was very high, showing a ~ 1000 mm precipitation anomaly compared to the past 14 yrs. (1999-2013; Appendini et al., 2014). As a result of this anomalous precipitation event, the study site experienced localized flooding (Fig. 2 b, c). Both Ingrid and Manuel were retired as hurricane names due to their impact.

3.3 Methods

3.3.1 Study Area

Yax Chen is a 2.7 km passage in the world's longest underwater cave, the Ox Bel Ha Cave System located in Quintana Roo, Mexico near the town of Tulum (Fig. 1; 256,909 m; Quintana Roo Speleological Survey, 2014). Yax Chen's main passage has seven cenotes along its length with a combined cenote area of ~ 35,000 m^2 (this study). The cave passage runs sub-perpendicular to the coastline and opens into Cenote Yax Chen which is ~ 300 m from the shoreline (Fig. 3a, b). There are no mapped cave passages that directly connect Yax Chen to the open ocean. Hydrologic connection to the sea is via matrix flow and small scale dissolution features but may be variable as a result of caliche zones at the coast (Perry, et al., 1989). Like many of the cave systems in the Yucatan, flow is low (< 12 cm/sec; Moore et al., 1992) and directed towards the coast. The main cave passage is relatively shallow (~ 10 mbsl) and within the ML, although there are some deeper areas in small pits along the passage (14 mbsl). Several of the side passages that feed into the main passage attain greater depths but they are limited in number and extent (e.g. Little Chen 34 mbsl). The water masses are stratified with a ML from 0 ~ 10.6 mbsl (6 PSU, 25.75 °C), a stepped MZ from 10.6 ~ 15.0 mbsl (6 - 34 PSU, 25.75 - 26.8 °C) and a MWM which begins at ~ 15.0 mbsl (34 PSU, 26.8 °C; Fig. 4). Yax Chen was selected since it transected overlying terrestrial forested areas (i.e. Cenote

Gemini; Fig. 3a) but also downstream mangroves allowing comparisons between sediment inputs from different terrains. Yax Chen also contained numerous cenotes of varying size to investigate the effects of their surface area and productivity on cave sedimentation (Fig. 3b). The cave is also being used for paleohydrological analysis and this study provides baseline data for comparison of the long-term sedimentary records.

3.3.2 Cave Mapping

The cave from Cenotes Gemini to Yax Chen was mapped using the exploration line that generally follows the central passage. The orientation of the passage was mapped using compass bearing and distance between tie-off points on the exploration line. Sidewall measurements from the exploration line (~ every 30m) were recorded using a tape measure obtaining passage widths while bottom and ceiling heights were collected using a digital depth gauge (± 0.1 m) to obtain the overall geometry of the passage. Field measurements were compiled in Arc GIS and spatially corrected with cenote GPS locations (Garmin etrex) and overlain on pansharpened Landsat 7 satellite imagery (15 meter resolution) provided by Google Earth ™. Cenote areas were calculated in Arc GIS using open water exposed on the satellite imagery (Fig. 3b).

3.3.3 Sediment Flux

Sediment flux data was recorded using the trap design of Gardner (1980 a, b) who determined that accurate sediment trap accumulation was controlled by container shape and fluid velocity rather than simply gravity settling of sediment. He found that trap proportions for fine grained sediment (<63 μm) with low flow velocities (< 9 cm/s) should have a height/width ratio ~ 2-3, and that a cylindrical shape prevented resuspension of sediment. The traps used in Yax Chen were constructed with PVC central vacuum tubing with a height of 13.7 cm and diam. of 5.08 cm (height/width = 2.7; Fig. 5a) which were sealed at the bottom with a cap. PVC water pipe (diam. = 2.5 cm) was used as "stakes" to anchor the traps to the bottom. A threaded pipe connector (female) was attached to the bottom of the trap with the opposing male end attached to the water pipe. This allowed the traps to be replaced underwater at annual and bi-annual intervals. Divers attached a top cap, which was secured with a small plastic bag and electrical tie-wrap, then the trap was removed and the new one installed. During initial deployment, the PVC "stake" was pushed into the sediment until refusal, and then cut at ~ 30 cm above the sediment surface using a saw (Fig. 5b). The numbered sediment trap was attached to the stake with a top cap installed and removed once disturbed sediment (if any) had settled.

In May of 2011, a total of 21 traps at seven locations were installed using self-contained breathing apparatus (SCUBA) equipment. Placement of the traps was designed to document the downstream effects of cenote size but also record the effects of overlying vegetation - namely mangrove vs. terrestrial areas. At each location, three traps were installed to transect the width of the cave and placed in open areas avoiding fluid hydraulic jumps with flow obstructions. Additional traps were added as the study progressed to increase spatial resolution with a total of 51 traps at 17 locations covering the 2.7 km of cave passage (Fig. 3b). Sediment traps were collected on a yearly basis in May (2011/12, 2012/13) but were collected bi-annually in 2013/14 (Dec and May) to capture the sedimentation effects of Hurricane Ingrid.

Trap samples were filtered and sediment weighed after drying in an oven at 30°C for 48 hours. The flux and bulk density were calculated for each sample using:

$$Flux = \frac{Ws}{Ta * Di} \qquad\qquad Bd = \frac{Md}{Sv}$$

Where:

Ws = Dry weight of the sediment (mg)

Ta = Area of the trap (20.27 cm^2)

Di = Days trap was deployed (d)

Bd = Bulk density g/cm^3

Md = Mass of dried sediment (g)

Sv = Total sediment volume (cm^3)

Uncertainty on the calculated flux values was assumed to be consistent with Gardner (1980b) who conducted experiments (e.g. water velocity, sediment concentration, etc.) with similar H/W ratio traps (2.3 vs 2.7) and found a ± 17% error on the results.

Organic carbon content was measured using loss on ignition (LOI) following the procedure of Heiri et al., (2001). Approximately 1.25 ml of sediment was dried at 60 °C for 24-48 hours. Samples were weighed (uncertainty on mass ±0.0001g) and combusted in a muffle furnace for 4 hours at 550 °C, cooled in a desiccator and reweighed. Results from each transect (3 traps) were averaged to provide a mean flux (mg/cm2/day) and organic carbon content (LOI %) per station.

3.3.4 Mangrove Detection

Meacham (2012) used the spectral signature of mangrove trees to produce an overall map of mangrove distribution in the Municipality of Tulum. The results classified mangrove type using the physiognomic classification of Lugo and Snedaker (1974). Utilizing the spectral signature of mangrove leaves and other vegetation, Meacham (2012) discriminated fringe and dwarf classes of mangrove using Landsat 5 Thematic Mapper imagery (Fig. 3a, b). The resulting vector map identified dwarf versus fringe mangrove stands and had an 88% accuracy delineating over 19,000 ha of mangrove forest in the municipality. Fringe mangroves tend to dominate in areas of protected shorelines where the elevations are higher than mean high tides while dwarf mangroves are generally found in flat coastal areas (Lugo and Snedaker, 1974). The most characteristic feature of the dwarf mangrove is the limited vertical extent of the trees <1.5m (Lugo and Snedaker, 1974). The physiognomic classification system is not species specific, however, Mexico is limited to three types of mangroves including: *Rhizophora mangle* (red mangrove), *Avicennia germinans* (Black mangrove), *Laguncularia racemosa* (White mangrove) (Lopez Fuerte et al., 2010).

3.3.5 Kriging of Flux Data

Kriging was used to extrapolate the flux data to other areas of Yax Chen to document trends. Kriging is based on the assumption that there is some autocorrelation between values at locations nearest to each other while autocorrelation decreases as you move further away from a given point (Matheron, 1963). This spatial variance in the measured variable (in this case sediment flux) is plotted on a semivariogram. Once the data has been plotted, a model is fitted to the semivariogram to determine coefficients to calculate the values at unmeasured locations and determine the error of the estimate.

Assessment of the data showed that the sediment flux dataset consisted of a small number of points, were slightly non-stationary and non-parametric. Based on these factors, Empirical Bayesian Kriging (EBK) is the most appropriate Kriging method for this dataset. Kriging the data produces measured standard errors of the predictions that are more accurate as the uncertainties of the semivariogram are included in the calculation.

3.3.6 Weather Data

Daily weather data was collected from the closest weather station to Cenote Yax Chen, which is in the Sian Ka'an Biosphere Reserve (4 km south; Servicio Meteorológico Nacional, 2014). Weather data was collected in 10 min. intervals from March 3, 2012 - May 13, 2014. Precipitation (mm/day) and air temperature (°C) was aggregated/averaged into daily values with the temperature data smoothed using a 10 point boxcar filter.

3.3.7 Water Level Data

Water level data was collected using ReefNet Sensus Ultra dive loggers which continuously measured depth (± 1.3 cm) at 30 min intervals. The Yax Chen sensor was fixed mid-point in the cave in the ML at the Little Chen monitoring station (Fig. 3b). Due to the minimal hydraulic gradient of the Yucatan aquifer (7-10 mm/km) and the proximity of the study area to the coast, the top of the water table was assumed to be slightly above or equal to mean sea-level (Morin, 1990). The water table fluctuations are relative changes from the averaged calculated position of the sensors. The data shows variations in the water table above the sensor and are reported in this study as meters below sea-level (mbsl).

Three other caves in two additional systems were also instrumented for comparative purposes, two are from nearby locations including Mayan Blue (Ox Bel Ha) and Temple of Doom (Sac Actun) while Xtabay (Ponderosa) is located ~ 40 km northeast of Yax Chen (Fig. 1). These sensors were also fixed at different points in their respective caves. All water level data was averaged to daily depths.

3.4 Results

3.4.1 Sediment Flux and LOI

The sediment composition and the flux data (Fig. 6) both showed transitions at Station 8 upstream of the L-shaped Cenote and also upstream of Cenote Gemini (Station 1). The dominant composition of trap sediment was fine (mud-sized) brown OM flocs (gyttja like; stns. 3-17 station) but some stations contained light tan carbonate mud (esp. stn. 1). The data showed that stations in the upper region of the cave (stns. 2-8) had ~ 2 x lower LOI (21 ± 5 % vs 43 ± 3 %; Table 1) and 3 x lower sediment flux values (0.11 $mg/cm^2/day$) compared with downstream stations (stns. 13-17; 0.32 $mg/cm^2/day$). The OM content (LOI %) in these two areas did not vary much from year to year (< 5 %), however the sediment flux data did show some variability. The average sediment flux in the upper region varied by ± 0.05 $mg/cm^2/day$ (1σ) over the three years monitored, whereas the downstream areas varied by ± 0.15 $mg/cm^2/day$ (1σ). Two stations in the downstream area showed elevated rates in 2011/12 (stns. 13, 14) relative to the other two years and there were some small variations in flux in the upper region but they were small (e.g. stns. 7 and 8). Station 1 is unique in that it is upstream of Cenote Gemini where there is marked change with sediment accumulation and had very low flux values of 0.014 mg/cm^2/day and low OM at 6% (LOI) (Fig. 6).

Mean sediment flux rates correlated well with the corresponding upstream cenote areas (m^2) showing a direct relationship (r^2= 0.70; Fig. 7a; Table 2). The data from station 2 had a higher than usual flux relative to cenote area (Gemini), however this value is only based on measurements from one station. LOI results also showed a strong direct relationship with the areas of corresponding upstream cenotes (r^2= 0.99; Fig.7b; Table 2).

Yearly sediment flux was not significantly different with Hurricane Ingrid in 2013/14, although LOI values in the upper region of the cave had higher values (~ 5%; Fig. 6). However, the bi-annual collection of sediment traps showed that sediment flux was higher in the months after the hurricane in September 2013 (Fig. 8). Sediment flux was low during May to December 2013, but increased significantly from December to May 2013/14. Sediment flux in upper region of the cave had relatively constant sedimentation throughout the year (~ 0.06 to 0.2 mg/cm^2/day) while downstream areas showed more contrast. From May - December (2013) sedimentation was lower (stns. 13-17; ~ 0.1 to 0.2 mg/cm^2/day) in the downstream area but increased during December – May (stns. 9-17; 2013/14; ~ 0.2 to 0.5 mg/cm^2/day). LOI results showed slight increases in the upstream area (<5%) but overall the proportion of OM did not change significantly.

The kriging results decrease in predictability with increased distance from measured points. A standard error map was generated for each surface with 2011/12 showing the greatest standard errors ranging from 0.08 – 0.2 $mg/cm^2/day$. Error estimates generated for data in 2012/13 and 2013/14 showed the same range of errors from 0.03 - 0.06 $mg/cm^2/day$. The model showed the highest level of error in the zone between cenotes L-shaped and Tarpon 1 which correlated to zones of no measured values until December of 2013.

Kriging yearly sediment flux data demonstrated spatially consistent sedimentation rates from year to year (Fig. 9). The extrapolated surface demonstrated that for all years, sediment deposition was elevated for downstream areas with the highest levels of sedimentation between Cenotes Tarpon 1 and Yax Chen. The seasonal results show relatively uniform low sedimentation in all parts of the cave during the summer/fall (Fig. 10a; May - Dec, 2013) vs higher sedimentation in downstream areas during the winter/spring (Fig. 10b; Dec- May 2013/14).

3.4.2 Mangrove extent

Regional mangrove location tend to be shore parallel, narrowing at the north and becoming wider in the south connecting to the Sian Ka'an Biosphere lagoon system (Fig 3a). The distribution of fringe and dwarf mangrove likely follows an elevational trend with the fringe mangrove in deeper areas surrounding the cenotes while the dwarf mangrove is located at higher elevations in the karst terrain (Fig. 3a). In the immediate area overlying the Yax Chen cave system, the transition from mangrove to terrestrial forested areas is approximately 100 m upstream from Cenote ISOD 2. The mangrove is mostly dwarf, but there is fringe mangrove on the southern margins of the L-shaped, Tarpon 1 and Tarpon 2 cenotes that continues in a SE trend to the coast which may be in a trough at a lower elevation (~ 200 - 400m wide; SE trend; Fig. 3a).

3.4.3 Weather and Water Data

Aggregated daily weather data from March 2012 – May 2014 showed seasonal variations (winter/summer; Fig. 11). Higher rainfalls occurred from April to October 2012 and then in May to December 2013. Total annual rainfall for May 2012 - May 2013 was 1026 mm and for May 2013 - May 2014 it was nearly twice the amount at 2031mm. Over the course of study, the area had five larger than normal precipitation events with daily rainfall exceeding 90 mm. Precipitation on September 18, 2013 as a result of Hurricane Ingrid exceeded 320 mm for a single 24 hour period. Air temperature showed seasonal trends ($\bar{u}$ = 26.7 ± 2.3° C) punctuated by smaller scale weather related fluctuations. During the five major storm events the air temperature decreased (~ 1.9 °C) before and during the storm and rebounded after the event.

The average daily water table depth at the Little Chen Monitoring Station in Yax Chen was 7.58 mbsl varying by ~ 1 m from March 2012 to May 2014 (Fig.11). The water level data showed an overall broad response to seasonal variations with an increase during the rainy season (~ 7.65 - 7.75 mbsl) and depressed levels during the dry season (~ 7.45 - 7.50 mbsl) with a ~ 30 cm variation over seasonal cycles. The data also showed large precipitations events caused rapid short term water level rise (days to weeks) superimposed on the broad seasonal trend. The largest water level change occurred with Hurricane Ingrid on September 18, 2013. Water table level increased by ~70 cm from 7.74 mbsl on September 12th to 8.42 mbsl on September 18th and decreased to pre-storm level (7.73 mbsl) ~ 13 days after the storm (Fig. 11). The months prior to Hurricane Ingrid (August - September) were also unusual compared to the same time period in 2012. In 2013, the frequency and amount of rainfall was higher compared to the same period in 2012 (14 days, 141mm vs. 30 days, 878 mm).

Similar seasonal patterns including large rainfall events were seen in the daily averaged water table data from the other cave systems, although the magnitude of water level change does vary (Fig. 11). Hurricane Ingrid created larger magnitude increases in the water table in caves near-by including; Mayan Blue (Ox Be Ha) and Temple of Doom (Sac Actun) caves which were ~ 1.5 m higher than the pre-storm water level and returned to pre-storm levels ~ 12 days after the hurricane. In comparison, the water table, at Xtabay (Ponderosa) which is ~ 40 km northeast of Yax Chen, did not rise as high, only reaching 0.3 m (daily average) and the water table returned to pre-storm levels in 16 days. Not all the water table increases corresponded with precipitation events (e.g. August 1, 2012) which may be due to spatial patterns of rainfall which may have not been as great at the Sian Ka'an Reserve.

3.5 Discussion

3.5.1 Precipitation and hydrologic response

Water table data showed broad seasonal variation (rise and fall), as well as short-term events from storm induced precipitation. The amount of water table rise depended on the amount of precipitation and its timing with respect to the rainy or dry seasons but also likely the degree of connectivity between the cave and the ocean (i.e. the number and size of discharge vents). Seasonal fluctuations in both 2012 and 2013 showed a stepwise water table rise (rapid rise and then a moderate fall) at the start of the rainy season which elevated the water table spanning the summer and fall seasons (Fig. 11). In Yax Chen during 2012, the elevated water table (~7.65 mbsl) lasted from July to October, while in 2013 it lasted from May to December with greater magnitude and more variability, mostly 7.65 - 7.75 mbsl but also reaching 8.42 mbsl with Hurricane Ingrid in September 2013. Overall, the rainy season in 2013 was more sustained, lasting until December vs October in 2012. On average water levels dropped over ~ 2 weeks following precipitation events.

A sustained higher water table during the rainy season is likely due to delays in groundwater drainage through the karst (i.e. epikarstic zone) to the ocean (Bauer-Gottwein et al., 2011; Neuman and Rahbek, 2007). Based on the similarity of water table response in unconnected cave systems it appears to be a regional phenomenon (Fig. 11), however, short-term rainfall events and their localized elevated water tables were more variable. Hurricane Ingrid was the most extreme of the recorded events with very high rainfalls over a short time period which amplified minor differences between the cave systems. The water table in Yax Chen rose by ~ 0.75 m during the hurricane and was considerably higher in nearby cave systems (e.g. ~ 1.5m in Temple of Doom, Mayan Blue; Fig. 11), but also much lower in Xtabay (~ 0.3m) which is ~ 40 km to the northeast. The seasonal water table response in all the caves is very similar (approx. ± 6 cm), so the difference with the hurricane maybe due to spatial patterns of rainfall and/or differences in hydraulic conductivity on a local scale (also coastal plugging; Perry et al., 1989; Stanley and Warne, 1994).

There are important differences in the pathway for rainwater between cave systems that have overlying mangrove vs. forested areas (Fig. 12). Rainfall in Yax Chen with its extensive mangrove would retain water through the rainy season, versus forested areas where rainfall would immediately percolate through thin soils to the vadose zone (Bauer-Gottwein et al., 2011; Neuman and Rahbek, 2007; Wolanski and Gardner, 1981). The underlying mangrove sediments would effectively prevent or slow penetration of surface water to the phreatic zone. The effect of mangroves appears to be an increase in runoff at the expense of recharge. Wolanski and Gardner (1981) found that the density of mangrove roots created water gradients on the order of 1 m per 1000 m in a wetland in Nakawa Gawa, Japan lowering current velocities and increasing the residence time of the meteoric water in the wetland. In Yax Chen, precipitation falling on the mangrove would potentially create a reservoir of water which would drain overland into the cenotes over the rainy season. Most ponded mangrove water would drain through the cenotes but may also follow smaller pathways in the mangrove sediment through crab burrows or desiccation cracks which may have formed during the previous dry season when the water table was low (Ovalle et al., 1990; Wattayakorn et al., 1990; Wolanski and Gardner, 1981). Areas in forested terrain that do not have mangrove would not experience this focused drainage through the cenotes, as rainwater would percolate directly through the karsted limestone to the phreatic zone and immediately flow to the coast. In areas with extensive mangrove, water could be stored in the mangrove before draining and become nutrient rich from biological activity and weathering (Lopez Fuerte et al., 2010; Mazda et al., 1990). This would be in contrast with forested areas where rainwater would not inherit these properties but simply percolate to the water table. This process appears to be important for sedimentation patterns in the caves explaining differences between forested and mangrove areas in Yax Chen.

3.5.2 Controls on sedimentation patterns in Yax Chen

The pattern of sediment flux in the cave passages was consistent over the three years of study (2011-2014) showing only minor deviations. The data discerned three areas in the cave associated with low, moderate and high sediment flux patterns which corresponded with the presence of overlying mangrove as well as cenote size.

3.5.3 Low Sediment Flux

The low sediment flux area was upstream of Cenote Gemini where flux was very low (0.02 mg/cm^2/day; stn. 1; Figs. 6, 8, 9 and10). The sedimentation dropped to negligible amounts upstream of Gemini due to the prevalence of terrestrial forested areas dominated with little low-lying topography. Further upstream areas were not measured, but observations found little to no sedimentation in the cave other than in the immediate vicinity of cenotes (e.g. Actun Ha cave systems). Large OM sediment from forest litter is predominately deposited in close proximity to the cenotes as found in the inland cave of Hoyo Negro (Collins et al., 2015a). Sediment flux from primary productivity in the sunlit cenotes would be limited as cenote areas tend to be smaller in the upstream areas of the cave system and rainfall predominately percolates through the limestone with little overland flow towards the cenote openings (see below). There also seems to be little variation in seasonal flux patterns (e.g. 2012/2013 data; Fig. 6) in the upstream area indicating rainfall events have little impact. These areas do not seem to retain OM sediment accumulations over any extended period of time, if fine OM particulate is deposited; it seems to decay quickly leaving no record.

3.5.4 Moderate to High Sediment Flux

Areas with moderate to high sediment flux were dominated by the presence of overlying mangrove but also importantly larger and more numerous cenotes. Moderate sediment flux was found from Cenote Gemini to the L-shaped Cenote (0.11 $mg/cm^2/day$; stns. 2-8) where dwarf mangrove tended to dominate while areas from L-shaped to Cenote Yax Chen (0.32 $mg/cm^2/day$; stns. 13-17) had high flux with more fringe mangrove. More importantly, the cenote area showed that upstream of L-shaped Cenote ($8954 \pm 90\ m^2$) surface area was 2.5 times smaller than the downstream portions of the cave ($22448 \pm 240\ m^2$). This relationship not only corresponded with average sediment flux, which was three times as large in downstream areas, but also with OM content which was twice as abundant. There is also a direct relationship between upstream cenote size, sediment flux and OM content (LOI %; Fig. 7).

Inputs of particulate OM (POM) into the cave would be sourced from the extensive prop roots of lower-lying fringing mangrove. Fringe mangrove tend to be located in areas with slightly deeper water compared to the dwarf mangrove stands which would have less direct connection with the cenote water body (Fig. 12). Inputs of POM but also dissolved organic matter (DOM) and associated nutrients are likely greater in the fringe mangrove, as was evidenced by the data, however, cenote primary productivity would also be influenced by this input, which would be greater with larger cenote size. As discussed with the water table data, ponding of water in the mangrove through precipitation and water table rise would drain mainly through the cenote openings versus the terrestrial areas which would infiltrate directly through the karst. The retention of water in the mangrove during the rainy season would allow nutrient build-up with release into the cenotes during the start of the dry season. Larger sunlit cenote areas would have increased primary productivity but also would have higher inputs of nutrients with the larger surrounding cenote circumferences. At the end of the rainy season, when the water table drops, the nutrients stored in the mangrove waters are fully released into the cenotes. Monthly sediment flux data was not collected but this is likely occurring during and immediately after the stored water has drained causing a slightly increased flow and transport of sediment into the cave. The areas in Yax Chen with no mangrove are largely nutrient poor and do not respond to these changes in primary productivity and as a result this area is subject to lower sediment flux and minimal OM (LOI) content (i.e. upstream of Cenote Gemini).

There does not appear to be an effect on sedimentation in Yax Chen as a result of the morphology of the cave as there isn’t a significant difference in height or width of the cave passage along the measured length. There are some deeper pits in the cave passage but these are limited in number and extent. Localized patterns in sediment flux due to cave morphology are likely present on a smaller scale (e.g. stn. 3 where the cave narrows and abruptly changes direction), but the trap spacing and density was not high enough to confidently determine these localized patterns.

3.5.5 Hurricane Ingrid

Sedimentation data showed that the effects of Hurricane Ingrid on sediment flux were minimal in Yax Chen as yearly flux rates and OM content did not vary considerably from non-hurricane years. There are some minor increases in the upstream areas but their magnitude varied from station to station. The lack of response is likely due to rapid rise and then fall of the water table. Similar flashy water table fluctuations were observed in Wakulla Springs Florida in 2005 with Hurricane Dennis as the water table rose and fell by ~1.5 meters in 5 days (Loper et al, 2008). Water dropped by ~70 cm in two weeks after the hurricane versus ~20-30 cm at the end of the rainy season which drained over six weeks. The rapid flushing of nutrient rich mangrove water likely by-passed the cenotes entering the dark cave passages with no light and thus little primary productivity. Draining after the wet season would be more gradual (i.e. leaky) allowing higher residence times in the cenotes and higher primary productivity. It doesn't appear that there is much POM transported from the mangroves during or after the hurricane, there were no unusually large OM fragments in the traps during the 2013/2014 season and there was no significant difference in sediment flux or OM contents (LOI). The lack of response suggests that most mangrove POM is deposited in the cenotes or is retained in the mangroves by baffling due to the extensive prop roots (Lugo and Snedaker, 1974).

It doesn't appear that flows in the cave created much if any resuspension of sediment. Flow meters were not employed in this study, but observations made while diving Yax Chen after the hurricane found increased flows but no obvious signs of bed erosion (e.g. scour). Resuspension of sediment would have caused increased accumulation of trap sediment which as stated was not found in this study.

3.6 Implications

3.6.1 Cave Sediment as a Sea-Level Indicator

In Yax Chen, the cenote area and overlying vegetation is having a significant effect on the production and accumulation of sediments in the cave. In this instance, there is virtually no sedimentation in areas upstream of Cenote Gemini which is significant, since water has flooded this cave passage for thousands of years and there is no sediment record of that water table rise (van Hengstum et al., 2015; van Hengstum et al., 2011). It is only with continued sea-level rise and flooding of the upper karst surface and movement of the mangrove/wetland inland that we will expect sedimentation to occur in this area. The nature of the karst topography (among many other factors) has a significant role in determining where and when mangrove/wetlands will develop with sea-level rise (Delgado et al., 2001; McKee et al., 2007; Soares, 2009; Torrescano and Islebe, 2006). Sedimentation in this instance is based on sea-level rise and flooding of the epikarstic surface, allowing the colonization by mangroves which provide nutrients for primary productivity in the cenotes versus presence of water (Collins et al., 2015a, b).

3.6.2 Sinkhole as Hurricane Recorders

The relationship between sedimentation and overlying mangrove/wetlands is also important for hurricane studies. Our results show that sediment flux does not respond to hurricane deposition, but it does show that above average rainfall events cause increased nutrient inputs and productivity in open water locations. Coastal sinkholes (vs. shelf blueholes) which are connected to cave passages may receive inputs from surrounding mangroves and wetlands transporting OM and nutrients to the sunlit sinkholes. Each system will likely have a unique response, but this connectivity with the overlying terrestrial surface should be considered when examining hurricane sedimentation. As demonstrated in Yax Chen, surficial environments (mangroves/wetlands) upstream of the sinkhole can affect deposition through the transport of sediment but also nutrients affecting primary productivity in the sunlit sinkhole months after the hurricane. Each system may respond differently, this work only demonstrated one example, but connectivity of the sinkhole with regional cave passages is a consideration that needs to be addressed for sinkholes to be utilized as hurricane recorders.

3.6.3 Paleo-hydrological studies

The result of the sediment trap studies in Yax Chen showed that the average sedimentation rate is steady with respect to location in the cave from year to year. There is variability in the sedimentation flux depending on location (i.e. mangrove and cenote extent) but seems to remain consistent from location to location albeit with only a limited three year data set. Continued monitoring may reveal differences (e.g. very dry years) but extreme rainfalls do not appear to have a significant effect on the sediment flux rate and OM composition as discussed above. This is one of the more extreme events to have affected the cave system over the last decade (Devos pers. communication) and yet there were no unusually high rates of sedimentation. In terms of using cave sediments from Yax Chen as a paleohydrological proxy, sedimentation rates will be relatively constant from location to location and will provide good accumulation histories and high resolution records of the paleohydrology of the aquifer (see also; Collins et al., 2015b). The results from this study provide important baseline data for interpreting the older accumulation histories.

3.7 Conclusion

The sediment trap data from Yax Chen showed a strong correlation between cenote area and downstream sedimentation flux but also showed the contributory role of mangrove and associated wetlands on primary productivity in the cenotes. Nutrient rich water draining through the mangrove with the onset of the dry season showed that primary productivity in the sunlit cenotes is largely determining the sediment flux in the dark cave. Hurricane Ingrid had a strong effect on water table elevation, but this caused little effect on sedimentation patterns likely due to precipitation rapidly draining the mangroves and flowing into the cave with little residence time in the cenotes.

This study provides important baseline data for interpreting further paleohydrological studies in Yax Chen, but also provides comparative data for other cave systems. It also emphasizes that cave connectivity needs to be considered when using sinkholes for paleo-hurricane studies. In differing hydrological systems large water table fluctuations may result in upstream areas contributing nutrients and sediment to the sunlit sinkhole during higher than normal rainfalls, complicating the resulting sedimentary record.

3.8 Acknowledgements

The authors would like to thank Dr. Todd Kincaid for his insightful review and comments on the original manuscript. We would also like to thank David Carrillo for his cartography skills and AutoCAD digitation of Yax Chen Cave Map. We gratefully acknowledge the support of; Global Underwater Explorers, The Mexican Cave Exploration Project, Cindaq, and the wonderful staff at Zero Gravity for dive support and logistics. This research was only possible due to all of the talented MCEP Science Week volunteers from around the world. Special thanks go to; Onno van Eijk, Ali Perkins, Arno Mol and Jan Duikt for your repeated support each year. Sediment trap underwater photography thanks to Fred Boer. Funding was provided by National Sciences and Engineering Research Council of Canada (EGR – Discovery); National Geographic Research and Exploration Grant (EGR).

3.9 References

Appendini, C. M., Rafael Meza, P., Pedrozo-Acuña, A., Raga, G. B., and Farfán, L. M., Storm Surge Estimation Due to the Incidence of Simultaneous Tropical Cyclones in Mexico, *in* Proceedings 31st Conference on Hurricane and Tropical Meteorology, San Diego, March 31, 2014 2014, American Meteorological Society.

Back, W., 1995, Water Management by early people in the Yucatan, Mexico: Environmental Geology, v. 25, p. 239-242.

Bauer-Gottwein, P., B.R.N. Gondwe, G. Charvet, L.E. Marin, M. Rebolledo-Vieyra, and G. Merediz-Alonso, 2011, Review: The Yucatan Peninsula karst aquifer, Mexico: Hydrogeology Journal, v. 19, p. 507-524.

Beddows, P. A., 2004, Groundwater Hydrology of a Coastal Conduit Carbonate Aquifer: Caribbean Coast of the Yucatan Peninsula, Mexico [Doctor of Philosophy: University of Bristol, 332 p.

Beddows, P. A., Smart, P. L., Whitaker, F. F., and Smith, S. L., 2007, Decoupled fresh-saline groundwater circulation of a coastal carbonate aquifer: Spatial patterns of temperature and specific electrical conductivity: Journal of Hydrology, v. 346, p. 18-32.

Benavente, J., M.c. Hidalgo, and F. Carrasco, Influence of a high recharge episode following a drought period in an aquifer affected by seasonal seawater intrusion (Granada Coast S. Spain). *in* Proceedings First International Conference on Saltwater Intrusion and Coastal Aquifers - Monitoring, Modeling and Management, Essaouira, Morocco, April 2001, p. 23-25.

Beven, J. L. I., 2014, Hurricane Ingrid, National Hurricane Centre Tropical Cyclone Report, Volume 2014, National Weather Service.

Boose, E. R., D.R. Foster, A. Barker Plotkin, and B. Hall, 2003, Geographical and historical variation in hurricanes across the Yucatan Peninsula, *in* Gomez-Pompa, A., M.F. Allen, S. F., and Jimenez-Osornio, J. J., eds., Lowland Maya Area: Three Millennia at the Human-Wildland Interface: New York, Haworth Press, p. 495-516.

Budd, D. A., and Vacher, H. L., 1991, Predicting the thickness of fresh-water lenses in carbonate paleo-islands: Journal Sedimentary Petrology, v. 61, no. 1, p. 43-53.

Chatters, J. C., D.J. Kennett, Y. Asmerom, B.M. Kemp, V. Polyak, A.N. Blank, P.A. Beddows, E. Reinhardt, J. Arroyo-Cabrales, D.A. Bolnick, TR.S. Malhi, B.J. Culleton, P. Luna Erreguerena, D. Rissolo, S. Morell-Hart, and T.W. Stafford Jr., 2014, Late Pleistocene Human Skeleton and mtDNA Link Paleoamericans and Modern Native Americans: Science, v. 344, p. 750-754.

Coke, J., 1991, Sea-level Curve: Nature, v. 353, no. 5, p. 25.

Collins, S. V., E.G. Reinhardt, D. Rissolo, J.C. Chatters, A. Nava Blank, and P. Luna Erreguerena, 2015a, Reconstructing water level in Hoyo Negro with implications for early Paleoamerican and faunal access.: Manuscript submitted for publication.

Collins, S. V., Reinhardt, E. G., Devos, F., and LeMaillot, C., 2015b, Late Holocene Mangrove development and onset of sedimentation in Yax Chen cave system (Ox Bel Ha) Yucatan, Mexico.: Manuscript submitted for publication.

Delgado, P., P.F. Hensel, J.A. Jimenez, and J.W. Day, 2001, The importance of propagule establishment and physical factors in mangrove distributional patterns in a Costa Rican estuary: Aquatic Botany, v. 71, no. 3, p. 157-178.

Finch, W. A., 1965, The Karst Landscape of Yucatan, University of Illinois at Urbana-Champaign.

Gabriel, J. J., E.G. Reinhardt, M.C. Peros, D.E. Davidson, P.J. van Hengstum, and P.A. Beddows, 2009, Palaeoenvironmental evolution of Cenote Aktun Ha (Carwash) on the Yucatan Peninsula, Mexico and its response to Holocene sea-level rise: Journal of Paleolimnology, v. 42, p. 199-213.

Gardner, W. D., 1980a, Field Assessment of Sediment Traps: Journal of Marine Research, v. 38, no. 1, p. 41-52.

-, 1980b, Sediment trap dynamics and calibration: A laboratory evaluation: Journal of Marine Research, v. 38, no. 1, p. 17-39.

Gondwe, B. R. N., S. Lerer, S. Stisen, L. Marin, M. Rebolledo-Vieyra, G. Merediz-Alonso, and P. Bauer_Gottwein, 2010, Hydrogeology of the south-eastern Yucatan Peninsula: New insights from water level measurements, geochemistry, geophysics and remote sensing: Journal of Hydrology, v. 389, p. 1-17.

González, A. H., C. Rojas Sandoval, A. Terrazas Mata, M. Benavente Sanvicente, W. Stinnesbeck, J. Aviles O. Magdalena de los Rios, and E. Acevez, 2008, The arrival of humans on the Yucatan Peninsula: evidence from submerged caves in the state of Quintana Roo, Mexico: Current Research in the Pleistocene, v. 25, p. 1-25.

Hanstenrath, S., and Greischar, L., 1993, Circulation Mechanisms Related to Northeast Brazil Rainfall Anomalies: Journal of Geophysical Research, v. 98, no. D3, p. 5093-5102.

Heiri, O., A.F. Lotter, and G. Lemcke, 2001, Loss on ignition as a method for estimating organic and carbonate content in sediments: reproducibility and comparability of results: Journal of Paleolimnology, v. 25, p. 101-110.

Horstman, E. M., C. Marjolein Dohmen-Janssen, and S.J.M.H. Hulscher, 2013, Flow routing in mangrove forests: A field study in Trang province Thailand: Continental Shelf Research, v. 71, p. 52-67.

Hughen, K. A., J.T. Overpeck, L.C. Peterson, and Anderson, R. F., 1996, The nature of varved sedimentation in the Cariaco Basin, Venezuela, and it's paleoclimatic significance: The Geological Society, London, Special Publication, v. 116, p. 171 - 183.

Leyden, B. W., M. Brenner, and B.H. Dahlin, 1998, Cultural and Climatic History of Coba a Lowland Maya City in Quintana Roo, Mexico: Quaternary Research, v. 49, p. 111-122.

Loper, D. E., Werner, C. L., Dehan, R., Kincaid, T., Chicken, E., and Davies, G., 2008,Probingthe Plumbing of Wakulla Spring: Instrumentation and Preliminary Results *in* Yuhr, L. B., Alexander, C., and Beck, B. F., eds., Sinkholes and the

Engineering and Environmental Impacts of Karst: Tallahassee, Florida, American Society of Civil Engineers.
Lopez Fuerte, F. O., D.A. Siqueiros Beltrones, and J.N. Navarro, 2010, Benthic Diatoms Associated with Mangrove Environments in the Northwest Region of Mexico: CICIMAR-Oceanides.
Lugo, A. E., and Snedaker, S. C., 1974, The Ecology of Mangroves: Annual Review of Ecology and Systematics, v. 5, p. 39-64.
Maas, K., 2007, Influence of climate change on a Ghijben-Herzberg lens: Journal of Hydrology, v. 347, no. 1-2, p. 223-228.
Marin, L. E., 1990, Field Investigations and numerical simulation of groundwater flow in the karstic aquifer of northwestern Yucatan, Mexico [Ph.D.: Northern Illinois University, 183 p.
Matheron, G., 1963, Principles of Geostatistics: Economic Geology, v. 58, p. 1246-1266.
Mazda, Y., H. Yokochi, and Y. Sato, 1990, Groundwater Flow in the Bashita-Minato Mangrove Area, and its Influence on Water and Bottom Mud Properties: Estuarine, Coastal and Shelf Science, v. 31, p. 621-638.
McKee, K. L., D.R. Cahoon, and I.C.Feller, 2007, Caribbean mangroves adjust to rising sea level through biotic controls on change in soil elevation: Global Ecology and Biogeography.
Meacham, S. S., 2012, Using Landsat 5 TM Data to Identify and Map Areas of Mangrove in Tulum, Quintana Roo, Mexico [Masters of Science: University of New Hampshire, 105 p.
Moore, Y. H., R.K. Stoessell, and D.H. Easley, 1992, Fresh-water sea-water relationship within a groundwater-flow system, northeastern coast of the Yucatan Peninsula: Ground Water, v. 30, no. 3, p. 343-350.
Neuman, B. R., and Rahbek, M. L., 2007, Modeling The Groundwater Catchment of the Sian Ka'an Reserve, Quintana Roo: National Speleological Society.
Ovalle, A. R. C., C.E. Rezende, L.D. Lacerda, and C.A.R. Silva, 1990, Factors Affecting the Hydrochemisty of a Mangrove Tidal Creek, Sepetiba, Brazil: Estuarine, Coastal and Shelf Science, v. 31, p. 639-650.
Pasch, R. J., and Zelinsky, D. A., 2014, Hurricane Manuel, National Hurricane Centre Tropical Cyclone Report, Volume 2014, National Weather Service.
Perry, E., J. Swift, J. Gamboa, A. Reeve, R. Sanborn, L. Marin, and M. Villasuso, 1989, Geologic and envirnomental aspects of surface cementation, north coast, Yucatan, Mexico: Geology, v. 17, no. 9, p. 818-821.
Peterson, L. C., J.T. Overpeck, N.G. Kipp, and J. Imbrie, 1991, A high-resolution late Quaternary upwelling record from the anoxic Cariaco Basin, Venezuela: Paleooceanography, v. 6, p. 99-120.
Pohlman, J. W., T.M. Iliffe, and L.A. Cifuentes, 1997, A stable isotope study of organic cycling and the ecology of an anchialin cave ecosystem: Marine Ecology Progress Series, v. 155, p. 17-27.
Quintana Roo Speleological Survey, 2014, List of Long Underwater Caves in Quintana Roo, Mexico: Tulum, Quintana Roo Speleological Survey.

Rissolo, D., 2001, Ancient Maya Cave Use in the Yalahau Region, Northern Quintana Roo, Mexico: National Speleological Society.
Servicio Meteorológico Nacional, 2014, Daily Weather Data: Tulum Mexico, Servicio Meteorológico Nacional
Smart, P. L., P.A. Beddows, J. Coke, S. Doerr, S. Smith, and Whitaker, F. F., 2006, Cave Development on the Caribbean coast of the Yucatan Peninsula, Quintana Roo, Mexico, *in* Harmon, R. S. a. C. W., ed., Perspectives on Karst geomorphology, hydrology and geochemistry - A tribute volume to Derek C. Ford and William B. White, Volume 404, Geological Society of America Special Paper, p. 105-128.
Soares, M. L. G., 2009, A Conceptual Model for the Responses of Mangrove Forests to Sea Level Rise: Journal of Coastal Research, v. 56, p. 267-271.
Stanley, D. J., and Warne, A. G., 1994, Worldwide initiation of Holocene marine deltas by deceleration of sea-level rise: Science, v. 265, no. 5169, p. 228-231.
Steinich, B., and L.E. Marin, 1997, Determination of flow characteristics in the aquifer of the Northwestern Peninsula of Yucatan, Mexico: Journal of Hydrology, v. 191, no. (1-4), p. 315-331.
Stoessell, R. K., 1995, Dampening of Transverse Dispersion in the Haloclince in Karst Limestone in the Northern Yucatan Peninsula: Ground water, v. 33, no. 3, p. 366-371.
Stoessell, R. K., and Coke, J. G., 2006, An Explanation for the lack of a Dilute Freshwater Lens in Unconfined Tropical Coastal Aquifer: Yucatan Example: Gulf Coast Association of Geological Societies Transactions, v. 56, p. 785-792.
Torrescano, N., and Islebe, G. A., 2006, Tropical forest and Mangrove history from southeastern Mexico: a 5000 yr pollen record and implications for sea level rise: Veget Hist Archaeobot, v. 15, p. 191-195.
van Hengstum, P. J., D.A. Richards, B.P. Onac, and J.A. Dorale, 2015, Coastal caves and sinkholes, *in* Ian Shennan, A.J. Long, and B.J. Horton, eds., Handbook of Sea-Level Research, John Wiley and Sons Ltd.
van Hengstum, P. J., D.B. Scott, D.R. Grocke, and M.A. Charette, 2011, Sea level controls sedimentation and environments in coastal caves and sinkholes: Marine Geology, v. 286, p. 35-50.
van Hengstum, P. J., E.G. Reinhardt, P.A. Beddows, and J.J. Gabriel, 2010, Linkages between Holocene paleoclimate and paleohydrogeology preserved in a Yucatan underwater cave: Quaternary Science Reviews, v. 29, no. 19-20, p. 2788-2798.
Veni, G., 1984, Maya utilization of karst groundwater resources: Environ. Geol. Water Sci, v. 16, no. 1, p. 63-66.
Wattayakorn, G., E. Wolanski, and B. Kjerfve, 1990, Mixing, Trapping and Outwelling in the Klong Ngao Mangrove Swamp, Thailand: Estuarine, Coastal and Shelf Science, v. 31, p. 667-688.
Weidie, A. E., 1985, Geology of Yucatan Platform: Part 1, 19 p.:
Werner, C., 2007, Double-Diffusive Fingering in Porous Media [Doctor of Philosophy: Florida State University, 114 p.

Whitaker, F. F., and Smart, P. L., 1990, Active circulation of saline ground waters in carbonate platforms: Evidence from the Great Bahama Bank: Geology, v. 18, p. 200-203.

Wolanski, E., and Gardner, R., 1981, Flushing of salt from mangrove swamps: Australian Journal of marine and Freshwater Research, v. 32, p. 681-683.

3.10 Tables

Table 1. Aggregated sediment flux and corresponding cenote area for Yax Chen divided into low, moderate and high sediment flux zones.

Station	Cenote Area (m^2)*	Sediment Flux (mg/cm^2/day)			Organic Matter LOI (%)	
		Mean	*1 std*	*(± 17%)*	*Mean*	*1 std*
1	-	0.014	0.002	0.002	6	2
2-8	8955	0.11	0.05	0.02	21	5
13-17	22448	0.32	0.15	0.05	43	3

* Combined cenote area for Stations.

Table 2. Sediment flux, loss on ignition and cenote dimensions aggregated by spatial locations in Yax Chen (see Fig. 7 a, b).

Cenote	Area (m^2)	Perimeter (m)	Station	Mean Flux*	1 std	LOI (%)	1 std
Gemini	2893	368	2	0.26	0.04	22	3
Luna	4447	250	3,4	0.22	0.03	31	4
Isod 2	1615	306	5-8	0.12	0.06	19	2
Tarpon 1	7196	814	13-17	0.32	0.15	43	3

* Sediment flux mg/cm^2/day.

3.11 Figures

Fig. 1. The location of Cenotes Yax Chen, Mayan Blue, Temple of Doom and Xtabay on the Yucatan Peninsula, Mexico.

Fig. 2. a) Storm tracks for Hurricanes Ingrid and Manuel which made landfall in Mexico in 2013. Red lines indicate the storm had reached F1 hurricane status on the Saffir-Simpson scale (modified after, Beven, 2014; Pasch and Zelinsky, 2014). b) MCEP diver Fred Devos showing the flooding experienced in the rainy season of September 23, 2013 at the access point to Cenote Yax Chen, Quintana Roo, Mexico. c) MCEP cave diver Fred Devos indicating the high water mark at Cenote Yax Chen, Mexico (>1.0m above normal).

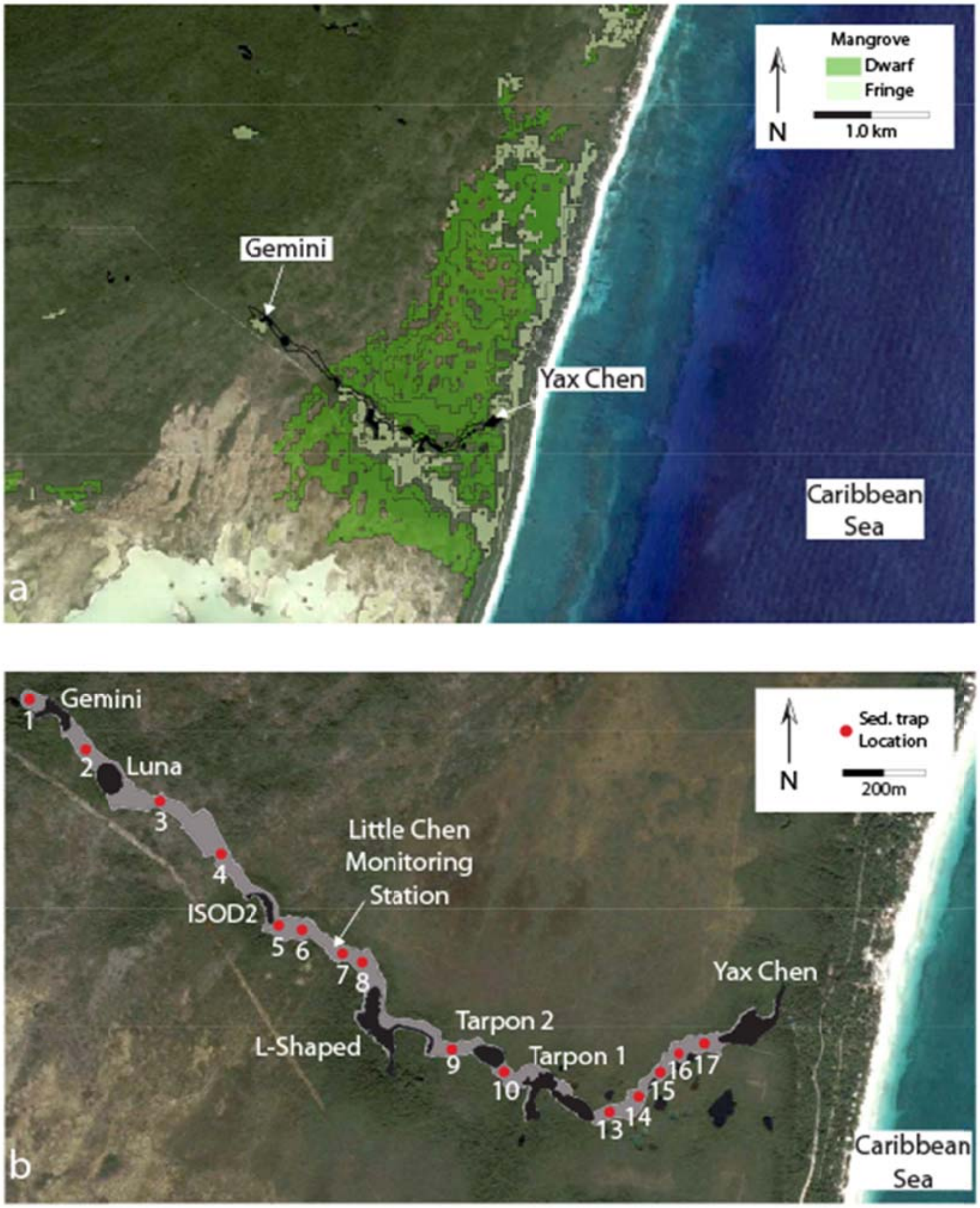

Fig. 3. a) Partial results of Landsat 5 supervised classification of mangrove forest in the Tulum Region (modified after, Meacham, 2012). b) Location of mapped cenotes, water level monitoring site and sediment flux stations in Yax Chen (Ox Bel Ha), Tulum, Mexico.

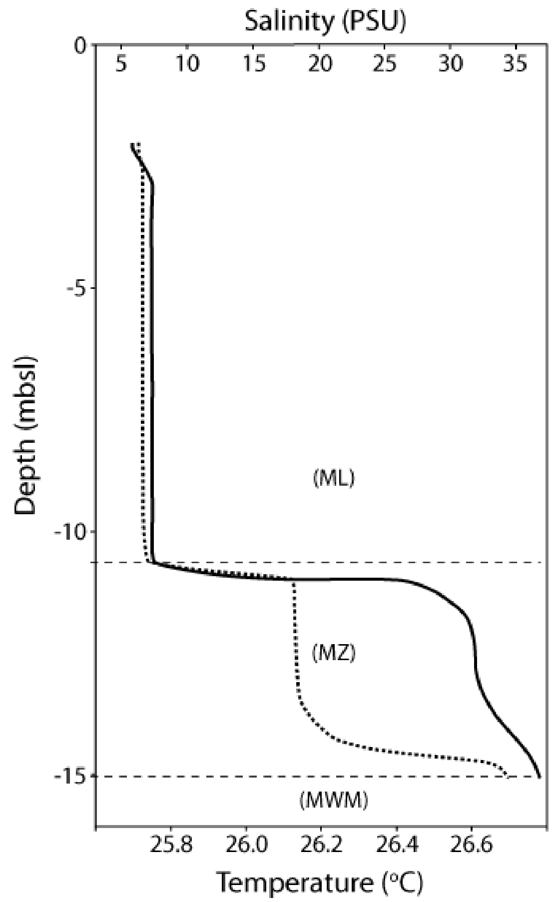

Fig. 4. Temperature (solid line) and salinity (dotted line) profile showing the positon of the meteoric lens (ML), mixing zone (MZ) and marine water mass (MWM) in Yax Chen (Ox Bel Ha). The profile was taken near the Little Chen Monitoring station in Yax Chen (Ox Bel Ha), Tulum, Mexico (see Fig. 3b).

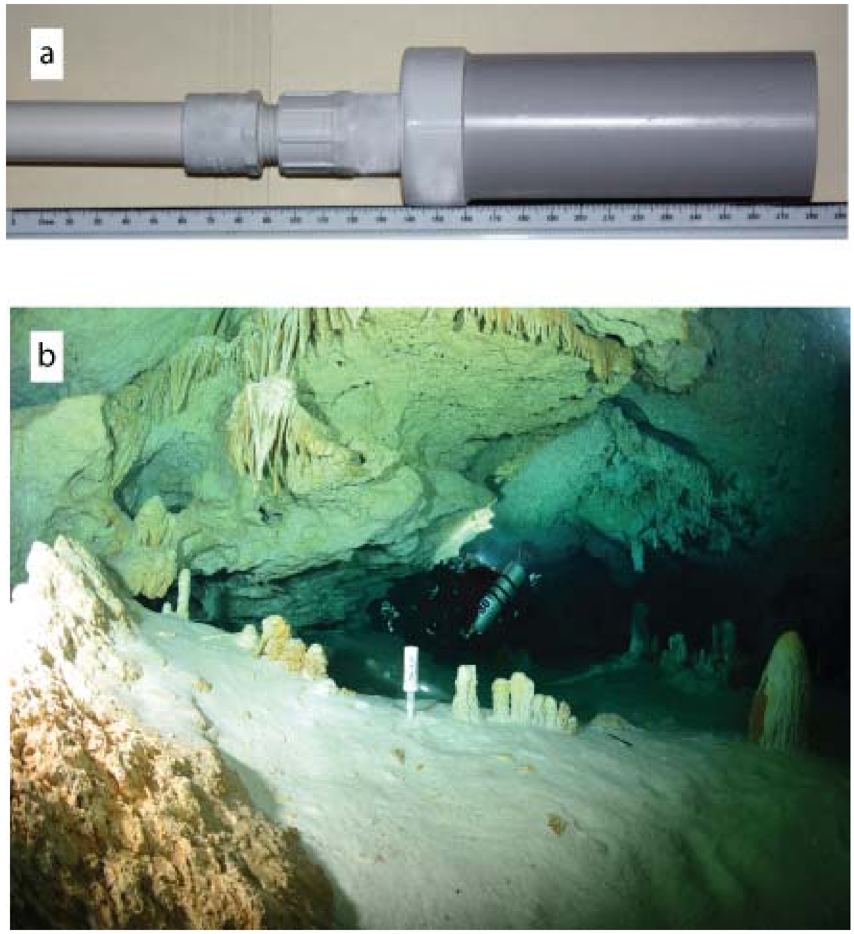

Fig. 5. a) Photo of cylindrical sediment trap constructed to monitor sediment flux (H/W ratio 2.7) b) Photo of installed sediment trap.

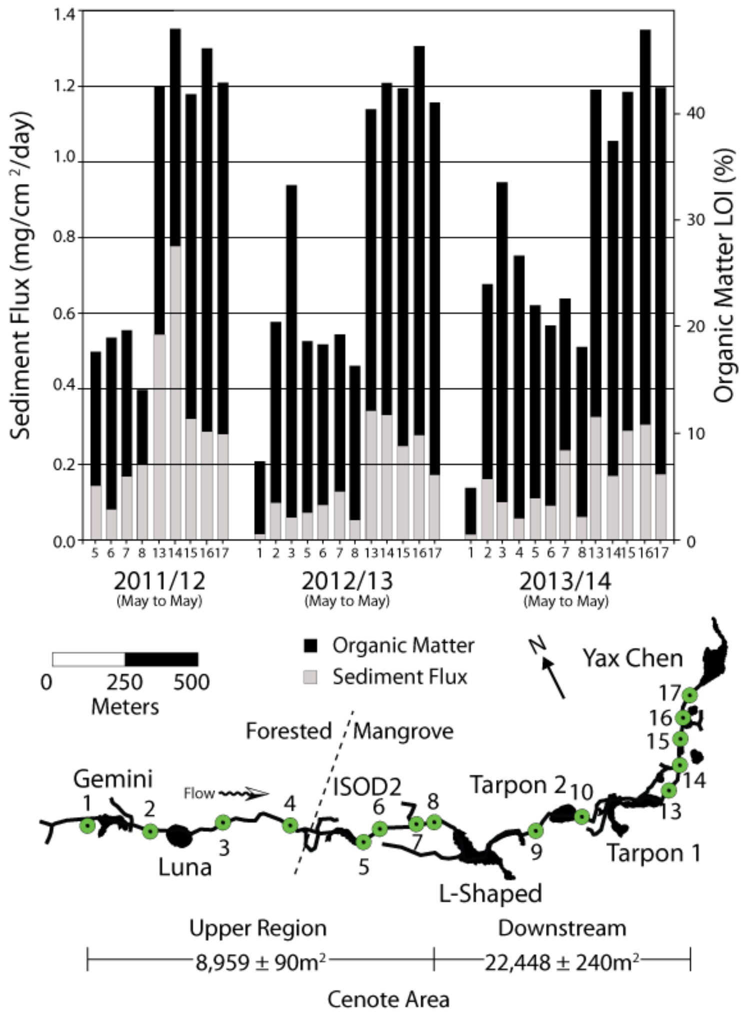

Fig. 6. Variation in the amount of yearly sediment flux and organic matter calculated for sediment trap locations in Yax Chen Cave, Mexico from May 2011 to May 2014. Aggregated cenote areas are shown.

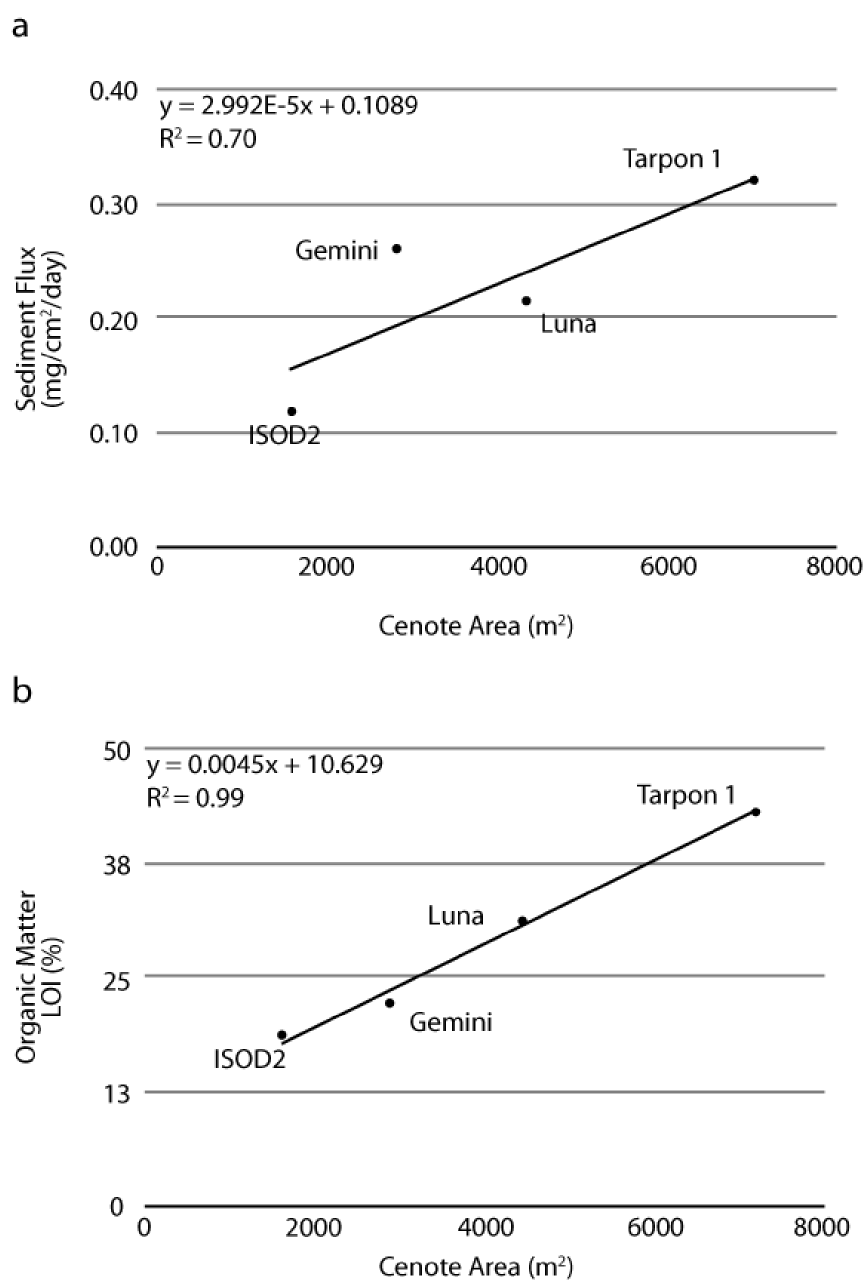

Fig. 7. a) Plot of calculated downstream sediment flux versus corresponding cenote area for Yax Chen (Ox Bel Ha). b) Plot of calculated downstream OM (LOI %) versus corresponding cenote area for Yax Chen (Ox Bel Ha).

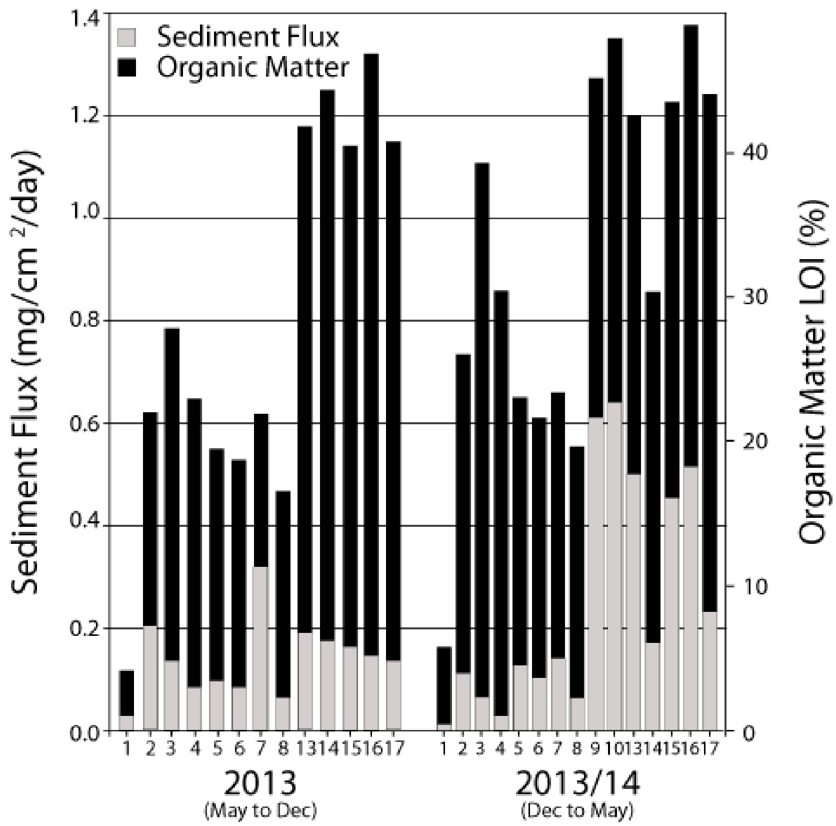

Fig. 8. Variation in the amount of biannual sediment flux and organic matter calculated for sediment trap locations in Yax Chen Cave, Mexico from May - Dec 2013 and Dec to May 2013/14.

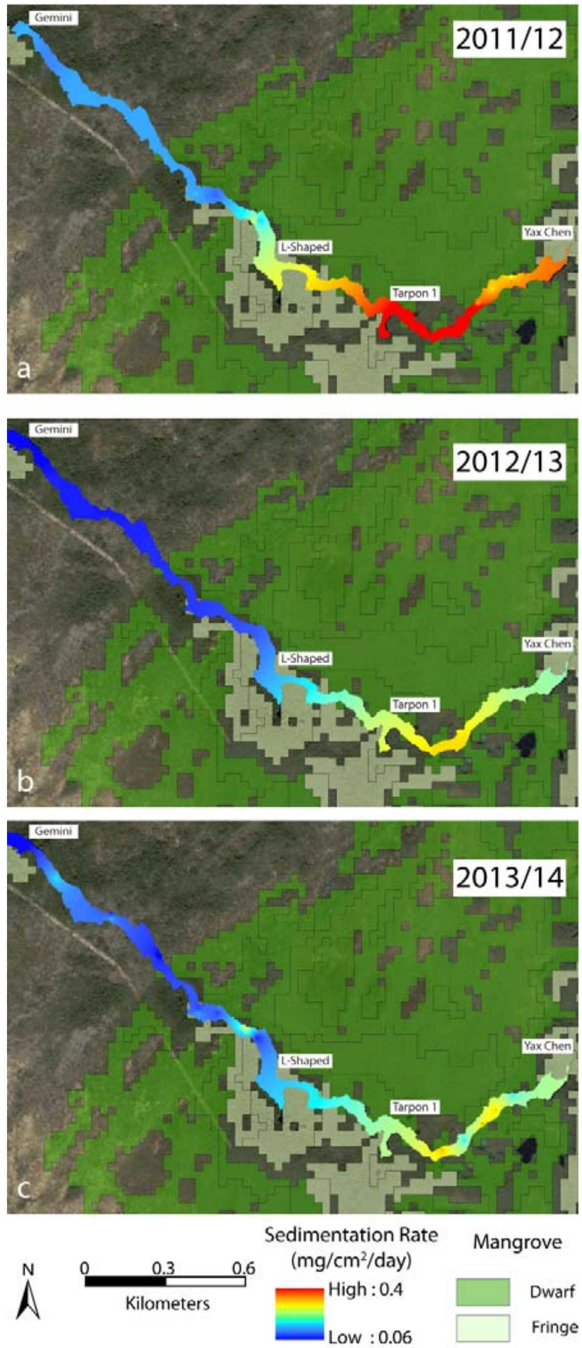

Fig. 9. Interpolated surface for Yax Chen (Ox Bel Ha) showing the results of kriged sediment flux data for annual collection periods from 2011-2014. Landsat supervised mangrove classification is overlaid for comparison (modified after, Meacham 2012).

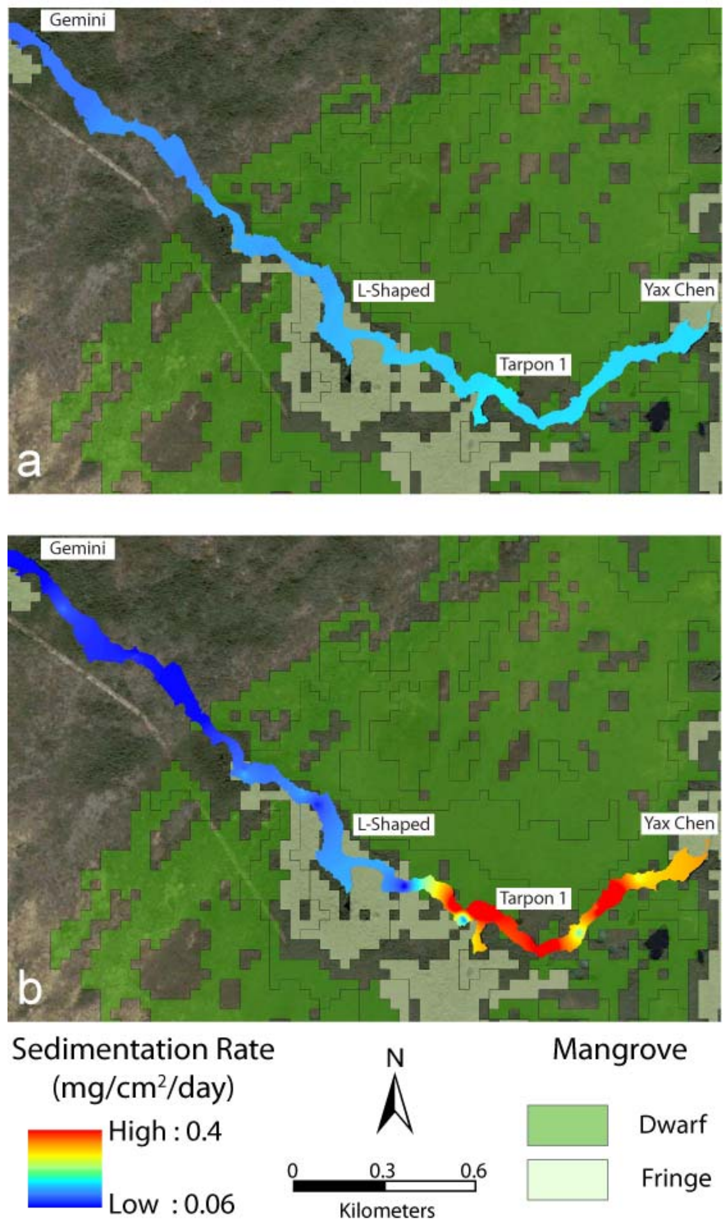

Fig. 10. Interpolated surface for Yax Chen (Ox Bel Ha) showing the results of kriged sediment flux data for biannual collection periods from May to Dec. 2013 and Dec to May 2013/14. Landsat supervised mangrove classification is overlaid for comparison (modified after, Meacham, 2012).

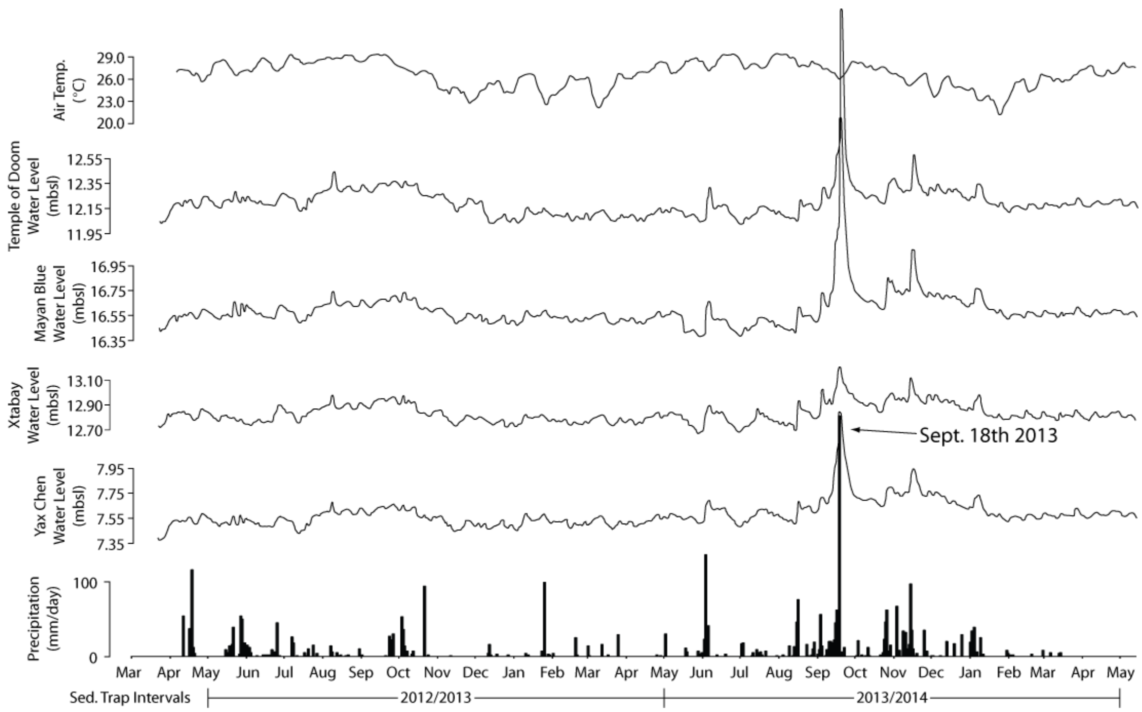

Fig. 11. Seasonal variation of mean air temperature (smoothed with a 10 point boxcar filter) and precipitation from automatic weather station in the Sian Ka'an Biosphere Reserve, Tulum, Mexico. Seasonal variations in water level of meteoric water lens at four locations in Quintana Roo, Mexico using ReefNet Sensus Ultra dive loggers. Locations include; Cenotes Yax Chen, Xtabay, Mayan Blue and Temple of Doom (see Fig. 1 for locations).

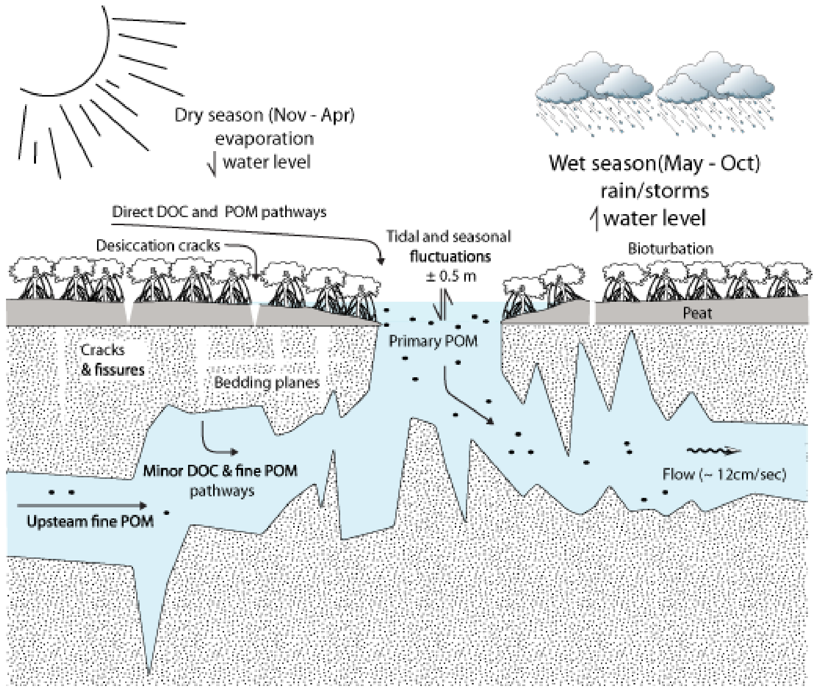

Fig. 12. An interpretive diagram showing the various organic matter pathways into Yax Chen (Ox Bel Ha) and the primary processes that control water level in the cave and mangrove forest.

Chapter 4 – Late Holocene Mangrove development and onset of sedimentation in the Yax Chen cave system (Ox Bel Ha) Yucatan, Mexico implications for using cave sediments as a sea-level indicator.

Paleogeography, Paleoclimatology, Paleoecology.

Collins S.V.*, Reinhardt E.G., Werner C., Le Maillot C., Devos F., Rissolo, D.

*Corresponding Author – shawnvcollins@icloud.com

Keywords: Cave Sediments; Anchialine; Yucatan; Hurricanes; Sea-level; Mangrove.

4.1 Abstract

This study examines the relationship between the formation of coastal mangrove with Holocene sea-level rise and the onset of aquatic sedimentation in Yax Chen, a cave system in Quintana Roo on Mexico's Yucatan Peninsula. Sediment depth measurements (n=180) were collected along 2.7 km of underwater cave passage and three cores were radiocarbon dated to examine both the extent and timing of sedimentation in the cave. Basal radiocarbon ages (~ 4 Ka) for aquatic sediments in the cave show that sea-level rise flooding the upper karst surface and the establishment of mangrove, initiated sedimentation in the cave rather than flooding of the cave bottom. Cenote surface area

controlled the long-term sediment accumulation in the cave passages through primary productivity in the sunlit open water areas of the cenotes. This primary productivity was enhanced with mangrove formation, which causes funneling of precipitation and nutrient rich waters into the cenotes from the mangroves which has also been documented with sediment trap studies in a previous study (Collins et al., 2015b). Accumulation histories from the radiocarbon dated sediment cores (n=3) were compared with accumulation histories in previously published studies including Actun Ha, Mexico and Green Bay Cave (GBC), Bermuda.

4.2 Introduction

Cave and sinkhole sediments have been used to document water level changes in anchialine systems and can be used as a proxy for sea-level (Gabriel et al., 2009; van Hengstum et al., 2015; van Hengstum et al., 2011). However, many of these studies were based on limited data sets or are speculative, as there are few studies which provide a basis for comparison. Recent research in Yax Chen (part of the Ox Bel Ha cave system) and the Outland Cave in Quintana Roo, Yucatan Peninsula, Mexico show that sedimentation can be ephemeral and non-continuous in cave passages (Collins et al., 2015a; Collins et al., 2015b). The study from the anchialine system of Sac Actun (Outland Cave) demonstrated the difficulty of reconstructing water levels and inferring sea-level from cave systems with an upper karst terrain dominated by tropical forests (Collins et al., 2015a). The study emphasized that not only bottom elevation but more importantly ceiling elevation can control sedimentation in the cave. Research using sediment traps in Yax Chen showed the role of mangroves and cenote area controlled the sediment flux in downstream cave passages (3 yrs. of data; Collins et al., 2015b). Little sediment was found in upstream cave passages dominated by tropical forest vegetation, while passages with overlying mangrove and large cenotes had abundant sediment. This study further examines long-term sedimentation patterns (1000s of yrs.) in Yax Chen and the role of sea-level rise and mangrove formation which has important implications for using cave sediments as a sea-level indicator (van Hengstum et al., 2015).

4.2.1 The Caves of Quintana Roo, Mexico

The Yucatan Peninsula is a carbonate platform of Paleogene to Quaternary age which has undergone multiple phases of diagenesis altering mineralogy and textural characteristics (Weidie, 1985). However, the platform has largely retained its sub-horizontal geometry with minimal differential tilting (Beddows, 2004; Coke, 1991; Weidie, 1985). The caves in the Yucatan have formed through repeated cycles of vadose and phreatic conditions associated with sea-level fluctuations over the Quaternary (Smart et al., 2006). The limestone matrix has a porosity of 17% but there is also a large anastomosing network of caves passages (> 2 m dia.) with smaller hydrologic pathways through fractures and bedding planes (Beddows, 2004; Smart et al., 2006). Cave passage formation has been attributed to Mixing Zone (MZ) dissolution that occurs at the transition between saline and meteoric groundwater which is undersaturated with respect to $CaCO_{3-}$ (Beddows, 2004; Esterson, 2003; Smart et al., 2006; Werner, 2007).

Cenotes (or sinkholes; karst windows) provide openings to the cave passages and act as point sources for sediments entering cave passage downstream (Collins et al., 2015b; Gabriel et al., 2009; Pohlman et al., 1997; van Hengstum et al., 2010 ; van

Hengstum et al., 2015). Cenotes form during sea-level low-stands when the weight of the ceiling exceeds the flexural strength of the limestone causing collapse resulting in a central breakdown deposit at the bottom of the cavern (Finch, 1965; Smart et al., 2006). The central breakdown deposit consists of angular, brecciated limestone boulders strewn on the floor of the cave. Organic Matter (OM) and phytoplankton (e.g. diatoms) sediment enter the cave passages largely through this cenote point source as there is no primary productivity in the dark cave passages (Benavente et al., 2001; Pohlman et al., 1997; van Hengstum et al., 2010). Other sediment includes; detrital carbonate (percolation from ceiling), calcium carbonate rafts and minor aeolian derived dust (Collins et al., 2015a; Collins et al., 2015b; Lopez Fuerte et al., 2010; Schmitter-Soto et al., 2002). Sediment can also enter through cracks and fissures in the bedrock but is minor in comparison to the cenotes (Mazda et al., 1990; Pohlman et al., 1997; Simon et al., 2007; Wolanski et al., 1992). Modern sediment trap studies in Yax Chen found that cenote area combined with mangrove extent strongly influenced the amount of sediment entering the cave (Collins et al., 2015b).

4.2.2 Hydrogeology

The Yucatan has no surficial lakes or rivers as the limestone has a high matrix porosity (~17%) with most of the water stored in the subsurface (>96%) and the cave passages accounting for ~ 99% of groundwater flow (Beddows, 2004). Due to this high porosity, water table elevation approximates sea-level and there is minimal hydraulic gradient (10^{-5}) which equates to a water table rise of 1-10 cm/km (Bauer-Gottwein et al., 2011; Beddows, 2004; Milne and Peros, 2013; van Hengstum et al., 2015).

Groundwater in the Yucatan is density stratified with a Meteoric Lens (ML) on top of saline groundwater (Marine Water Mass - MWM). Density contrasts between the warmer, denser MWM (~35 PSU) and the cooler ML (PSU <1) are responsible for the stratification (Moore et al., 1992; Neuman and Rahbek, 2007). In Yax Chen, the MZ between the ML and MWM ranges from 10 and 14 mbsl and is stepped (~ 6- 35 PSU; Collins et al., 2015b). The MZ can demonstrate changes in temperature, pH, dissolved oxygen and salinity depending on the location in the cave and the time of year (Esterson, 2003). There are numerous controls on the thickness and position of the MZ. Large scale changes are a result of eustatic sea-level fluctuations. As sea-level rises and falls, the aquifer tracks these changes and the MZ moves coincidently (Back et al., 1986; Florea et al., 2007; Raeisi and Mylroie, 1995). Short term fluctuations in position and thickness of the MZ in the cave are a result of flow velocity changes, channel morphology and sinuosity of the cave passage (Beddows et al., 2007; Smart et al., 2006). The majority of Yax Chen has cave passages that are within the ML (i.e. <10 mbsl).

Groundwater flow in Yucatan anchialine caves is low but varies with distance from the coastline with velocities ranging from 12 cm/s on the coast to ~ 1 cm/s 10 km inland (Moore et al., 1992). Cave passage morphology, flow patterns (Reynolds number) and sediment density can control patterns of sedimentation on the cave bottom (Beddows, 2004). The geometry of the passages are elliptical tubular, irregular and often subject to sudden elevational changes and abrupt bends (Smart et al., 2006). In addition to the changes in the shape, cave floors and ceilings tend to be obstructed with stalagmites, stalactites and central breakdown deposits which can affect the rate and Reynolds number of the flow. These factors all increase the turbulent mixing in the cave and can affect localized sedimentation (Beddows, 2004; Beddows et al., 2007; Esterson, 2003; Smart et al., 2006). Broad depositional patterns are controlled by OM productivity in cenotes, which act as point sources for sediment entering the cave (Collins et al., 2015b).

4.2.3 Climate

Quintana Roo, Mexico has a tropical climate with heavy rains in the summer months and drier conditions in the winter (Hodell et al., 2005; Metcalfe et al., 2000). Seasonal variation is controlled by the movement of the Intertropical Convergence Zone (ITCZ) with its northern movement bringing extensive precipitation from May to October which overlaps with the hurricane season in the Caribbean (June to November; Hanstenrath and Greischar, 1993; Hughen et al., 1996; Peterson et al., 1991). On average the Yucatan Peninsula receives 550 – 1500 mm of precipitation per annum (Bauer-Gottwein et al., 2011). During the dry season (November to April) the ITCZ moves south resulting in dry, cool conditions (Hanstenrath and Greischar, 1993; Hughen et al., 1996; Peterson et al., 1991). The average temperature for the area ranges from 34°C in the summer months to 25°C in the winter (Bauer-Gottwein et al., 2011; Beddows, 2004; Hodell et al., 2005).

4.2.4 Study Site

Yax Chen is part of the Ox Bel Ha Cave System which is 9 km south of the town of Tulum and on the northern border of the Sian Ka'an Biosphere (Fig. 1, 2a). The Ox Bel Ha Cave System is currently the world's longest underwater cave with over 256 km of explored underwater passage (Quintana Roo Speleological Survey, 2014). Yax Chen is a 2.7 km long section of Ox Bel Ha that trends in a NW direction inland from the coastline with access to the cave through a large cenote (Cenote Yax Chen) proximal to the coast (Fig. 2b). Downstream from Cenote Yax Chen porous matrix and fractures through the beach head connect to the open ocean. Yax Chen has seven large cenotes which range in size from 1600 – 9000 m^2 and at least five other unnamed smaller cenotes (250 – 1050 m^2; Fig. 2b). The average depth of the cave is ~10 m but some sections are >14 m. The cave passages are generally sub-perpendicular to the coast with some passages trending sub-parallel, with an average width of 45 m. The flow direction is generally from west to east moving towards the Caribbean coast.

Collins et al., (2015b) conducted a sediment trap study of Yax Chen over three years (May, 2011 – May, 2014) capturing the effects of Hurricane Ingrid (September, 2013) and showing how cenote size and mangrove coverage influenced sedimentation in downstream cave passages. The present study examines whether these trends apply to long-term sedimentation patterns in Yax Chen over the mid-late Holocene.

4.3 Methods

4.3.1 Cave Mapping

The cave from Cenotes Gemini to Yax Chen was mapped using the exploration line that generally followed the central line of the passage. The orientation of the passage was mapped using compass bearings and distance between tie-off points on the exploration line. Sidewall measurements from the exploration line (~ every 30m) were recorded using a tape measure to obtain passage widths while bottom and ceiling heights were collected using a digital depth gauge (± 0.1 m) to obtain the overall geometry of the passage. Field measurements were compiled in Arc GIS (Geographical Information System v10.2) and spatially corrected with cenote GPS locations (Garmin etrex) and overlain on pansharpened Landsat 7 satellite imagery (15 meter resolution) provided by Google Earth ™.

The area of each mapped cenote in Yax Chen was calculated remotely using satellite imagery available on Google Earth™. The satellite image was imported into Arc GIS and georectified to insure accurate positioning with existing cave survey maps. Each cenote was digitized into polygons and the area for each polygon was calculated.

4.3.2 Sediment Depth

A total of 180 sediment depth measurements were collected by self-contained underwater breathing apparatus (SCUBA) throughout the length of Yax Chen using foldable avalanche poles (3 m) which were graduated every centimeter. Depth of the sediment water interface and ceiling height for each location was measured using a digital depth gauge (±10 cm). At least three measurements were recorded across the width of the cave passage to provide an average accumulation thickness. The sediment depth data was tabulated and entered into Arc GIS to calculate the kriging weights and plot the final models. Assessment of the data revealed that the sediment depth data consisted of a moderate number of points, was slightly non-stationary and non-parametric. Based on these factors, ordinary kriging was determined to be the most appropriate interpolation method for this dataset. Data was plotted and a model fitted to the semivariogram to determine coefficients and values at unmeasured locations to determine the error of the estimate. The validity of the model was tested using cross validation, which compared the measured sediment depths with modeled values in the interpolation and calculated statistics on the difference (Arlot and Celisse, 2010).

4.3.3 Sedimentation Rate

Sediment cores (5 cm diam.) were collected using SCUBA at depths of 9.2 (Core 2 and Core 33) and 7.6 mbsl (Core 3). Cores were logged and bulk OM used for radiocarbon dating (AMS) as there were no seeds or discernible OM that could be isolated. Samples were analyzed at Beta Analytic, Miami, Florida, NOSAMS, Woods Hole Oceanographic Institute, Massachusetts and Direct AMS, Seattle, Washington. Raw radiocarbon ages were calibrated with the northern hemisphere terrestrial calibration curve IntCal13 (Reimer et al., 2013) using the R statistical software package Clam (Blaauw, 2010; version 2.2, Table 1). Sediment accumulation histories used an inferred date of 0 yrs. BP (± 1 yrs. BP) for the core top and a linear age model to fit the data. Cores from Actun Ha cave system, Mexico, near Yax Chen and also GBC, Bermuda (Core 5) were also analyzed for comparative purposes.

Collins et al., (2015b) used sediment trap data to calculate modern sedimentation rates for Yax Chen and found the average bulk density of the sediment was 0.01 g/cm^3. Sedimentation rates for the cores were calculated using this average bulk density estimate. Based on the volume of the 5 cm core tube, sedimentation rate was calculated using the following formula:

Sedimentation Rate =

$$\frac{\text{(Bulk density of mangrove gyttja*volume of core tube/cm)*Length of core interval (cm)}}{\text{(number of years*365 days)}}$$

Sedimentation rate was calculated for radiocarbon dated intervals in the cores, and compared with modern day rates reported in Collins et al., (2015b).

4.3.4 Mangrove Distribution

Meacham (2012) used the physiognomic classification of mangrove forests developed in Lugo and Snedaker, (1974) to map the extent of mangroves in the vicinity of Yax Chen. The classification used the spectral signature of mangrove leaves and other vegetation to discriminate fringe and dwarf classes of mangrove forest. Fringe mangroves tend to dominate in areas of protected shorelines where the elevations are higher than mean high tides. Fringe mangroves tend to have well developed prop roots that are excellent at entrapping sediment (Lugo and Snedaker, 1974). Dwarf mangroves are generally found in flat coastal areas. The most characteristic feature of the dwarf mangrove stand is the limited vertical extent of the trees <1.5m (Lugo and Snedaker, 1974). The physiognomic classification system is not species specific however, Mexico has only three species of mangrove including; Rhizophora mangle (red mangrove), Avicennia germinans (Black mangrove), Laguncularia racemosa (White mangrove; Lopez Fuerte et al., 2010).

4.4 Results

4.4.1 Age model and sedimentation rates

All three cores from Yax Chen contained fine OM (gyttja) with only minor variation in color due variable amounts of small shell fragments. Both Core 2 and 3 penetrated to the cave bottom (limestone) while Core 33 did not reach refusal (Fig. 2b).

The age model for Core 2 used four radiocarbon dates, contained no age reversals and had a 95% confidence interval ranging from 131 – 355 years (mean = 198 years; Fig. 3; Table 1). The age model for Core 3 used five dates and excluded the date at 2.5 cm which was likely contaminated with fragments of older organic matter. The age model for Core 3 had a 95% confidence interval ranging from 70 - 369 years (mean = 152 years; Fig. 3; Table 1). The age model for Core 33 used four dates and had a 95% confidence interval ranging from 4 - 147 years (mean = 79 years; Fig. 3; Table 1). For comparison an age model was calculated from the nearby Actun Ha cave system using the radiocarbon dates from van Hengstum et al. (2010; Core 2) and two additional radiocarbon dates (Table 1). The core was retrieved 40 m downstream of Cenote Carwash at a depth of 16 mbsl (see Fig. 8 for location). The resulting age model using eight radiocarbon dates had a 95% confidence interval ranging from 4 – 338 years (mean = 127; Fig. 3; table 1) and had two age reversals that were within the uncertainty of the model. Core 5 from GBC, Bermuda was also age modelled based on the radiocarbon ages in van Hengstum et al. (2011). The age model for GBC core 5 used nine radiocarbon dates, contained no age reversals and had a 95% confidence interval ranging from 4 – 391 years (mean = 145 years; Fig. 3; Table 1).

Based on the age models, accumulation histories in Yax Chen were very similar and largely linear between the three cores. Cores 2 and 3 have similar basal ages (~ 3500 cal yr BP) and accumulation profiles, while Core 33 showed a largely linear accumulation rate but had a basal age of only ~1600 cal yr BP, as the core did not reach refusal. The upper age (~ 700 cal yr BP, 18 cm) may contain older OM fragments and the lower three ages show a similar linear accumulation as Core 2 and 3. The accumulation rate of sediment in Core 33 is ~ 2x the rate in Cores 2 and 3 and is likely due to its close proximity to the cenote (Fig. 2b).

In contrast, the cores from Actun Ha and GBC show stepped sediment accumulation histories that indicate episodic deposition of sediment with hiatuses or possibly erosional events between depositional episodes (Fig. 3). The basal age of Actun Ha is similar to the Yax Chen cores (~3500 cal yr BP) while the GBC is much older (13,000 cal yr BP).

Sedimentation rates calculated using bulk density values from (Collins et al., 2015b) showed slight changes through time varying from ~ 0.1 to 0.5 ±0.05 $mg/cm^2/day$ (Fig. 4). The mean accumulation rate for the two cores was 0.3 ± 0.05 (1σ) $mg/cm^2/day$ which was comparable to the average accumulation rates calculated for the modern sediment traps (Point B Fig. 4; Collins et al., 2015b) indicating only minor variation in sedimentation rates over the last ~3500 yrs. Points A and C represent the mean sedimentation rate downstream and upstream of the mangrove extent respectively.

4.4.2 Sediment Depth, Kriged Surface

Sediment depth measurements were taken at over 60 stations with each station consisting of three measurements transecting the width of the cave passage. The ceiling heights and average sediment thickness (n=3) were plotted along the length of Yax Chen showing the relationship with the overlying mangrove (Fig. 5). The average sediment thickness for the entire cave was 1.21 ± 0.75 (1σ) m with a maximum thickness of 3.6 m. Sediment thickness was lowest in the western section of the passage (mean = 1.03 m) dominated by overlying tropical forest vegetation and increased (mean = 1.27 m) moving east with the presence of mangrove (Fig. 5).

The kriged interpolated sediment depth surface was overlaid on the extent of the mangrove to show the spatial relationships (Fig. 6). Cross-validation of the model results indicated that the average error for sediment depth was between 0.18 – 0.53 meters, with the largest error in the cenotes. This was expected as minimal measurements were taken in the cenotes as there was little exposed sediment. As previously mentioned, collapsed central breakdown deposits in the cenotes preferentially concentrated sediment in the voids and crevices between boulders. The model indicated the sediment thickness was deeper east of the mangrove with the greatest concentration of sediment located between Cenotes L-Shaped and Tarpon 2 (1.67-2.17 meters) where there is fringing mangrove (Fig. 6). The interpolation also identified two zones in the area with overlying tropical forest vegetation, which had elevated sediment thicknesses above the mean of 1.03 meters. The model predicted the sediment thicknesses in these regions as 1.67 – 2.17

meters (red) and 1.16 – 2.17 meters (yellow) highlighting localized zones of increased sediment thickness not readily apparent on Fig. 5

4.4.3 Cenote Area and Modern Sedimentation Rates

The area of each cenote was plotted against the average sedimentation rate for 2011-2014 reported in Collins et al. (2015b; Fig. 7). The cenotes ranges in size from 250 – 9000 ± 30 m^2 with the mean size being 3200 ±30 m^2. L-Shaped Cenote was the largest with an area in excess of 9000 ± 30 m^2 (Figs. 2b, 7). The data showed that currently the average sedimentation rate upstream of L-Shaped cenote is 0.09 ± 0.02 $mg/cm^2/day$ while in downstream locations it is four times greater (0.4 ±0.07 $mg/cm^2/day$). Sedimentation rates increase downstream of L-shaped Cenote with contributions of sediment from cenotes Tarpon 1 and 2 and other smaller cenotes.

4.5 Discussion

4.5.1 Mangrove development and the onset of cave sedimentation in Yax Chen.

Rising Holocene sea-level flooded the Yax Chen cave passages (~10 mbsl) at ~ 7500 cal yr BP based on the Toscano and Macintyre (2003) and Milne and Peros (2013) sea-level curves (Fig. 8). However, the basal ^{14}C age from the aquatic sediments in Core 2 and Core 3 is ~ 3500 cal yr BP indicating sedimentation in the cave did not begin until 4000 years after flooding of the cave bottom. During cave flooding (~ 7500 cal yr BP) until the cave passages were completely flooded (~4000 cal yr BP) sedimentation in the cave would be negligible and consist predominately of calcite rafts and minimal fine OM (Fig. 9). The ages for the onset of sedimentation in Yax Chen are better explained with the rise of sea-level flooding the subaerial karst terrain allowing for the formation of the mangrove, which based on the sea-level curves occurred at ~ 4500 - 3800 cal yr BP (Fig. 8). Our basal ages from Yax Chen match this flooding age but also match the onset of mangrove development recorded at other locations along the coast. Torrescano and Islebe, (2006) documented the initiation of mangrove at El Palmar swamp located southwest of Cenote Yax Chen, near the City of Chetumal by ~ 3800 cal yr BP (see Fig. 1 for location; Table 2). Basal mangrove peats ^{13}C dated at Casa Cenote show a similar age (3395 - 3788 cal yr BP) and are coincident with the basal ages from Yax Chen (Fig. 8; Table 2). During this period sedimentation in the cave was high, consisting of OM derived from upstream cenotes (Fig. 9).

Based on the modern sediment trap study from Collins et al., (2015b) it appears that mangrove peat creates an aquitard slowing downward percolation of rainwater through the vadose zone. In mangrove areas, precipitation funnels nutrient rich waters into the cenotes during the seasonal drop in the water table during the dry season (November - April). This nutrient rich water then causes increased primary productivity in the sunlit cenotes and the draining water also causes slightly increased flows into the downstream cave passages (Moore, 1999). In the sediment trap study; there was a strong direct relationship between cenote area and sediment flux with the presence of mangrove (Collins et al., 2015b; Fig. 7). In contrast, tropical forest terrains, with their thin soils allow rainwater to immediately penetrate through the vadose zone to the water table resulting in minimal nutrient inputs to cave passages (Pohlman et al., 1997).

This effect is also seen in the long-term sediment depth data where areas upstream of L-Shaped Cenote generally have thinner sediment deposits vs. downstream areas where they are thicker (Figs. 5, 6). This corresponds with both more extensive mangrove but also increased cenote area and associated primary productivity which matches similar trends in the modern sediment trap study (Collins et al., 2015b). There are departures from this trend, notably downstream from Cenote Luna where the kriged data shows high sediment depths which may be due to nutrient inputs from side cave passages that connect to the Sian Ka'an Biosphere wetlands. Cenote Luna has a relatively large surface area and nutrient inputs from side passages maybe increasing its primary productivity and resulting sedimentation in the downstream areas of Yax Chen. Sediment coverage thins to negligible amounts upstream of Cenote Gemini (Figs. 5, 6). As sea-level rise continues, sedimentation would be expected to extend further inland as new mangrove stands develop on the karst surface (McKee et al., 2007).

Similar but multiple phases of punctuated sedimentation are likely causing stepwise sediment accumulation patterns in cores from GBC, Bermuda and Actun Ha, Mexico (Fig. 3). In GBC, the shift in sedimentation occurs with the abrupt onset of carbonate mud deposition throughout the cave (C12, C7, C11, C2; Fig. 8 in, van Hengstum et al., 2011). When sea-level breaches a sill at the entrance of GBC connecting Harrington Sound (a marine embayment) with the cave passages, micrite from the lagoon is transported into the cave. In Actun Ha, the basal age for the onset of cave sedimentation is too young (~3400 cal yr BP) for its elevation (-16.4 mbsl) but similar in age to Yax Chen. The coincident age is likely due the topography of Cenote Carwash (entrance to Actun Ha) which is shallow (-4.5 mbsl). Sea-level rise and flooding of the central breakdown deposit occurred after (~6500 cal yr BP) and continued to rise thereafter forming deeper open water conditions in the cenote (Gabriel et al., 2009). The initiation of sedimentation likely represents connection through flooding of the cenote of the two sections of the cave (upstream and downstream) allowing siphoning of sediment from the sunlit cenote into the cave passage through increased flow. This occurred at approximately the same time as the formation of the mangrove around Yax Chen with rising Holocene sea-level.

The emphasis of this study is how inherited topography (i.e. karst surface) and sea-level change dictates the distribution and development of surficial vegetation, additionally however, the hydrological connection and flow regime in the cave passages are important variables on cave sedimentation. This in turn determines when, and what type of sediment will be deposited in the cave, which will be affected by climate induced hydrological change (e.g. more rainfall events) but it does appear that sea-level triggers abrupt shifts in sedimentation in the cave (van Hengstum et al., 2011; van Hengstum et al., 2015). The nature of the phase-shift in sedimentation will depend on cave physiography and its connection with outside sources of sediment, however, it is sea-level coupled with the topography that is triggering large and rapid shifts in sedimentation.

4.5.2 Implications for using Cave Sediments as a Sea-level Indicator

Plots of basal peats/aquatic sedimentation from a variety of locations in the vicinity of Yax Chen show discrepancies from Caribbean sea-level curves (Fig. 8). Some points show good correlation, while others demonstrate considerable departures (~16 m). Generally, the sites that were located in cenotes had good correspondence (e.g. Chum Kopo, Carwash), while cave sediments tended to show some significant discrepancies. Yax Chen and Actun Ha have notable departures as discussed; however, data from Cenotes Ich Balam and Oasis with ages that are too old for a given depth likely reflect contamination with older allochthonous OM. Cenotes have better correspondence between the onset of sedimentation and flooding likely because OM has a higher chance of accumulating and being preserved in the open water areas. Deposition in the cenote is a result of gravitational settling and does not rely on transportation processes necessary for deposition in the cave (see also, Collins et al., 2015b; Fig. 9). As discussed in Gabriel et al., (2009), it isn't until the water table reaches the top of the central breakdown deposit that mangrove and other vegetation can grow, allowing autochthonous sedimentation in and around the open waters zones of the cenote. In the case of Cenotes Ich Balam and Oasis in the Outland Cave system, basal ages demonstrated a better fit with sea-level. This was shown to be the result of bats transporting OM (seeds and guano) deep into the cave which was then preserved in shallow water on the cave bottom allowing for better resolution of sea-level changes. In the Actun Ha system, this is not the case, even though distances from the cenote are very similar. As discussed in Collins et al., (2015a), numerous cores are required to isolate the flooding age for cave passages. Basal ages in these circumstances should be considered as a minimum date for cave inundation, as flooding may have occurred previous to sediment deposition / preservation. The basal ages likely reflect a change in the hydrology as explained, causing movement of sediment into the cave with water level rising and flooding the central breakdown deposit. The ceiling height and its relationship with flooding is also very important for the movement of floating OM but also airway access for bats and birds entering the cave (Collins et al., 2015a). Work at the Hoyo Negro archaeological site demonstrated how these airways affected the loci of OM deposition in the cave with rising sea-level over the Holocene (Collins et al., 2015a), and emphasized the need to measure and document the cave physiography (bottom and ceiling heights) to understand what controls sedimentation in the cave. As demonstrated in Hoyo Negro but also GBC, Bermuda, the elevation of sills or restrictions (e.g. ceiling) is required information to associate sediment records with sea-level change in the cave environment.

4.6 Conclusions

Sediment did not begin accumulating in Yax Chen until ~3500 cal yr BP when the upper karst terrain became flooded with Holocene sea-level rise allowing the development of mangrove. These results match ages for the establishment of mangrove from nearby sites (e.g. 3800 cal yrs BP ; Chetumal; Torrescano and Islebe, 2006) on the coast. The development of mangrove, coupled with cenote size largely determined the long-term pattern of sedimentation in the cave as measured with sediment thickness. This trend matched those from modern sediment trap studies conducted previously in Yax Chen (Collins et al., 2015). Based on these results, basal ages for the onset of aquatic cave sedimentation should be scrutinized with respect to karst physiography and their connectivity with surficial terrestrial environments as phase shifts in sedimentation may not be coincident with the flooding of the cave with sea-level rise.

4.7 Acknowledgements

The authors would like to thank Dr. Todd Kincaid for his insightful review and comments on the original manuscript. We would also like to thank David Carrillo for his cartography skills and AutoCAD digitation of Yax Chen Cave Map. We gratefully acknowledge the support of; Global Underwater Explorers, The Mexican Cave Exploration Project, Cindaq, and the wonderful staff at Zero Gravity for dive support and logistics. This research was only possible due to all of the talented MCEP Science Week volunteers from around the world (especially the Dutch contingent). Special thanks go to; Onno van Eijk, Ali Perkins, Arno Mol, Jan Duikt, Steve and Chantel Blanchard for your repeated support each year. Funding was provided by National Sciences and Engineering Research Council of Canada (EGR – Discovery); National Geographic Research and Exploration Grant (EGR).

4.8 References

Arlot, S., and Celisse, A., 2010, A survey of cross-validation porcedures for model selection: Statistics Surveys, v. 4, p. 40-79.

Back, W., B.B. Hanshaw, J.S. Herman, and J.N. Van Driel, 1986, Differential dissolition of a Pleistocene reef in the ground-water mixing zone of coastal Yucatan, Mexico: Geology, v. 14, p. 137-140.

Bauer-Gottwein, P., B.R.N. Gondwe, G. Charvet, L.E. Marin, M. Rebolledo-Vieyra, and G. Merediz-Alonso, 2011, Review: The Yucatan Peninsula karst aquifer, Mexico: Hydrogeology Journal, v. 19, p. 507-524.

Beddows, P. A., 2004, Groundwater Hydrology of a Coastal Conduit Carbonate Aquifer: Caribbean Coast of the Yucatan Peninsula, Mexico [Doctor of Philosophy: University of Bristol, 332 p.]

Beddows, P. A., Smart, P. L., Whitaker, F. F., and Smith, S. L., 2007, Decoupled fresh-saline groundwater circulation of a coastal carbonate aquifer: Spatial patterns of temperature and specific electrical conductivity: Journal of Hydrology, v. 346, p. 18-32.

Benavente, J., M.c. Hidalgo, and F. Carrasco, Influence of a high recharge episode following a drought period in an aquifer affected by seasonal seawater intrusion (Granada Coast S. Spain). *in* Proceedings First International Conference on Saltwater Intrusion and Coastal Aquifers - Monitoring, Modeling and Management, Essaouira, Morocco, April 2001, p. 23-25.

Blaauw, M., 2010, Methods and code for "classical" age-modelling of radiocarbon sequences: Quaternary Geochronology, v. 5, p. 512-518.

Brown, A. L., E.G. Reinhardt, P.J. van Hengstum, and Pilarczyk, J. E., 2014, A Coastal Yucatan Sinkhole Records Intense Hurricane Events: Journal of Coastal Research, v. 30, no. 2, p. 418-428.

Coke, J., 1991, Sea-level Curve: Nature, v. 353, no. 5, p. 25.

Collins, S. V., E.G. Reinhardt, D. Rissolo, J.C. Chatters, A. Nava Blank, and P. Luna Erreguerena, 2015a, Reconstructing water level in Hoyo Negro with implications for early Paleoamerican and faunal access.: Manuscript submitted for publication.

Collins, S. V., E.G. Reinhardt, C.L. Werner, S. Meacham, F. Devos, and C. LeMaillot, 2015b, Regional response of the coastal aquifer to Hurricane Ingrid and sedimentation flux in the Yax Chen cave system (Ox Bel Ha) Yucatan, Mexico Manuscript submitted for publication.

Esterson, K., 2003, Mixing Corrosion in a Coastal Aquifer [Masters of Science: Florida State University, 66 p.]

Finch, W. A., 1965, The Karst Landscape of Yucatan, University of Illinois at Urbana-Champaign.

Florea, L. J., H.L. Vacher, B. Donahue, and D. Naar, 2007, Quaternary cave levels in peninsular Florida: Quaternary Science Reviews, v. 26, p. 1344-1361.

Gabriel, J. J., E.G. Reinhardt, M.C. Peros, D.E. Davidson, P.J. van Hengstum, and P.A. Beddows, 2009, Palaeoenvironmental evolution of Cenote Aktun Ha (Carwash) on the Yucatan Peninsula, Mexico and its response to Holocene sea-level rise: Journal of Paleolimnology, v. 42, p. 199-213.

Gabriel, J. J., and Reinhardt, E. G., 2006, Late Holocene (3500yBP) Salinity Changes and Their Climatic Implications as Recorded in an Anchialine Cave System, Ox Bel Ha, Yucatan,Mexico [Masters: McMaster University, 120 p.]

Gischler, E., E.A. Shinn, W. Oschmann, J.Fiebig, and N.A. Buster, 2008, A 1500-Year Holocene Caribbean Climate Archive from the Blue Hole, Lighthouse Reef, Belize: Journal of Coastal Research, v. 24, no. 6, p. 1495-1505.

Hanstenrath, S., and Greischar, L., 1993, Circulation Mechanisms Related to Northeast Brazil Rainfall Anomalies: Journal of Geophysical Research, v. 98, no. D3, p. 5093-5102.

Hodell, D. A., M. Brenner, J.H. Curtis, R. Medina-Gonzalez, E. Ildefonso-Chan Can, A. Albornaz-Pat, and T.P. Guilderson, 2005, Climate change on the Yucatan Peninsula during the Little Ice Age: Quaternary Research, v. 63, p. 109-121.

Hughen, K. A., J.T. Overpeck, L.C. Peterson, and Anderson, R. F., 1996, The nature of varved sedimentation in the Cariaco Basin, Venezuela, and it's paleoclimatic significance: The Geological Society, London, Special Publication, v. 116, p. 171 - 183.

Lopez Fuerte, F. O., D.A. Siqueiros Beltrones, and J.N. Navarro, 2010, Benthic Diatoms Associated with Mangrove Environments in the Northwest Region of Mexico: CICIMAR-Oceanides.

Lugo, A. E., and Snedaker, S. C., 1974, The Ecology of Mangroves: Annual Review of Ecology and Systematics, v. 5, p. 39-64.

Mazda, Y., H. Yokochi, and Y. Sato, 1990, Groundwater Flow in the Bashita-Minato Mangrove Area, and its Influence on Water and Bottom Mud Properties: Estuarine, Coastal and Shelf Science, v. 31, p. 621-638.

McKee, K. L., D.R. Cahoon, and I.C.Feller, 2007, Caribbean mangroves adjust to rising sea level through biotic controls on change in soil elevation: Global Ecology and Biogeography.

Meacham, S. S., 2012, Using Landsat 5 TM Data to Identify and Map Areas of Mangrove in Tulum, Quintana Roo, Mexico [Masters of Science: University of New Hampshire, 105 p.

Metcalfe, S. E., S.L. O'Hara, M. Caballero, and S.J. Davies, 2000, Records of Late Plistocene-Holocene climate change in Mexico - a review: Quaternary Science Reviews, v. 19, p. 699-721.

Milne, G. A., and Peros, M., 2013, Data-model comparison of Holocene sea-level change in the circum-Caribbean Region: Global and Planetary Change, v. 107, p. 119-131.

Moore, W. S., 1999, The subterranean estuary: a reaction zone of ground water and sea water: Marine Chemistry, no. 65, p. 111-125.

Moore, Y. H., R.K. Stoessell, and D.H. Easley, 1992, Fresh-water sea-water relationship within a groundwater-flow system, northeastern coast of the Yucatan Peninsula: Ground Water, v. 30, no. 3, p. 343-350.

Neuman, B. R., and Rahbek, M. L., 2007, Modeling The Groundwater Catchment of the Sian Ka'an Reserve, Quintana Roo: National Speleological Society.

Peterson, L. C., J.T. Overpeck, N.G. Kipp, and J. Imbrie, 1991, A high-resolution late Quaternary upwelling record from the anoxic Cariaco Basin, Venezuela: Paleooceanography, v. 6, p. 99-120.

Pohlman, J. W., T.M. Iliffe, and L.A. Cifuentes, 1997, A stable isotope study of organic cycling and the ecology of an anchialin cave ecosystem: Marine Ecology Progress Series, v. 155, p. 17-27.

Quintana Roo Speleological Survey, 2014, List of Long Underwater Caves in Quintana Roo, Mexico: Tulum, Quintana Roo Speleological Survey.

Raeisi, E., and Mylroie, J. E., 1995, Hydrodynamic behaviour of caves formed in the fresh-water lens of carbonate islands: Carbonates and Evaporites, v. 10, no. 2, p. 207-214.

Reimer, P. J., M.G.L. Bard, A. Bayliss, J.W. Beck, P.G. Blackwell, C.B. Ramsey, C.E. Buck, R.L. Edwards, M. Freidrich, P.M. Groots, T.P. Guilderson, H. Haflidason, I. Hajdas, C. Hatté, T.J. Heaton, D.L. Hoffmann, A.G. Hogg, K.A. Hughen, K.F. Kaiser, B. Kromer, S.W. Manning, M. Nui, R.W. Reimer, D.A. Richards, E.M. Scott, J.R. Southon, C.S.M. Turney, and J. van der Plicht, 2013, IntCal13 and Marine13 radiocarbon age calibration curves, 0-50,000 years Cal BP.: Radiocarbon, v. 55, p. 1896-1887.

Schmitter-Soto, J. J., F.A. Comin, E. Escobar-Briones, J. Herrera-Silveira, J. Alcocer, E. Suarez-Morales, M. Elias-Gutierrez, V. Diaz-Arce, and B. Steinich, 2002, Hydrogeochemical and biological characteristisc of cenotes in th Yucatan Peninsula (SE Mexico): Hydrobiologia, v. 467, p. 215-228.

Simon, K. S., T. Pipan, and D.C. Culver, 2007, A Conceptual Model of the Flow and Distribution of Organic Carbon in Caves: Journal of Cave and Karst Studies, v. 69, no. 2, p. 279-284.

Smart, P. L., P.A. Beddows, J. Coke, S. Doerr, S. Smith, and Whitaker, F. F., 2006, Cave Development on the Caribbean coast of the Yucatan Peninsula, Quintana Roo, Mexico, *in* Harmon, R. S. a. C. W., ed., Perspectives on Karst geomorphology, hydrology and geochemistry - A tribute volume to Derek C. Ford and William B. White, Volume 404, Geological Society of America Special Paper, p. 105-128.

Torrescano, N., and Islebe, G. A., 2006, Tropical forest and Mangrove history from southeastern Mexico: a 5000 yr pollen record and implications for sea level rise: Veget Hist Archaeobot, v. 15, p. 191-195.

Toscano, M. A., and Macintyre, I. G., 2003, Corrected western Atlantic sea-level curve for the last 11,000 years based on calibrated ^{14}C dates from Acropora framework and intertidal mangrove peat: Coral Reefs v. 22, p. 257-270.

van Hengstum, P. J., D.A. Richards, B.P. Onac, and J.A. Dorale, 2015, Coastal caves and sinkholes, *in* Ian Shennan, A.J. Long, and B.J. Horton, eds., Handbook of Sea-Level Research, John Wiley and Sons Ltd.

van Hengstum, P. J., D.B. Scott, D.R. Grocke, and M.A. Charette, 2011, Sea level controls sedimentation and environments in coastal caves and sinkholes: Marine Geology, v. 286, p. 35-50.
van Hengstum, P. J., Donnelly, J. P., Toomey, M. R., Albury, N., and Kakuk, B., 2014, 3000 Years of Intense Hurricane Surge in the Northern Bahamas, Geological Society of America: Vancouver.
van Hengstum, P. J., E.G. Reinhardt, P.A. Beddows, and J.J. Gabriel, 2010, Linkages between Holocene paleoclimate and paleohydrogeology preserved in a Yucatan underwater cave: Quaternary Science Reviews, v. 29, no. 19-20, p. 2788-2798.
Weidie, A. E., 1985, Geology of Yucatan Platform: Part 1, 19 p.:
Werner, C., 2007, Double-Diffusive Fingering in Porous Media [Doctor of Philosophy: Florida State University, 114 p.
Wolanski, E., Y. Mazda, and P. Ridd, 1992, Coastal and Estuarine Studies - Mangrove Hydrodynamics, American Geophysical Union, Tropical Mangrove Ecosystems, 329 p.:

4.9 Tables

Table 1: Conventional and calibrated radiocarbon ages measured by atomic mass spectrometry, from Gabriel and Reinhardt, 2009; van Hengstum et al., 2010 and van Hengstum et al., 2011.

Location	Core No.	Sample Depth (mbsl)	Depth (cm)	Laboratory no.	Age 14C yr B.P.	Age Range (2σ) cal yr B.P.
Aktun Ha	C2	-16.07	7	Beta-279531	570 ± 40	581 - 651
	C2	-16.10	10	Beta-239981	780 ± 40	666 - 766
	C2	-16.12	12	Beta-271308	750 ± 40	653 - 739
	C2	-16.16	16	Beta-272082	800 ± 40	673 - 782
	C2	-16.21	21	Beta-239982	2640 ± 40	2722 - 2811
	C2	-16.26	26	Beta-279532	2480 ± 40	2434 - 2718
	C2	-16.31	31	Beta-271309	3110 ± 40	3239 - 3404
	C2	-16.36	39	Beta-239983	3210 ± 40	3361 - 3486
Ox Bel Ha	C2	-9.29	9	Beta-257280	950 ± 40	776 -934
	C2	-9.49	29	Beta-257281	1840 ± 40	1696 - 1874
	C2	-9.71	51	Beta-257282	2460 ± 40	2362 - 2618
	C2	-9.93	73	OS-74418	3310 ± 30	3466 - 3618
	C3	-7.81	21	OS-74462	435 ± 35	439 - 533
	C3	-8.01	41	OS-74420	1410 ± 30	1286 - 1358
	C3	-8.21	61	OS-74422	2270 ± 25	2301 - 2346, 2178 - 2243
	C3	-8.29	69	OS-74423	2730 ± 25	2769 - 2868
	C3	-8.39	79	OS-74424	3240 ± 30	3388 - 3491
	C33	-9.38	18	D-AMS 008367	725 ± 26	652 - 699
	C33	-9.64	44	D-AMS 008366	953 ± 26	796 - 885
	C33	-9.79	59	D-AMS 008368	1339 ± 27	1239 - 1303
	C33	-9.95	75	D-AMS 008369	1724 ± 28	1564 - 1701
Green Bay Cave Bermuda	GBC5	-19.65	15	OS-79473	645 ± 25	246 - 378
	GBC5	-19.78	28	OS-78020	1610 ± 25	1096 - 1253
	GBC5	-19.81	31	OS-78019	2040 ± 25	1533 - 1687
	GBC5	-19.88	38	OS-78451	3590 ± 30	3834 - 3974
	GBC5	-19.96	46	OS-74180	3800 ± 40	4082 - 4298
	GBC5	-20.00	50	OS-74179	4930 ± 45	5590 - 5742
	GBC5	-20.02	52	OS-80321	6800 ± 50	7233 - 7418
	GBC5	-20.11	61	OS-79218	7160 ± 65	7509 - 7765
	GBC5	-20.15	65	OS-79474	11100 ± 65	12802 - 13086

Table 2: Conventional and calibrated radiocarbon basal sediment ages measured by atomic mass spectrometry from various locations around Quintana Roo, Mexico.

Location (Author)	Core/Sample No.	Sample Depth (mbsl)	Depth (cm)	Laboratory no.	Age 14C yr B.P.	Age Range (2σ) cal yr B.P.
Cenote Ich Balam (Collins et al., 2014a)	C1	-11.5	64	D-AMS 002363	7088 ±31	7914-7970
	C2	-9.4	131	Beta 333187	7270 ±40	8009-8172
	C3	-11.2	38	D-AMS 002368	6994 ±31	7742-7817
	C4	-12.3	77	D-AMS 002374	7269 ±38	8010-8170
	C5	-11.8	120	Beta 333188	6300 ±40	7163-7310
	C6	-4.9	26	D-AMS 002372	3510 ±31	3698-3865
Cenote Oasis (Collins et al., 2014a)	OAC2	-4.1	66	D-AMS 003397	4704±29	5322-5418
	OAC3	-1.8	76	D-AMS 003400	3887±38	4230-4420
Ox Bel Ha Cave/Cenote Yax Chen (Gabriel et al., 2006)	C1	-7.8	32	Beta-244014	3460±40	3636-3836
	C2	-10.0	75	OS-74418	3310±30	3466-3618
	C3	-8.4	80	OS-74424	3240±30	3388-3491
	C4	-7.9	43	OS-74426	3160±30	3343-3447
Cenote Casa (Kovacs and Gregory, unpublished)	1	-4.0	-	D-AMS 002350	3519±31	3701-3874
	2	-4.3	-	D-AMS 002353	3607±39	3831-3994
	3	-5.5	-	D-AMS 002355	3579±33	3826-3977
	4	-4.6	-	D-AMS 002357	3392±29	3567-3699
El Palmar Swamp (Torrescano and Islebe, 2006)	C1	-0.8	80	NSRL 11098	3870±50	4153-4418
	C1	-2.2	220	NSRL 11099	5080±40	5739-5913
Laguna Chumkopó (Brown et al., 2014)	CK2	-7.3	91	Beta-270693	6160±40	6951-7164
Cenote Carwash (Gabriel et al., 2009)	C1	-4.1	6	Beta-226967	5790±40	6488-6675
	C1	-4.6	57	Beta-235036	6390±40	7262-7418
Actun Ha Cave (Van Hengstum et al., 2010)	C2	-16.4	40	Beta-239983	3210±40	3361-3486
	C4	-20.5	53	Beta-237363	3890±40	4229-4422

4.10 Figures

Fig. 1: The location of Cenote Yax Chen on the Yucatan Peninsula, Mexico.

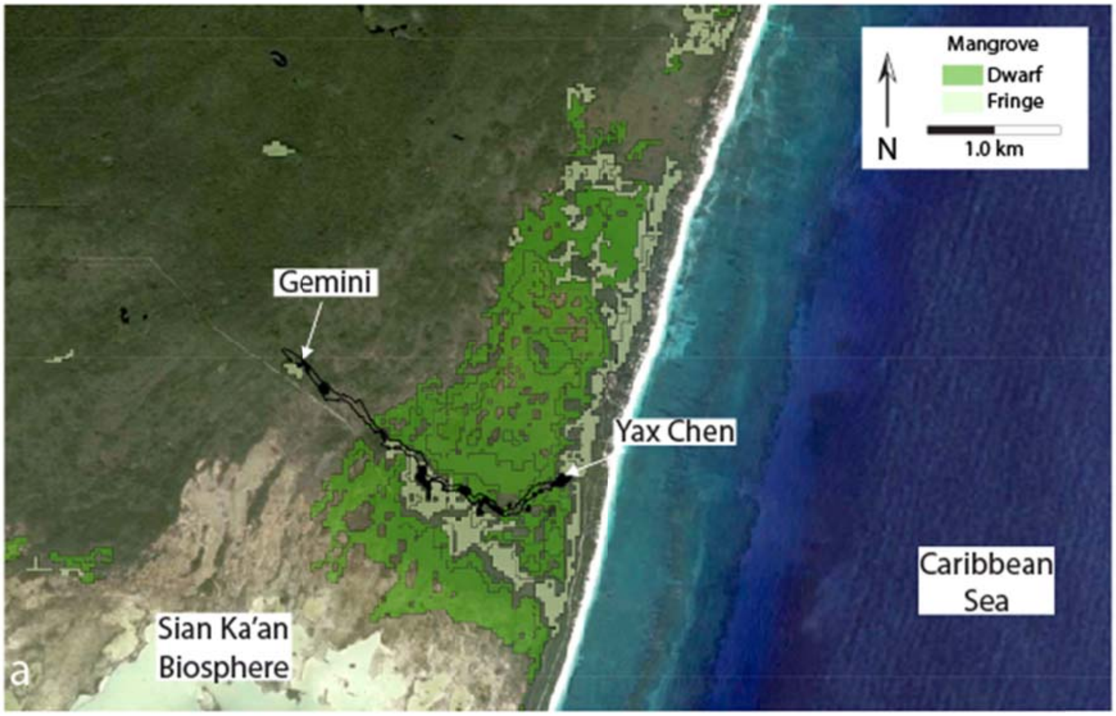

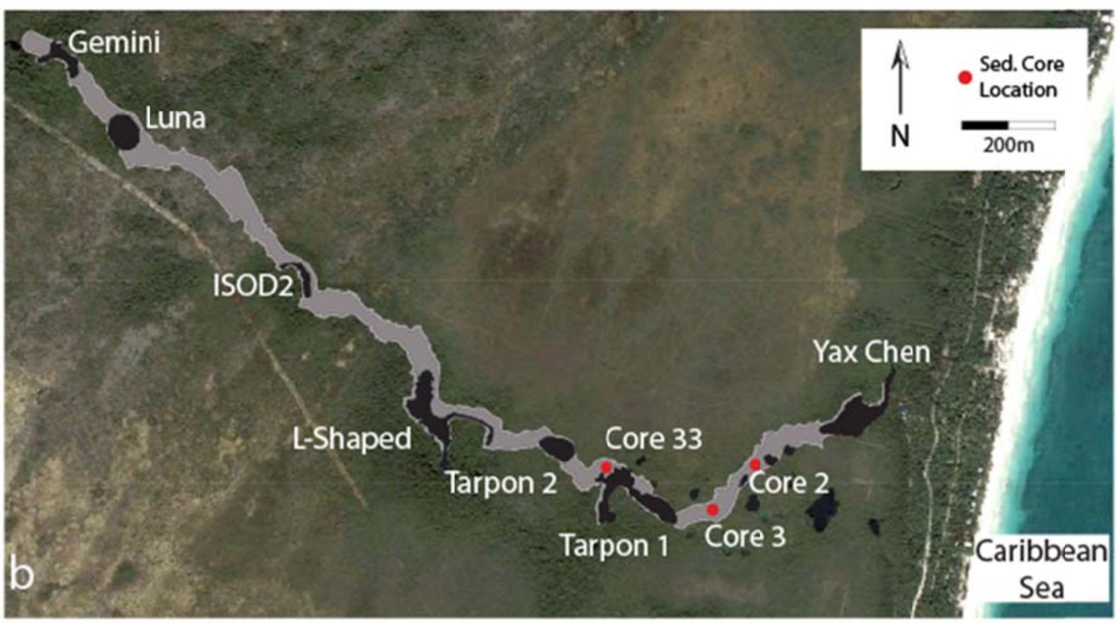

Fig. 2: (a) Partial results of Landsat 5 supervised classification of mangrove forest in the Tulum Region (modified after, Meacham, 2012). (b) Location of mapped cenotes and core locations in Yax Chen, Quintana Roo, Mexico.

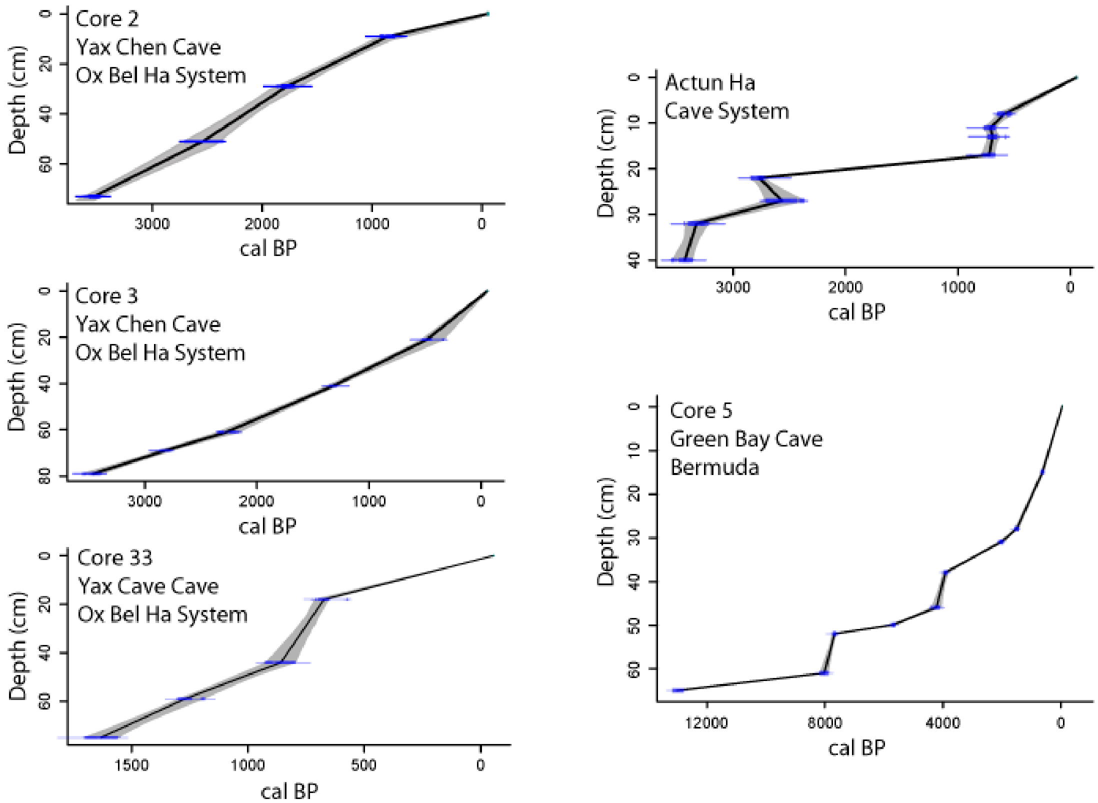

Fig. 3: Age/depth models calculated using Clam R statistical software for sediment cores from Yax Chen, Actun Ha, Green Bay Cave, Bermuda (van Hengstum et al., 2011). Blue lines represented calibrated distributions of dated material. Black lines represent the age weighted mean value for a given depth. The grey shaded area corresponds to the 95% confidence interval for the age/depth model.

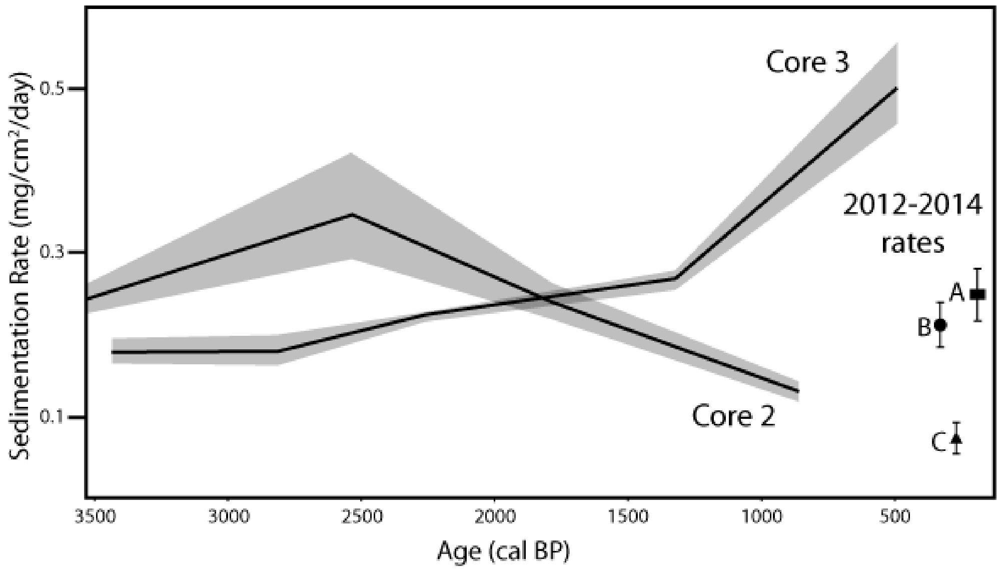

Fig. 4: Calculated sedimentation rates for cores 2 and 3 from Yax Chen. Also plotted are modern sedimentation rates and standard deviations from Collins et al, (2015b). Point A is the modern sediment flux downstream of the mangrove forest. Point B is the modern overall sediment flux for the entire Yax Chen Cave Passage. Point C is the modern sediment flux upstream of the main mass of mangrove forest (see Fig. 5 for detailed mangrove extent).

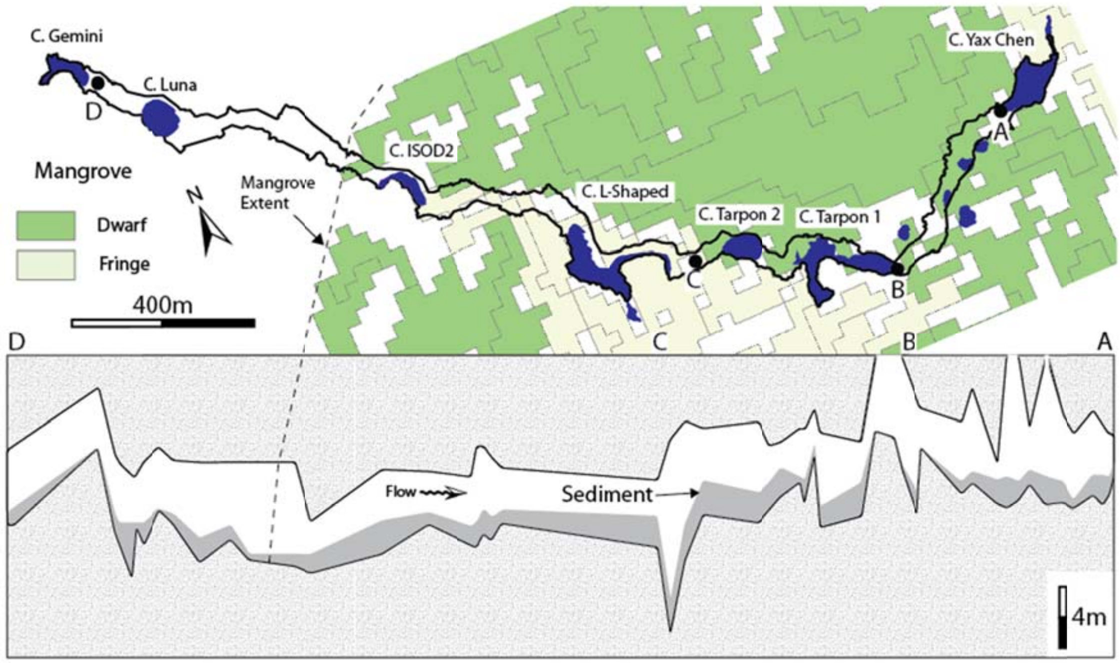

Fig. 5: Results of sediment depth measurements in the eastern section of the Ox Bel Ha Cave system from Cenote Yax Chen to Cenote Gemini. The vector map of the extent of overlying fringe and dwarf mangrove is shown for comparison (Vertical exaggeration = 100; vector overlay, modified after, Meacham, 2012).

.

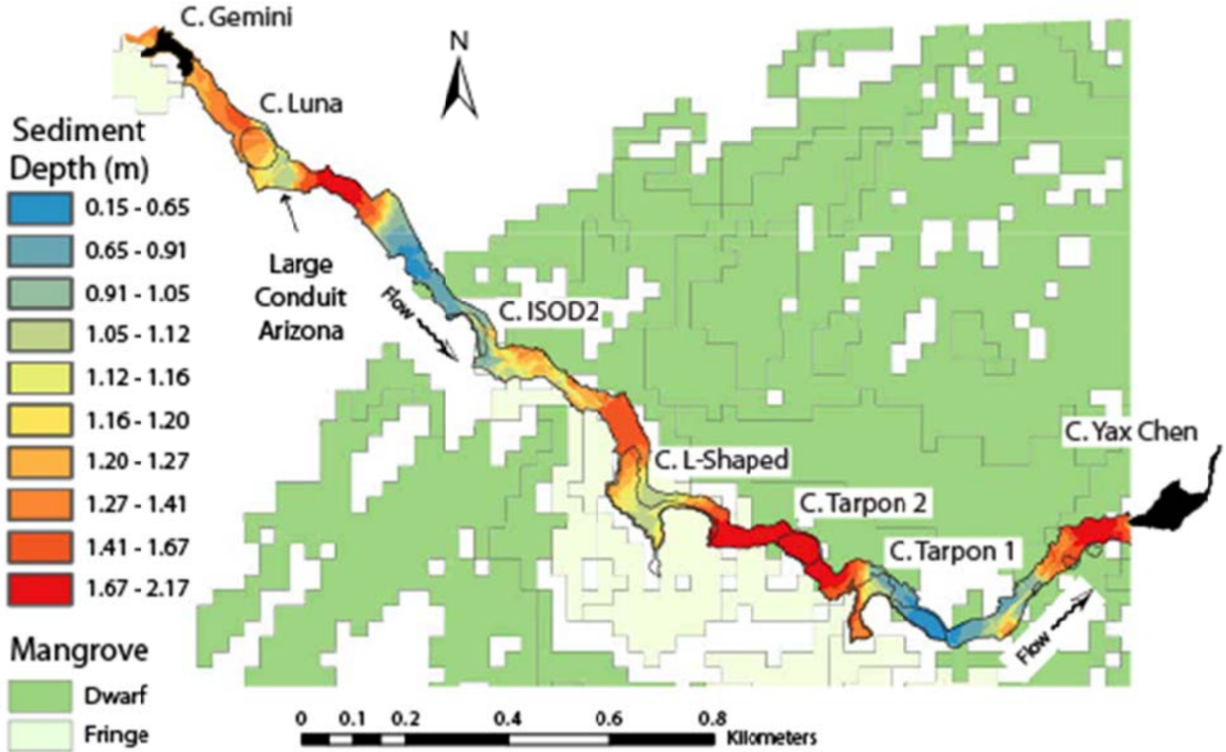

Fig. 6: Interpolated sediment depth surface for Yax Chen showing areas of increased sediment thickness. Partial results of supervised mangrove classification, overlaid to show relationship between sediment thickness and mangrove forest, (modified after, Meacham , 2012).

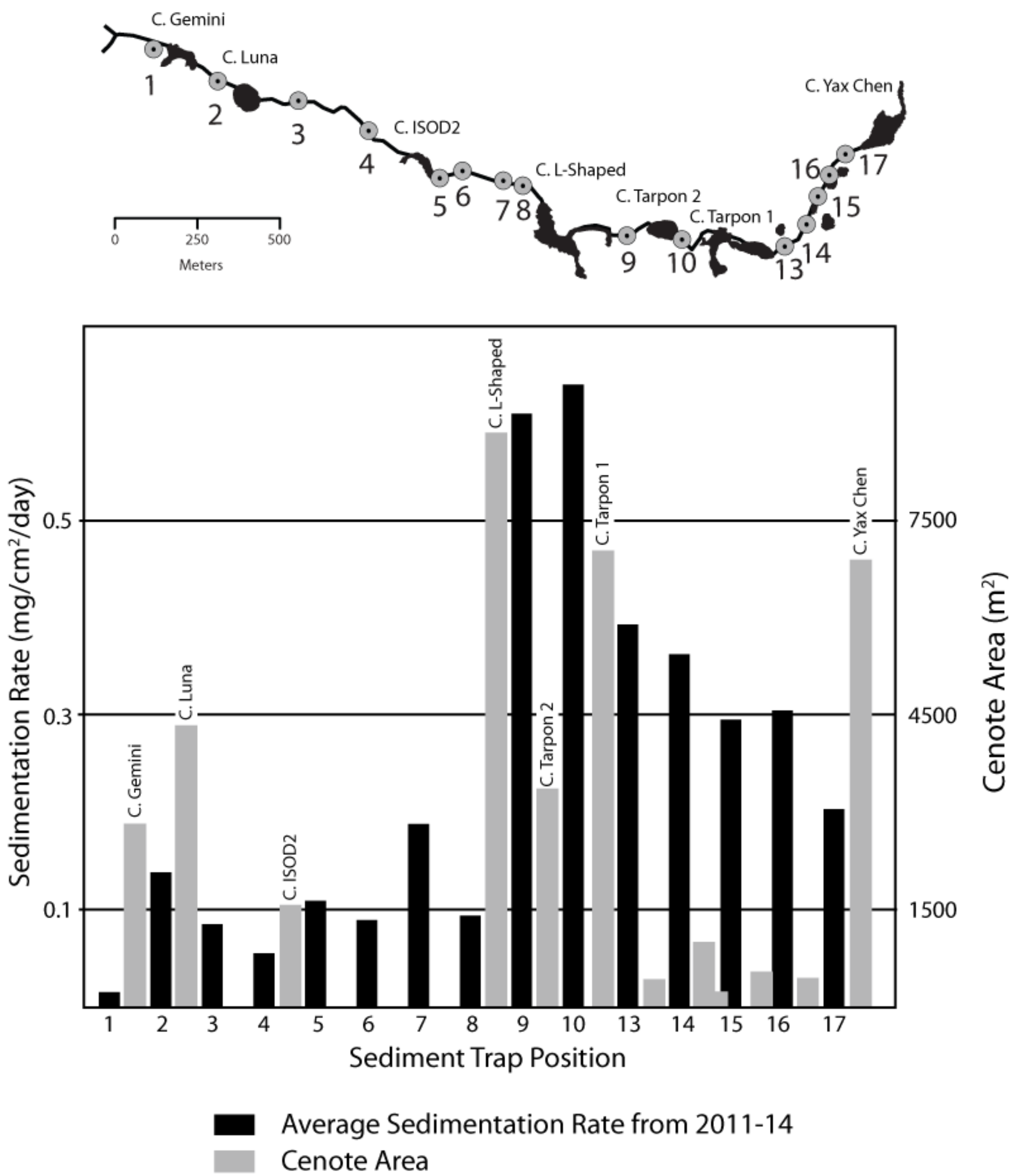

Fig. 7: Average sedimentation rate calculated in $mg/cm^2/day$ from 2011-2014 and cenote area in m^2, plotted in order from Cenote Gemini to Cenote Yax Chen (Collins et al, 2015b).

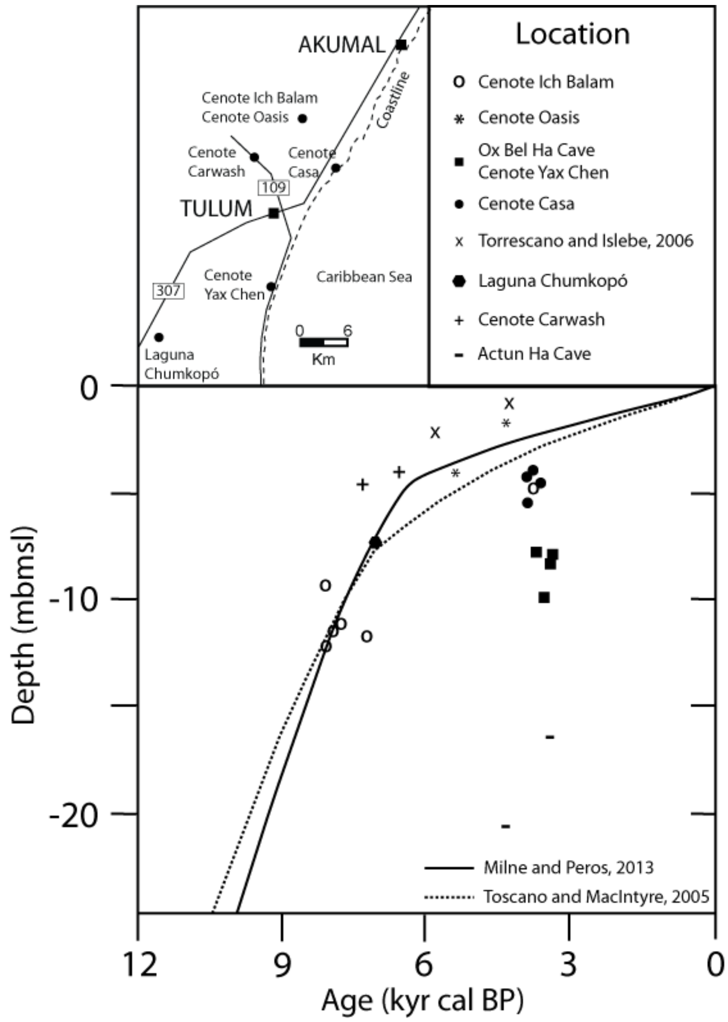

Fig. 8: Radiocarbon ages from previous studies at eight different locations around Quintana Roo, Mexico were plotted on the local Caribbean sea-level curve from Toscano and MacIntyre (2005) and Milne and Peros (2013). Dating results; Cenotes Ich Balam and Oasis from Collins et al., (2015a); Ox Bel Ha Cave/Cenote Yax Chen from Gabriel and Reinhardt, (2006), unpublished; Cenote Casa from Kovacs and Gregory, (2013), unpublished; El Palmar Swamp from Torrescano and Islebe, (2006); Laguna Chumkopó from Brown et al., (2014); Cenote Carwash from Gabriel et al., (2009); Actun Ha from van Hengstum et al., (2010).

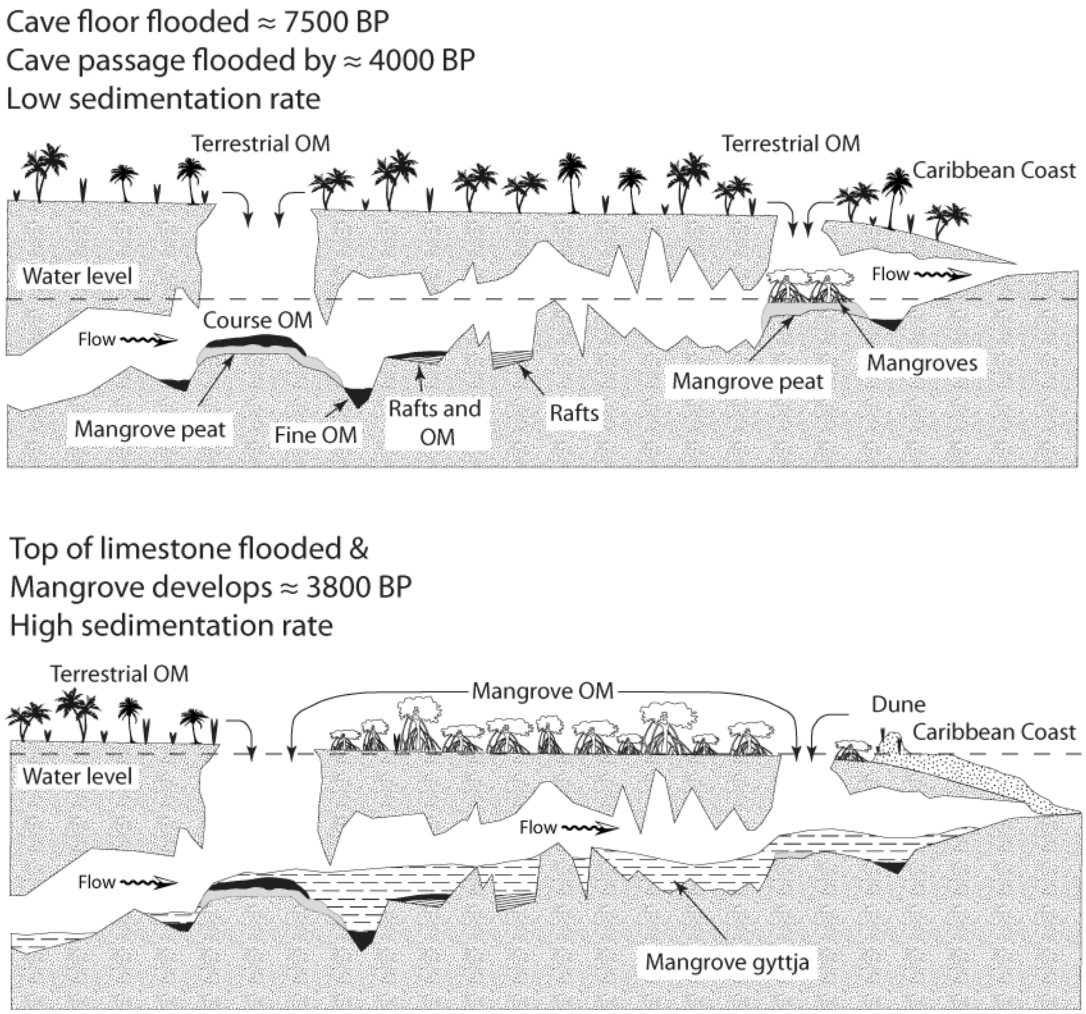

Fig. 9: An interpretative drawing of the initiation of sedimentation for Yax Chen Cave and the nature of sediment being deposited. Initial inundation of cave passage with rising sea level results in low sedimentation rates limited to cenote proximal zones of the cave. Initiation of mangrove swamp over Yax Chen Cave resulted in elevated sedimentation in the cave passage. Cave flooding did not correspond directly with initiation of sedimentation in the cave passage.

Chapter 5 - Conclusions

The subaqueous caves of the Yucatan Peninsula are proving to be a flourishing source of information for geologic study. Previous work has documented the usefulness of these sedimentary environments by providing information on paleoenvironmental changes during phreatic and vadose conditions. Earlier research has focused on the sediments in the cave and the information that was contained therein. Little attention was given to the providence and processes responsible for transporting the sediment into the cave environment. This dissertation was the first to address these two fundamental questions in a multifaceted series of projects.

In project one, the providence, mechanisms of transport and subsequent deposition of sediment were investigated in an archaeological context in the Actun Ha Cave System. A traditional geologic facies methodology was undertaken, utilizing sediment cores and microfossil analysis. Identifying that cave physiography was a controlling factor; this study was one of the first to incorporate detailed cave conduit ceiling and floor measurements as part of the geologic investigation. During the course of laboratory analysis, differences in calcite crystal habit were reported at systematic depths in multiple sediment cores. Combining these data provided inferences on important questions regarding the paleoenvironmental history of Hoyo Negro and the adjacent cave passages. Determining that sedimentation patterns in the cave were transient in time and space and were not controlled by water-level alone, provided a geologic framework to interpret future sediment cores in similar karstic environments. This information will help identify areas of interest for the numerous cores necessary to determine the flooding history of an anchialine cave. The contribution of animals (specifically bats) was documented as a significant sediment transportation vector in the subaerial caves and cenote of the Yucatan Peninsula. This was not previously documented in a geologic context for the caves in the Yucatan. This process represents a poorly understood sediment transport mechanism which may prove to be a significant factor in future studies utilizing cave and cenotes sediments as a proxy for sea-level reconstructions. Further study needs to be completed in analogous areas to understand the temporal and spatial variables that control bat rookeries and habitats, in an effort to better understand the associated organic matter/guano deposits. The exact mechanisms controlling genesis and crystal morphology of calcite rafts in the caves of the Yucatan are not entirely known. Further research on the controls of calcite morphology may provide additional definitive information regarding paleo water chemistry and water levels.

The research conducted in the Ox Bel Ha Cave System was the first study in the Yucatan Peninsula to collect continuous hydrological data on aquifer characteristics and applied innovative sediment trapping techniques to document the sediment flux in an anchialine cave. The continuous monitoring of aquifer characteristics and sediment flux provided important information on the aquifer's response to seasonal variability and large storms such as, Hurricane Ingrid in 2013. Previous to this thesis, data regarding the hydrologic response of the aquifer to large storms were limited to visual observations and sporadic measurements taken in widely dispersed cenotes. Analysis of the data showed a link between sediment entering the cave and the overlying cenote area and vegetation cover. Previously undocumented, initiation of the organic matter sediment entering the cave was predominately sourced from the overlying mangrove forest. The relationship between cenote area, surficial vegetation and cave sediments helped to explain the vastly different sediment regimes in nearby cave passages of the same system. The response of the open karst aquifer to large storm events was documented and showed minimal spatial or temporal variations in sedimentation, as a result of the storm. This project provided a successful methodology to determine sedimentation rates in the phreatic caves in the Yucatan. Additional monitoring should be conducted in side passages, as sediment transport in these areas is poorly understood for Yax Chen. Instrumenting these passages with sediment traps will provide important data on spatial patterns of sediment deposition and remobilization.

Using sediment depths and sediment core data from Yax Chen confirmed the importance of the overlying mangrove forest and cenote area to the historical sediment budget for this area of the cave. The calculated sedimentation rates from sediment cores were consistent with present day rates and appeared to have remained largely constant since the initiation of the mangrove forest. This is in contrast to the varying sedimentation rates seen in caves and cenotes which underlie tropical forest vegetation. Comparisons with Green Bay Cave in Bermuda and Actun Ha Mexico revealed that sedimentation in anchialine caves can undergo significant shifts in sedimentation which can appear rapidly in the sedimentary record. The triggering mechanism for the punctuated sedimentation at both locations appears to be related to Holocene sea-level rise, but in the case of Yax Chen is not simultaneous with cave flooding. By providing research that documented the onset and processes controlling sedimentation in the cave, a better understanding of the ancient sedimentary record was possible. In Yax Chen, sedimentation was initiated when Holocene sea-level rise flooded the karstic surface and provided a niche for mangrove development. The trigger for sedimentation in Yax Chen was the development and transgression of the surficial mangrove and not the flooding of the cave passage. The gap in the sedimentary record of Yax Chen demonstrates that cave sediments may not show the required resolution necessary for use as a sea-level proxy. The data obtained in this study does not automatically preclude the use of cave sediments in sea-level studies, but demonstrates that a greater understanding of individual cave passages is critical to accessing a caves utility as a sea-level proxy. Collecting numerous sediment cores and completing high resolution radiocarbon dating to determine the sedimentation history of a cave passage will be a necessary first step before data can be utilized in sea-level reconstructions.

Documenting supplementary sedimentation histories should be attempted in other caves passages with overlying mangrove forest, to collect enough information to refine the facies model for the various sediment regimes in phreatic caves. Further to this, the regional connectedness of the phreatic cave and cenote system should also be considered when developing sedimentation models to interpret the sediment record for paleohydrolgical endeavors. Transported organic matter and nutrients, located in areas up-stream may represent a significant source of sediment during and after extreme weather events. The baseline data collected for this research provided a framework for understanding the sediment providence and processes controlling sedimentation rates in the Yax Chen and Outland Caves and represents advancement in the understanding of the sedimentary processes active in a complex anchialine cave environment.

References

Back, W., 1995, Water Management by early people in the Yucatan, Mexico: Environmental Geology, v. 25, p. 239-242.

Back, W., B.B. Hanshaw, J.S. Herman, and J.N. Van Driel, 1986, Differential dissolition of a Pleistocene reef in the ground-water mixing zone of coastal Yucatan, Mexico: Geology, v. 14, p. 137-140.

Bauer-Gottwein, P., B.R.N. Gondwe, G. Charvet, L.E. Marin, M. Rebolledo-Vieyra, and G. Merediz-Alonso, 2011, Review: The Yucatan Peninsula karst aquifer, Mexico: Hydrogeology Journal, v. 19, p. 507-524.

Beddows, P. A., Smart, P. L., Whitaker, F. F., and Smith, S. L., 2007, Decoupled fresh-saline groundwater circulation of a coastal carbonate aquifer: Spatial patterns of temperature and specific electrical conductivity: Journal of Hydrology, v. 346, p. 18-32.

Chatters, J. C., 2000, The recovery and first analysis of an early Holocene human skeleton from Kennewick, Washington: American Antiquity, v. 65, no. 2, p. 291-316.

Chatters, J. C., D.J. Kennett, Y. Asmerom, B.M. Kemp, V. Polyak, A.N. Blank, P.A. Beddows, E. Reinhardt, J. Arroyo-Cabrales, D.A. Bolnick, TR.S. Malhi, B.J. Culleton, P.L. Erreguerena, D. Rissolo, S. Morell-Hart, and T.W. Stafford Jr., 2014, Late Pleistocene Human Skeleton and mtDNA Link Paleoamericans and Modern Native Americans: Science, v. 344, p. 750-754.

Coke, J., 1991, Sea-level Curve: Nature, v. 353, no. 5, p. 25.

Colas, P. R., P. Reeder, and J. Webster, 2000, The Ritual Use of a Cave on the Northern VACA Plateau, Belize, Central America: Journal of Cave and Karst Studies, v. 62, no. 1, p. 3-10.

DeDeckker, P., and R.M. Forester, 1988, The use of Ostracods to reconstruct continential paleoenvironmental records, *in* P. De Deckker, J. P. C., J.P. Peypouquet, ed., Ostracoda in the Earth Sciences, Elsevier, p. 175-199.

Dixon, E. J., 1999, Bones Boats and Bison, New Mexico, Univesity of New Mexico Press, 322 p.:

Gabriel, J. J., E.G. Reinhardt, M.C. Peros, D.E. Davidson, P.J. van Hengstum, and P.A. Beddows, 2009, Palaeoenvironmental evolution of Cenote Aktun Ha (Carwash) on the Yucatan Peninsula, Mexico and its response to Holocene sea-level rise: Journal of Paleolimnology, v. 42, p. 199-213.

Gill, R. B., P.A. Mayewski, J.Nyberg, G.H. Haug, and L.C. Peterson, 2007, Drought and the Maya Collapse: Ancient Mesoamerica, no. 18, p. 283-302.

Gondwe, B. R. N., S. Lerer, S. Stisen, L. Marin, M. Rebolledo-Vieyra, G. Merediz-Alonso, and P. Bauer_Gottwein, 2010, Hydrogeology of the south-eastern Yucatan Peninsula: New insights from water level measurements, geochemistry, geophysics and remote sensing: Journal of Hydrology, v. 389, p. 1-17.

Gonzalez, A. H., A. Terrazas, W. Stinnesbeck, M.E. Benavente, J. Aviles, C. Rojas, J.M. Padilla, A. Velasquez, E. Acevez, and E. Frey, 2013, The First Humans in the Yucatan Penninsula Found in Drowned Caves: The Days of the Late Pleistocene-

Early Holocene in a Changinf Tropic, *in* K.E. Graf, C.V. Ketron, and M.R. Waters, eds., Paleoamreican Odyssey: New Mexico, Center fo rthe Study of the First Americans, p. 223-238.

Mahler, B. J., J.C. Personne, F.L. Lynch, and P.C. Van Metre, 2007, Sediment and Sediment-Associated Contaminant Transport Through Karst, SpringerLink, Studies of Cave Sediments:Physical and Chemical Records of Paleoclimate.

Milne, G. A., and M. Peros, 2013, Data-model comparison of Holocene sea-level change in the circum-Caribbean Region: Global and Planetary Change, v. 107, p. 119-131.

Neuman, B. R., and Rahbek, M. L., 2007, Modeling The Groundwater Catchment of the Sian Ka'an Reserve, Quintana Roo: National Speleological Society.

Patterson, T. R., John Blenkinsop, and William Cavazza, 1995, Planktic foraminiferal biostratigraphy and 87Sr/86Sr isotopic stratigraphy of the Oligocene-to-Pleistocene sedimentary sequence in the Southeastern Calabrian Microplate, Southern Italy: Journal of Paleontology v. 69, no. 1, p. 7-20.

Pohlman, J. W., T.M. Iliffe, and L.A. Cifuentes, 1997, A stable isotope study of organic cycling and the ecology of an anchialin cave ecosystem: Marine Ecology Progress Series, v. 155, p. 17-27.

Quintana Roo Speleological Survey, 2012, List of Long Underwater Caves in Quintana Roo, Mexico: Tulum, Quintana Roo Speleological Survey.

Reinhardt, E. G., M. Little, S. Donato, D. Findlay, A. Krueger, C. Clark, and J.I.Boyce, 2005, Arcellacean (thecamoebian) evidence of land-use change and eutrophication in Frenchman's Bay, Pickering, Ontario: Environmental Geology, v. 47, p. 729-739.

Rissolo, D., 2001, Ancient Maya Cave Use in the Yalahau Region, Northern Quintana Roo, Mexico: National Speleological Society.

Smart, P. L., P.A. Beddows, J. Coke, S. Doerr, S. Smith, and Whitaker, F. F., 2006, Cave Development on the Caribbean coast of the Yucatan Peninsula, Quintana Roo, Mexico, *in* Harmon, R. S. a. C. W., ed., Perspectives on Karst geomorphology, hydrology and geochemistry - A tribute volume to Derek C. Ford and William B. White, Volume 404, Geological Society of America Special Paper, p. 105-128.

Steinich, B., and L.E. Marin, 1997, Determination of flow characteristics in the aquifer of the Northwestern Peninsula of Yucatan, Mexico: Journal of Hydrology, v. 191, no. (1-4), p. 315-331.

Toscano, M. A., and Macintyre, I. G., 2003, Corrected western Atlantic sea-level curve for the last 11,000 years based on calibrated ^{14}C dates from Acropora framework and intertidal mangrove peat: Coral Reefs v. 22, p. 257-270.

van Hengstum, P. J., D.B. Scott, and E.J. Javaux, 2009a, Foraminifera in elevated Bermudian caves provide further evidence for +21 m eustatic sea-level during Marine Isotope Stage 11: Quaternary Science Reviews, v. 28, p. 1850-1860.

van Hengstum, P. J., E.G. Reinhardt, P.A. Beddows, H.P. Schwarcz, and J.J., G., 2009b, Foraminifera and testate amoebae (thecamoebians) in an anchialine cave: Surface distributions from Aktun Ha (Carwash) cave system, Mexico: Limnology and Oceanography, v. 54, no. 1, p. 391-396.

van Hengstum, P. J., E.G. Reinhardt, P.A. Beddows, H.P. Schwarcz, R.J. Huang, and J.J. Gabriel, 2008, Thecamoebians (testate amoebae) and foraminifera from three anchialine cenotes in Mexico: low salinity (1.5-4.5 psu) faunal transitions Journal of Foraminiferal Research, v. 38, no. 4, p. 305-317.
van Hengstum, P. J., E.G. Reinhardt, P.A. Beddows, and J.J. Gabriel, 2010, Linkages between Holocene paleoclimate and paleohydrogeology preserved in a Yucatan underwater cave: Quaternary Science Reviews, v. 29, no. 19-20, p. 2788-2798.